PRE-CLINICAL STRATEGIES TO OVERCOME DRUG-RESISTANT MULTIPLE MYELOMA: PREDICTIVE TRANSCRIPTOMICS AND TARGETING THE MYELOMA EPIGENOME

A DISSERTATION
SUBMITTED TO THE FACULTY OF THE GRADUATE SCHOOL
OF THE UNIVERSITY OF MINNESOTA
BY

TAYLOR STIVER HARDING

IN PARTIAL FULFILLMENT OF THE REQUIREMENTS
FOR THE DEGREE OF
DOCTOR OF PHILOSOPHY

BRIAN VAN NESS, PHD
ADVISOR

APRIL 2018

ACKNOWLEDGEMENTS

I would first and foremost like to advise my mentor, Brian Van Ness, Ph.D., continued to push me to take ownership over my projects and mature as a scientist. Brian has always been very accessible and has a clear interest in the education of his students. It has been wonderful to have an advisor who has made me a better scientist while also being someone I genuinely enjoy working for. Working in the Van Ness lab had provided me with a long list of great experiences and opportunities. I am sure that any success that I (hopefully) reach in my professional life will, in part, be due to the fantastic graduate education I received working in the Van Ness laboratory.

I would like to thank all of my past and present lab mates who have made working in the Van Ness all that much more enjoyable. Thank you to Holly Stessman, Samantha Quandahl and Aatif Mansoor for welcoming me into the lab when I first rotated in 2012. I owe a great deal of gratitude to Amit Mitra. Amit shared the most time with me in the Van Ness lab and was a wonderful person to work and interact with. Amit's extensive bioinformatics acumen was an invaluable resource for me to learn from. It would have been unimaginably difficult to have tackled certain aspects of my projects without his advice. Although we only briefly shared time in the Van Ness, Monica Akre was a welcome addition to the lab where company was at times rather scarce. And finally a special thanks to all of the undergraduate students in the lab who have been wonderful to mentor and/or work with over the years.

I would like to thank my thesis committee: York Marahrens, Ph.D., David Largaespada, Ph.D., Ran Bleckman, Ph.D., Chad Myers, Ph.D. and Pamala Jacobson, Ph.D. You have all provided me with invaluable advice and guidance over the last several years. It has been a pleasure to get to know all of you.

I want to extend a special thank you to all my graduate student friends. Although graduate school has not *always* been fun, you all have made these years in Minneapolis some of the enjoyable times in my adult life. I will always cherish our friendships.

Finally, I want to thank my family who have always encouraged me to peruse my academic goals and provided support whenever I needed it. I absolutely would not have made it this far without you.

ABSTRACT

Multiple myeloma remains an incurable hematological malignancy due to the failure of standard-of-care therapies to broadly target a genetically heterogeneous disease and an inability overcome inevitable drug-resistant relapse. This dissertation will address this outstanding problem through two approaches: transcriptomic profiling to predict resistance to proteasome inhibitors and pre-clinical evaluation of epigenetic-targeting therapies to broadly target the myeloma epigenome.

First, our goal was to develop a gene expression signature that predicts response specific to proteasome inhibitor (PI) treatment in MM. Using a well-characterized panel of human myeloma cell lines (HMCLs) representing the biological and genetic heterogeneity of MM, we created an in vitro chemosensitivity profile in response to treatment with the four PIs as single-agents. Through gene expression profiling and machine learning-based computational approaches we identified a 42-gene expression signature that could not only distinguish good and poor PI-response in the HMCL panel, but could also be successfully applied to four different clinical datasets on MM patients undergoing PI-based chemotherapy to distinguish between extraordinary (good and poor) outcomes. Our results demonstrate the use of in vitro modeling and machine learning-based approaches to establish predictive biomarkers of response and resistance to drugs that may serve to better direct myeloma patient treatment options.

Epigenetic abnormalities are abundantly present in multiple myeloma and accumulating evidence suggests that the histone methyltransferase EZH2 is aberrantly active in MM. We tested the efficacy of EZH2 specific inhibitors in a large panel of human MM cell lines (HMCLs) and found that only a subset of HMCLs demonstrate single agent sensitivity despite ubiquitous global H3K27 demethylation. Pre-treatment with EZH2 inhibitors greatly enhanced the sensitivity of HMCLs to the pan-HDAC inhibitor panobinostat in nearly all cases regardless of single agent EZH2 inhibitor sensitivity. Transcriptomic profiling revealed large-scale transcriptomic alteration by EZH2 inhibition highly enriched for cancer-related pathways. Further analysis demonstrated that combination treatment further perturbed oncogenic pathways and signaling nodes consistent with an antiproliferative/pro-apoptotic state. We conclude that combined inhibition of HDAC and

EZH2 inhibitors is a promising therapeutic strategy to broadly target the epigenetic landscape of aggressive MM.

TABLE OF CONTENTS

Page

LIST OF TABLES

CHAPTER 1 Page

CHAPTER 2

CHAPTER 3

LIST OF FIGURES

CHAPTER 1 Page

CHAPTER 2

CHAPTER 3

CHAPTER 4

CHAPTER 1

INTRODUCTION

1.1 - Multiple Myeloma: Overview and History

Multiple Myeloma (MM) is a devastating hematologic cancer that remains largely incurable despite progressive advancements in disease management over the last several decades [1]. MM is the second most common hematologic cancer in the United States that has over 30,000 new cases each year and accounts for about two percent of all cancer deaths [2,3]. MM has a higher incidence among males and is primarily a disease of the elderly with a median age at diagnosis of roughly 70 years [3].

While MM has arguably been present for centuries [4], the first reports of MM date back to the late 19th century where ovular cells bearing prominent nuclei were observes in patients with “soft bones” [5]. It was later observed that these patients had an unusual urinary proteins that were then referred to as Bence Jones proteins named after their discoverer [6]. Today we know Bence Jones proteins as the immunoglobulin light chains produced by overabundant antibody-producing plasma cells [7]. The quantification of these overabundant paraproteins, known as an “M-spike”, is still used today to diagnose and monitor MM through all stages of the disease [8,9]. The term “multiple myeloma” first appeared in J.V. Rustizky’s 1873 description of eight bone tumors identified in one post-mortem patient [10]. However, it was not until 1900 that the above characteristics were fully appreciated to embody our current understanding of MM [11].

Today MM is defined as a lymphoid neoplasm characterized by clonal expansion of malignant post-germinal-center B-cell-derived plasma cells within the bone marrow compartment [2]. Clinically, this disease is characterized by several well-characterized symptoms [12]. The increasing burden of antibody-producing plasma cells in the bone marrow elevates serum Ig levels, which can directly lead to renal impairment/failure [13]. The presence of osteolytic bone lesions in MM is caused by an aberrant increase in osteoclast activity and a concomitant decrease in osteoblast activity induced through interaction with MM cells [14,15]. Bone resorption leads to the release of calcium into circulation leading to hypercalcemia [16]. Immunodeficiency is

also a common symptom of MM and in late stages of the disease the inability to combat additional illnesses can be the fatal attribute [12].

1.2 - Myeloma Biology: Lymphoid Differentiation, Myeloma Etiology and Stages of Disease

MM is a disease characterized by the malignant proliferation of antibody-producing plasma cells in the bone marrow. Understanding the biological origins of MM is predicated on an understanding of how plasma cells develop from their lymphoid progenitors. The human immune system is a constantly changing network of diverse cell types that coordinate to recognize foreign antigens and target them for removal from the host. Producing cells that express receptors and antibodies that are conjugated specifically to foreign antigens is a complicated developmental process that tightly regulates a balance between positive and negative selection. This persistent state of proliferation and selection throughout lymphoid development can, over time, present a myriad of opportunities for the acquisition of genetic aberrations. Under the right conditions these aberrations can lead to undue proliferation and result in the development of one of many lymphoid neoplasms distinguished by their genetic/epigenetic landscape and stage of lymphoid differentiation.

1.2.1 – Lymphoid Differentiation and the Origins of Lymphoid Neoplasms

The developmental path towards a malignant plasma cell (**Figure 1**) begins in the bone marrow with a multi-potent lymphoid progenitor stem cell population [17–20]. Commitment to the lymphoid lineage can produce several essential effectors of the immune system (B, T and natural killer cells) that progress through subsequent stages of maturation to produce and enhance antigen specificity [21]. The developmental process of establishing and refining B cell antigen specificity is achieved through the controlled multi-step rearrangement of the genomic loci encoding immunoglobulin chains [22]. Rearrangements of these loci will produce genes that encode peptides with unique antigen binding regions that can then be further altered (e.g. mutations) and selected for specificity. While these genomic modifications are generally restricted to specific loci, aberrant modifications can occur on other genes at several stages.

Figure 1: MM etiology and progression within the stages lymphoid differentiation

A simplified schematic of B-cell development and the initiation/progression of MM. Linear differentiation of the B-cell lineage from a common lymphoid progenitor to the terminal developmental stage: long-lived plasma cells expressing high-affinity antibodies. Aberrant genomic lesions (i.e. mutations and translocations) are produced during clonal expansion/selection in the germinal center via somatic hypermutation and class-switch recombination errors. These lesions may persist in long-lived plasma cells that return to the bone marrow microenvironment, elevating their proliferative capacity. Continued growth permits acquisition of additional oncogenic lesions that results in a progressive increase in monoclonal plasma cell burden in the bone marrow and a concomitant increase in serum Ig. Accumulation of genomic lesions promotes branching sub-clonal diversification and competition for the bone marrow micro-environment progressively selects more aggressive growth. Pre-malignant phases of disease (smoldering MM and MGUS) precede presentation of disease symptoms that characterize fully malignant MM. The terminal developmental stage of disease, plasma cell leukemia, is characterized by bone-marrow-independent growth in the host.

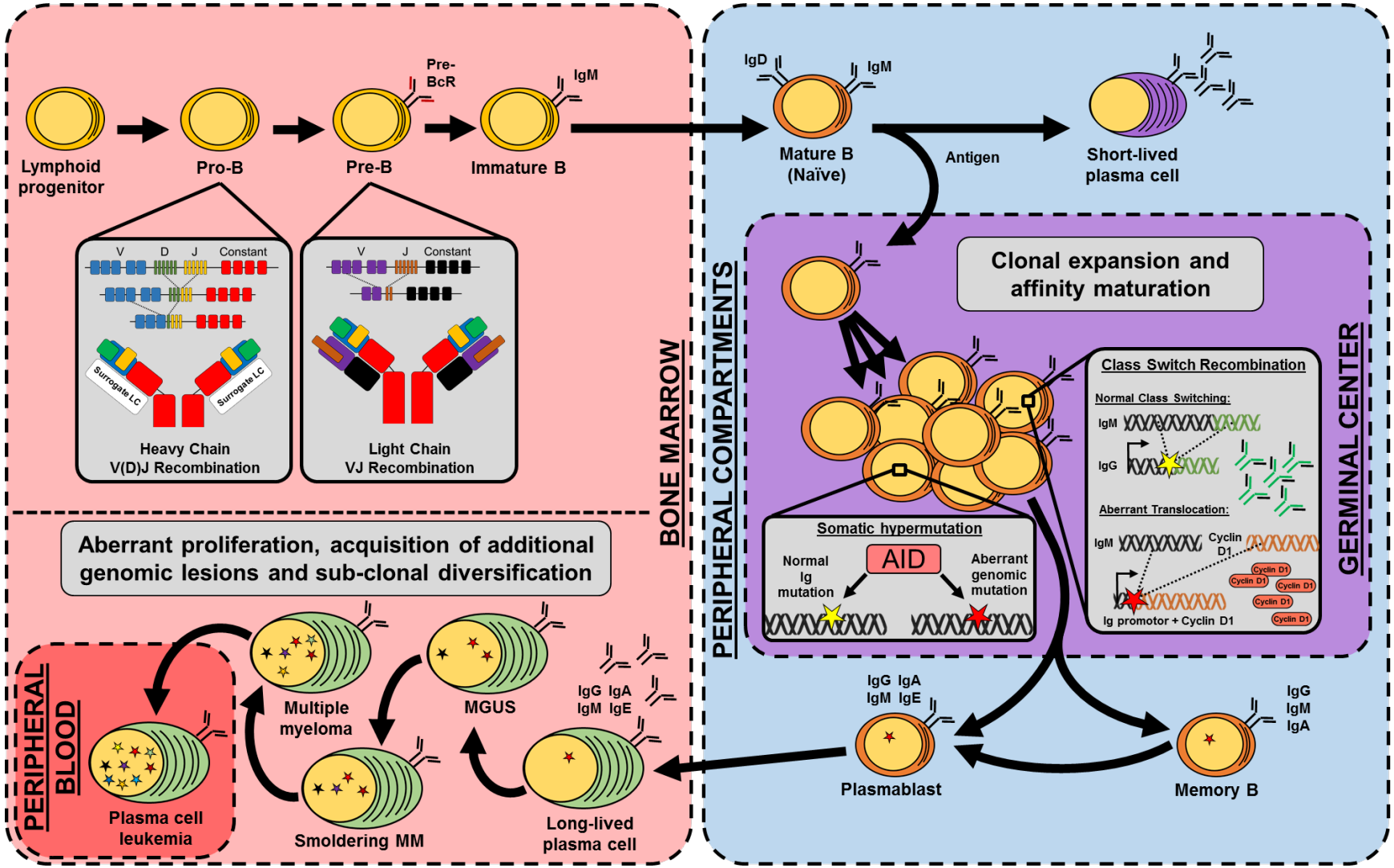
BONE MARROW
PERIPHERAL COMPARTMENTS
GERMINAL CENTER
PERIPHERAL BLOOD
Lymphoid progenitor
Pro-B
Pre-B
Pre-BcR
Immature B
IgM
V D J Constant
Surrogate LC
Surrogate LC
Heavy Chain V(D)J Recombination
V J Constant
Light Chain VJ Recombination
IgD
IgM
Mature B (Naïve)
Antigen
Short-lived plasma cell
Clonal expansion and affinity maturation
Class Switch Recombination
Normal Class Switching:
IgM
IgG
Aberrant Translocation:
IgM
Cyclin D1
Ig promotor + Cyclin D1
Somatic hypermutation
Normal Ig mutation
AID
Aberrant genomic mutation
Aberrant proliferation, acquisition of additional genomic lesions and sub-clonal diversification
Multiple myeloma
MGUS
Smoldering MM
Plasma cell leukemia
Long-lived plasma cell
IgG IgA IgM IgE
Plasmablast
Memory B
IgG IgM IgA

The process of establishing antigen specificity within the B cell linage begins with the pro-B cell stage of development [22]. Pro-B cells undergo recombination between the variable (V), diversity (D) and joining (J) regions of the immunoglobulin heavy chain locus (IgH) [23]. Completion of this process, termed V(D)J recombination, and the subsequent expression of Pax5 defines commitment to the B-cell lineage. Expression of the successfully recombined heavy chain in concert with a surrogate light chain forms the pre-B-cell-receptor (pre-BCR) complex. Pre-BCR establishment halts additional IgH recombination and promotes allelic exclusion to restrict pre-BCR complexes to the recognition of a single potential antigen.

The next stage of B cell development, the pre-B cell stage, initiates recombination of the Ig light chain locus. Similar to IgH V(D)J recombination in the previous stage, the light chain undergoes recombination between V and J regions. Successful rearrangement and expression of the light chain complexes with the heavy chain to produce IgM. Expression of IgM at the cell surface signifies the successful transition into the immature B cell. Immature B cells undergo selection where cells that recognize self-antigens and cannot persist outside the bone marrow microenvironment are negatively selected [24].

Positive selection for bone-marrow independence allows immature B cells to leave the bone marrow and become mature (naïve) B cells distinguished by cell surface expression of both IgM and IgD. Mature B cells enter the follicles of the spleen and lymph nodes as follicular B cells where they can become activated [22]. T-cell-independent activation of follicular B cells via exposure to antigen drives differentiation into short-lived plasma cells that secrete low affinity antibodies as part of a short lived immune response. Antigen activation of follicular B cells facilitated by T cells drives follicular B cells into the germinal center (GC) where they undergo further affinity maturation as part of establishing a long-term immune response [22].

Many opportunities for oncogenesis are present during the stages of genomic modification in B cell differentiation stages preceding activation of follicular B cells. Genomic lesions established during these stages can eventually manifest as MM, however, this can also

represent the origin for other lymphoid neoplasms including acute lymphoblastic leukemia, chronic lymphocytic leukemia, mantle cell lymphoma and mantle zone lymphoma [17].

In the GC, follicular B cells transition into GC B cells which undergo expansion and selection aimed at increasing antigen affinity [22]. GC B cells express the mutagenic enzyme activated-induced cytidine deaminase (AID) that is targeted to the V region of the heavy chain. At that locus AID mutagenesis increases diversity to allow further selection for enhanced antigen specificity in a process called somatic hyper mutation (SHM). Following SHM and matured specification AID also directs isotype switching from IgM to IgG or IgA. This process is referred to as class-switch recombination (CSR).

In the normal, non-pathogenic progression of the lymphoid lineage (i.e. sans aberrant genomic lesions) GC B cells that have high-affinity B cell receptors survive negative selection and are resigned to two fates as they exit the GC environment. A minority population of these GC B cells become long-lived non-secretory B-cells that are responsible for maintaining long-term recognition of antigens by the host immune system [25]. The remaining majority of these post-GC B cells differentiate into plasmablasts. Plasmablasts are an intermediate stage of differentiation between GC B cells and terminally differentiated plasma cells [26,27]. They initially maintain their highly proliferative GC behavior driven in part by BCL-6/PAX-5 repression of the plasma cell genes XBP-1 and BLIMP-1. Gradually, these intermediate plasmablasts begin adopting a transcriptomic profile consistent with mature plasma cells by elevating expression of IRF4 and NF-κB. This in turn represses BCL-6 and PAX-5 while enhancing Ig secretion, morphological changes and expression of XBP-1/BLIMP-1 [28]. BLIMP-1 in particular is considered a master regulator of plasma cell differentiation and its expression allows plasma cells to leave the lymph nodes and return to the bone marrow as long-lived plasma cells [29]. These terminally differentiated lymphoid cells reside in the bone marrow as non-dividing, Ig-secreting facilitators of the sustained immune response to foreign antigens [30].

1.2.2 – Multiple Myeloma: Pre-malignant Stages and Disease Progression

As outlined above, establishing and selecting for high affinity immunoglobulins is an essential process for the adaptive immune system. However, accomplishing robust

receptor/antibody diversity requires several stages of precise genomic modification, which, when executed erroneously, can set the stage for oncogenic transformation. As with V(D)J recombination, SHM and CSR present additional opportunities for aberrant genomic modification. The specific context of these aberrations and the stage at which they result in uncontrolled growth distinguishes several lymphoid malignancies that can arise from SHM and CSR. Follicular lymphoma, Burkitt lymphoma and diffuse large B cell lymphoma are thought to originate directly from GC B cells while Waldenström's macroglobulinemia and MM are thought to be derived from the post-GC B cell lineage [17]. With respect to MM, evidence has accumulated to implicate founding aberrations that have SHM/CSR signatures (e.g. IgH translocations at the switch locus) while the clonal nature of malignant plasma cell Ig's indicates a post-GC (post-affinity maturation/selection) origin [31–34]. This suggests that while the founding genetic events that result in MM occur in developmental stages well upstream of terminal differentiation.

MM originates from long-lived plasma cells residing in the bone marrow, however, malignant transformation is not an immediate consequence of terminal differentiation for cells harboring genomic lesions as discussed above. Rather, MM is thought to develop gradually the a series of pre-malignant stages that have specific clinical definitions [1]. Monoclonal gammopathy of undetermined significance (MGUS) is present in about 1% of adults over the age of 25 and has a roughly 1% chance per year of advancing to MM [35–37]. MGUS is diagnosed/monitored via serum Ig levels, lacks symptoms of end-organ damage associated with MM and is defined by a clonal bone marrow plasma cell burden below 10% [9]. MGUS often goes undiagnosed prior to progression in MM and the value of treating the disorder in light of low risk for progression remains an ongoing debate. Smoldering MM similarly lacks symptoms of end-organ damage and has a bone marrow plasma cell burden below 10%. Smoldering MM is distinct from MGUS in that is presents a higher serum monoclonal protein levels (≥3gm/dL) and has a much higher risk of progression to MM (~10% per year) [9,38]. Malignancy and the designation of MM is finally established as symptoms of end-organ damage (described above) appear and the plasma cell burden in the bone marrow exceeds 10% [1]. MM continues to persist in the bone marrow, however once bone marrow independence occurs and malignant plasma cells proliferate in the

peripheral blood, the disease has progressed to the exceptionally aggressive terminal stage: plasma cell leukemia [39].

The etiology of MM is established during the complex progression of B-cell development where a great diversity of founding genetic aberrations can be acquired and maintained through terminal differentiation. These diverse origins result in a diverse and complex disease that is equally diverse and complex in patients.

1.3 - The Genetic Landscape of Myeloma

MM is a highly heterogeneous disease. As described above, MM is distinct from other GC-based malignancies in that founding genetic lesions are not sufficient to dive malignant transformation but rather several additional abnormalities must be acquired after terminal differentiation. The genomic landscape of MM varies greatly from patient to patient due, in part, to the diverse set of initial genomic abnormalities that establish pre-malignancy. This heterogeneity is further exacerbated by genomic instability that continues throughout disease progression and persistent competition for the bone marrow microenvironment that maintains branching sub-clonal evolution within any individual case of MM [40,41].

The advent of several modern sequencing technologies and their application to large cohort studies has provided a large body of knowledge regarding the clonal and sub-clonal heterogeneity present in MM [40,42–48]. A great many genomic abnormalities have been identified in MM (**Table 1**). Among them, several have notable reoccurrence. Dissecting the wealth of genomic data available from numerous cases of MM reveals some genomic lesions that display clear characteristics of being founding events while others seem to more frequently accumulate during disease progression with less clear contribution. This dichotomy between early and late genomic lesions is more commonly referred to as ‘driver’ and ‘passenger’ events where drivers initiate/facilitate malignant proliferation and passengers accumulate due to persistent genomic instability. Characterizing all of the many reoccurring genetic abnormalities provides invaluable insights towards understanding the biology underlying MM’s ability to progress and evade therapy.

1.3.1 – Chromosomal Abnormalities

Chromosomal abnormalities are a classic hallmark of MM genomics. Such chromosomal abnormalities generally fall into two categories: hyperdiploidy found in 50% of patients and translocations on chromosome 14 with the IgH locus found in 45% of patients (distinguished as hyperdiploid or non-hyperdiploid MM) [49]. 10% bear both types and only 5% of patients have neither [49]. Acquisition of either of these abnormalities is considered a founding or initiating event in MM and their diverse effects on disease biology can have prognostic implications for therapy [49].

In non-hyperdiploid MM IgH translocations arise from either V(D)J recombination or SHM/CSR where double stranded DNA breaks at the IgH locus (Chr. 14q32) are aberrantly repaired through recombination with distant loci. The IgH gene is expressed after a strong promotor. When this promotor is translocated in front of a proto-oncogene, expression of that gene can be enhanced well beyond its normal level. The most common IgH translocations in MM all act in this way. In some cases this rapidly promotes malignant transformation as with IgH-MYC translocations observed in Burkitt lymphoma [50]. In MM, however, IgH translocations do not promote full transformation until after terminal differentiation and the acquisition of additional abnormalities ('second hits').

Common IgH translocations in MM include t(4;14), t(6;14), t(11;14), t(14;16) and t(12;20). In many of these cases cyclin D proteins are over expressed, promoting undue progression through the G1-S checkpoint of cell cycle regulation [51]. The most common translocation, t(11;14), occurs between 14q32 and 11q13 (in 15-20% of patients) and drives over expression of CCND1 (cyclin D1). Other cyclin D overexpressing translocations include t(6;14)(q21:q32)(cyclin D3) and t(12;14)(cyclin D2). Translocations t(14;16) and t(14;20) indirectly upregulate cyclin D2 by directly overexpressing c-MAF and MAFB respectively.

Other common translocations also drive expression of non-cyclin proteins. Translocation t(4;14), an indicator of poor prognosis, overexpresses MMSET (an epigenetic regulator discussed in more detail below) and FGFR3 (a receptor tyrosine kinase). Translocation t(6;14)(p25;q32) overexpresses IRF4 (a transcription factor significant for plasma cell differentiation).

Table 1: The most frequent genomic abnormalities observed in myeloma

Type of Genomic Lesion		Genomic Lesion(s)	Notable Genes or Processes Affected	MM Frequency or Notes
Primary Founding Events	**IgH Translocations (Non-hyperdiploid): 50% of MM cases** [48]	t(4;14)	MMSET & FGFR3	
		t(6;14)(q21;q32)	CCND3	
		t(6;14)(p25;q32)	IRF4	
		t(11;14)	CCND1	15-20%
		t(14;16)	c-MAF	
		t(12;20)	MAFB	
		t(12;14)	CCND2	
	Hyperdiploidy: 45% of MM cases [48]	Gain of odd numbered chromosomes: 3,5,7,9,11,15,19,21		Better prognosis than non-hyperdiploid
Secondary Events	**Secondary translocations** [48]	Translocations between MYC and strong promotors (e.g. IGH,IGL,IGK, FAM46C, FOXO3 or BMP6)	MYC	More prevalent in late-stage disease
	Common copy number variations [48]	Large gain of chromosome regions: 1q, 3, 5, 6p, 7, 9, 11q, 15, 18, 19, 21		
		Large loss of regions on chromosomes: 1q, 6p, 8,12, 13,14,16, 17p, 20 and 22	1q loss (30% of cases) removes FAM46C, CDKN2C and FAF1	17p loss removes TP53 in aggressive MM
		Focal Gain: 1q22, 2p14, 3p24.3, 3q26.2, 5q35.2,6p24.3, 7q22.1, 8q24.2, 9q34.13, 11q13.2, 12q34.21, 15q24.2, 17q23.2, 19p13.2, 20q11.22 and 22q13.1	1q22 minimally contains 679 genes including CKS1B and ANP23E	
		Focal loss: 1p21.3, 4p15.31, 4q13.1, 6q25.3, 7q11.22, 8p22, 9p24.1, 10q24.33, 12p13.1, 12q21.33, 13q21.33, 14q32.32 and 16p13.3		
	Most frequent somatic mutations [40,42,52]	KRAS	RAS/MAPK pathway	20-21%
		NRAS	RAS/MAPK pathway	19-20%
		FAM46C	Unknown	6-10%
		BRAF	RAS/MAPK pathway	7-12%
		TP53	DNA damage	3-12%
		DIS3	RNA stability	1-9%
		PRDM1	B cell development	<5%
		SP140	JAK/STAT signaling	4-6%
		EGR1	Transcription Factor	4-6%
		TRAF3	NF-κB signaling	2-5%
		ATM	DNA repair	3-4%
		CCND1	Cell cycle	2-4%
		HISTH1E	Histone 1	<3%
		LTB	NF-κB signaling	1-4%
		IRF4	B cell development	<3%
		FGFR3	RAS/MAPK pathway	<3%
		RB1	Cell cycle	<3%
		ACTG1	Cytoskeleton	<2%
		CYLD	Cell cycle	1-2%
		MAX	MYC regulation	<2%
		ATR	DNA repair	<1%

Hyperdiploidy is abundantly present in MM where affected patients generally have a better prognosis than patients with IgH translocations [49]. Chromosome copy number abnormalities seem to generally effect odd numbered chromosomes (3,5,7,9,11,15,19 and 21) and can produce chromosome numbers below 48 (hypodiploid) and as high as 74 (near-tetraploid) [53]. These karyotypic abnormalities appear to remain static throughout disease progression in most cases [54]. The specific mechanisms that cause these founding events remain less well understood than the mechanisms that produce IgH translocations. Current theories regarding the origin of abnormal karyotypes include mitotic errors [53].

While the IgH translocations and karyotypic abnormalities outlined above represent common primary events in the establishment of pre-malignancy, many secondary translocations produced through persisting genomic instability have been well characterized at disease diagnosis and relapse. A prime example of this is the proto-oncogene MYC which is translocated in 3-4% of MGUS/smoldering MM patients and 15-20% in newly diagnosed MM patients [55]. These translocations often occur with Ig-encoding genes IGH, IGL and IGK and other genes with strong promotors including FAM46C, FOXO3 and BMP6 [48].

Copy-number variations (CNVs) represent an additional class of frequent MM chromosomal abnormality that can span from small focal deletions/duplications to events effecting entire chromosome arms [56]. There are many documented CNVs and some regions appear to be affected more frequently than others [1,49,56]. For example, gain/amplification of 1q21 has been observed to minimally contain 679 genes including several oncogenes such as CKS1B and ANP23E. Deletions of the short arm of chromosome 1 (most often 1p12 or 1p32) occur in 30% of MM patients. This region contains several important tumor suppressors including FAM46C (protein translation), CDKN2C (cell cycle) and FAF1 (apoptosis). Deletion 17p, which removes the classic tumor suppressor TP53, can be present in roughly 10% newly diagnosed MM and up to 80% relapsed MM. Deletion 13q occurs in 40-50% of MM patients (more commonly in IgH translocated MM) where minimal loss includes the tumor suppressor RB1.

1.3.2 – Somatic Mutations

Acquisition of multiple oncogenic mutations is a hallmark of all cancers and MM is no exception. Several recent massive parallel sequencing studies have cataloged a large number of reoccurring mutations in MM [40,42,44,47]. Oncogenic mutations are generally (but not exclusively) divided into two categories: gain-of-function mutations that constitutively activate pro-growth signaling and loss-of-function mutations that suppress or abrogate tumor suppressor functions.

Among the genes identified in sequencing studies are KRAS and NRAS which harbor gain-of-function mutations in MM (~20% each). KRAS/NRAS mutations are found in many cancer types and are well characterized for constitutively promoting growth through the RAS/MAPK signaling cascade. BRAF gain-of-function mutations are less common (6-12% of cases) but also act through the RAS/MAPK pathway. Together, KRAS, NRAS and BRAFF somatic mutations occur in about 40% of MM cases [48]. Despite being the most commonly mutated genes KRAS,NRAS and BRAF in MM, sub-clonal analysis has revealed that these mutations (mean cancer clonal fractions at ~30%) are unlikely to represent founding events but rather contribute to progression as secondary lesions [44].

Several important tumor suppressors, many of which are also frequently reduced via recurring CNVs in MM, harbor recurring loss-of-function mutations. These include TP53(3-12%), RB1(2-3%), PTEN, CDKN2C and CDKN2A [1,40,44].

Network analysis performed on recurringly mutated genes has also elucidated several pathways that are biologically significant for MM. For example, the NF-κB pathway is a significant proliferation-promoting signaling pathway for MM and several genes with important functions in this pathway are frequently mutated including TRAF3 (2-5%), CYLD(1-5%), MAP3K14, BIRC2, BIRC3, IKBKB and others [1,40,44].

Several genes encoding epigenetic modifiers are also frequently mutated in MM [57–60]. This subject is discussed below.

1.4 – The Epigenetic Landscape of Myeloma: Characteristics and Therapeutic Strategies

The scientific community has long sought to understand the myriad of mechanisms malignant cells exploit to escape the homeostatic mechanisms that block overproliferation and evade eradication by the host immune system and therapy. Mutations and chromosomal abnormalities have been understood to drive cancer progression, yet exhaustive efforts to characterize cancer genomes have yet to provide a full picture of cancer biology. In recent decades, a growing understanding of epigenetics has fomented a new and important area of cancer research. Epigenetics, the sum total of all regulatory control of gene expression, is facilitated by several increasingly understood mechanisms including chemical modifications to DNA, post-translation histone modifications, histone composition/deposition and non-coding RNAs. A surge of interest in understanding cancer epigenetics has prompted the development of many compounds and strategies to study and target epigenetic mechanisms. It is now widely accepted that epigenetic abnormalities are abundantly present in cancer and are critically important for oncogenesis and disease progression. MM is no exception [57–60] (**Table 2**). As with other cancers, therapeutic strategies that target and exploit the epigenome have gained immense momentum in recent years. This has prompted many recent studies that have begun to elucidate the highly complex landscape of the myeloma epigenome.

1.4.1 – DNA Methylation

DNA methylation is one of the longest studied epigenetic mechanisms [61]. DNA methylation occurs at CpG sites (cytosine and guanine nucleotide pairs, in that order) where a methyl group is covalently added at the carbon-5 position of cytosine (5mC). This modification is predominantly restricted to intronic and intragenic CpG sites in healthy cells. In pathological contexts, large CpG clusters adjacent to transcription start sites, termed CpG islands (CPGIs), can be methylated to repress transcription initiation at the transcription start sites of adjacent genes. DNA methylation and demethylation is facilitated by DNA methyltransferases (DNMT1, DNMT3A and DNMT3B) and the TET protein family (TET1, TET2 and TET3) respectively. DNMT1 and DNMT3A are responsible for *de novo* DNA methylation while DNMT1 maintains DNA methylation after DNA replication. DNA-methylation was originally described to be a permanent genomic modification, however recent descriptions of demethylation via TET-induced base-

excision repair casts doubt on global 5mC permanency. DNA methylation is an important control mechanism that has rolls in differentiation, tissue specific gene expression, X-chromosome inactivation, silencing of transposable elements and genomic imprinting [61].

Many studies have attempted to characterize DNA methylation differences between heathy malignant cell types including healthy/malignant plasma cells. In some cases bisulfite sequencing has been used to measure global DNA methylation (the methylome).Generally, abnormalities in DNA methylation drive cancer progression through global hypomethylation and hypermethylation of tumor suppressor gene promotors [62]. In MM, several studies suggest that promotor hypermethylation indeed occurs at known tumor suppressor gene promotors and furthermore global hypomethylation/promotor hypermathylation gradually increases through the pre-malignant stages of MM, peaking in plasma cell leukemia [63–67]. Effected tumor suppressors are enriched in critical pathways/processes including cell cycle, DNA repair, apoptosis and important signaling cascades [58]. Promotor hypermethylation of SOCS-1 and DAPK have been reported to be early drivers of MM pathogenesis [65]. Interestingly, in a few cases hypomethylation of oncogene promotors (e.g. JAG2) has also been implicated as pathogenic in MM [68].

DNA methylation is also thought to contribute to MM progression by regulating other epigenetic mechanisms. Hypermethylation has been demonstrated to restrict the expression of tumor suppressor microRNAs, which can be reversed by inhibitors of DNA methylation (i.e. 5-azacytadine) [69–71]. It is also clear that DNA methylation and histone modifications share a regulatory relationship [62,72]. For example, DNA methylation seems to co-localize with loci harboring the repressive histone modification H3K27me3 (tri-methylated histone 3 lysine 27) and disruption of DNA methylation dramatically alters global H3K27me3 localization [72,73].

Somatic mutations in DNA methylation modifiers have been reported. A recent study examining whole exomes of 463 MM patients enrolled in the UK NCRI Myeloma XI study found that about 4% of those patients harbored a somatic mutations in DNA methylation modifiers [74]. Among those genes are TET1, TET2, TET3, DNMT1, DNMT3A, DNMT3B, IDH1 and IDH2. Mutations in DNMTs and TETs directly affect DNA methylation and demethylation respectively.

Table 2: Common epigenetic abnormalities in MM

Type of Abnormality		Sub-category	Notes or examples	
DNA Methylation [61,63,65,67]	**Global DNA methylation**		Decreases gradually through disease progression	Mutations frequent in writers (DNMT1/3A/3B), erasers (TET1/2/3) and indirect regulators (IDH1/2).
	Promotor CpG island methylation	**Hypermethylation**	Increases gradually through disease progression	
		Hypomethylation	Rare examples (e.g. JAG2)	
Non-coding RNAs [58,75–77]	**microRNAs**	**microRNA processing**	DICER mutations	Represses global microRNA levels
		Downregulated microRNAs	Targeting oncogenes:	miR-21/181a/106b-cluster (PTEN, BIM,p21 and PCAF) miR221/222 cluster (p27kip1, PTEN, PUMA and pKip2)
		Upregulated microRNAs	Targeting tumor suppressors:	Example tumors suppressors: CCND1, CCND2, NF-κB and AKT3
	Long non-coding RNAs		Very few MM-specific studies	MALAT1 overexpression
Chromatin [58,60]	**Chromatin remodeling**	**SWI/SNF complex**	Mutations in CHD2 and CHD4	SWI/SNF and NuRD complex members are affected by CNVs in ~40% of MM cases
		NuRD complex	Mutations in ARID1A/4A/5B	
	Histones		Recurrent HIST1H1B-E mutations	Low frequency of core histone mutations in MM
	Histone tail post-translational modifications	**Histone acetyl transferases**	Recurring mutations in EP300 and CREBBP	CREBBP mutations are particularly enriched in relapsed MM
		Histone deacetylases	Overexpression of HDAC1/2/3/6	HDAC6 counteracts proteasome inhibitors by facilitating lysosomal clearance of aggresomes
		Histone methyl transferases	MMSET (H3K36me2)	Overexpressed in t(4;14) MM or mutated (gain-of-function)
			EZH2 (H3K27me3)	Overexpressed in most cases of MM
			G9a (H3K9me3)	Overexpressed in MM
			GLP (H3K9me3)	Overexpressed in MM
			NSD1 (H3K36me2)	mutated (gain-of-function)
		Histone de-methylases	UTX/KDM6A (H3K27me3)	Mutated (loss-of-function)
			KDM3A/B (H3K9me3)	Upregulation drives IRF-4 and KLF-2 expression

IDH1/2 (Isocitrate dehydrogenases 1 and 2) loss of functions lead to aberrant buildup of 2-hydroxyglutarate, which is known to inhibit DNA demethylases (alpha-ketoglutarate dependent dioxygenases) [78].

Somatic mutations in these genes may explain abnormal methylomes observed in some cases of MM but fails to explain the broader prevalence of aberrant DNA methylation in MM. The regulatory contexts and mechanisms that govern changes in DNA methylation during the initiation and progression of MM are largely unknown and the broader mechanisms that control global methylation patters have yet to be fully elucidated. Given known protein-protein interactions between epigenetic-regulating protein complexes and other accumulating evidence, is likely that regulators of DNA methylation act in concert with regulators of chromatin dynamics in a complex high-dimensional network that has only begun to be fully described [79].

It is clear that DNA methylation is an attractive therapeutic target for MM. Indeed, DNA methyltransferase inhibitors (DNMTi's) such as 5-azacytidine (AZA, Vidaza) and 2-deoxy-5-aza-cytidine (DAC, Decitabine, Dacogen) have been evaluated via *in vitro* and *in vivo* pre-clinical models of MM [80,81]. Furthermore, AZA has been evaluated for efficacy in cancers including MM in recent clinical trials (NCT00006019) and encouraging results have prompted the development of new more stable DNMTi's [82].

1.4.2 – Non-coding RNAs

Since the completion of the human genome project scientists have been fascinated by the expanse of the non-protein-coding segment of the genome (98% by sequence, when including 5'/3' untranslated transcript regions) [83]. Further study of these regions have revealed that this so-called 'junk DNA' has important functional significance and that many loci are actively transcribed to confer an entire regulatory network of functionally active non-translated (non-coding) RNAs [84,85]. Non-coding RNAs (ncRNAs) that have structural functions (e.g. tRNAs, rRNAs, snRNAs and uRNAs) have been well studied. Regulatory ncRNAs are relatively new discoveries. Here regulatory ncRNAs are split into two types: long non-coding RNAs (lncRNAs) and microRNAs.

MicroRNAs are small (~22nucleotide) ncRNAs that regulate the transcriptome post-transcriptionally. MicroRNAs hybridize to specific complimentary sequences in target mRNAs and either initiate their degradation or inhibit their translation [86]. MicroRNAs regulate a great number of biological functions [87] including many that have a high impact on cancer initiation and progression [88,89].

Several studies have characterized microRNA abnormalities in MM and found that they are unsurprisingly altered by the same epigenetic abnormalities and genomic lesions that affect coding genes (e.g. mutations, translocations and CNVs) [75,76,90–92]. Additionally it appears that genes that encode core components of the microRNA machinery (e.g. DICER) may also by aberrantly repressed through the progression of MM [93].

MicroRNAs contribute to MM progression in several ways [75,76,90–92]. Many miRNAs upregulated in MM target tumor suppressors to promote malignancy. For example miR-21, miR-181a and the miR-106b cluster are known to target PTEN, BIM, p21 and PCAF. The miR-221/222 cluster promotes MM growth by targeting p27kip1, PTEN, PUMA and p57kip2 [94]. Other microRNAs with tumor suppressor functions are underexpressed in MM. For example CCND2 mRNA (cyclin D2) is targeted by several miRNAs that are underexpressed in MM including miR-196b, miR-135b, miR-320, miR-20a, miR-19b, miR-19a and miR-15a [95]. Other downregulated miRNAs share oncogenic targets such as NF-κB, AKT3 and cyclin D1 [58].

LncRNAs, the most numerous and least understood class of ncRNAs, are regulatory transcripts that coordinate with transcription factors and co-transcriptional regulators to control gene expression [96]. Unlike microRNAs, the direct consequence of lncRNA regulation can be either enhancing or repressing depending on the context. Recent studies have begun to reveal numerous roles for lncRNA dysfunction in cancer [97–100].

Only a small number of studies have explicitly examined lncRNA dysregulation in MM, yet despite this, it is clear that this class of ncRNA is abnormally regulated in MM to a significant degree [101,102]. One recent study found that in a small number of newly diagnosed MM patient samples over 3000 lncRNAs were differentially expressed compared to non-malignant controls

[103]. As a specific example, lncRNA MALAT1 is overexpressed in MM and coordinates with the Sp1 transcription factor to positively regulate the TGF-β signaling pathway [104].

1.4.3 – Chromatin Organization and Histone Modifications

Transcriptional regulation in eukaryotes relies, in part, on regulating the accessibility and compaction of chromatin. The fundamental unit of chromatin, the nucleosome, comprises of a core histone (H2A, H2B, H3 and H4) octamer linked by histone H1 and wrapped twice by a total of 147bps of genomic DNA [105]. The human genome encodes for over 70 different histone proteins and composition/remodeling of nucleosomes is an increasingly appreciated facet of epigenetic control [106,107].

Core histones have accessible N-terminal tails that are substrates for post-translational modifications (PTMs) (methylation, acetylation, phosphorylation, sumoylation, citullination, biotinylation, ribosylation and ubiquitination) at arginine, lysine and serine residues [108]. Histone tail PTMs regulate several essential functions including higher-order chromatin organization/compaction, DNA damage repair, sequestration of epigenetic/co-regulatory complexes and regulation of transcription [109]. Specific and global changes in histone tail PTMs are important for controlling expression of critical genes during development, maintaining tissue-specific gene expression and regulating higher-order nuclear organization [109]. Histone PTMs also present a means for facilitating broader context-specific gene expression changes that govern higher order processes (e.g. halting proliferative ‘stemness’ after terminal differentiation).

The numerous permutations of nucleosome compositions and histone PTMs allows much more regulatory information to be stored laterally along genomic DNA than is possible to convey with chemical modifications (i.e. methylation) to genomic DNA [107,110]. This sum total of this regulatory information along the genome is referred to as the histone code. As seen between DNA methylation and histone modification, a large and poorly understood global network of crosstalk exists between different pathways that modify and coordinate with histone modifications [23,111]. Understanding how these pathways focally and globally coordinate while sensing endogenous/exogenous signals and regulating the composition/plasticity of the histone code remains an immensely challenging systems biology problem.

Chromatin had classically been thought to exist in one of two states: active euchromatin and inactive heterochromatin. This notion, however, is an oversimplified description of the high-dimensional complexity inherent in the histone code. Recent studies have updated our understanding of chromatin classes to include several more nuanced distinctions based on clustering of histone PTMs and occupancy of chromatin binding proteins [112,113]. This includes chromatin found at 'bivalent promotors' that is poised for activation [114,115].

Extracting functional significance from the histone code begins by understanding the characteristics inherent in histone PTMs where some generalities can be drawn [110]. For example, acetylation of histone tail lysine (K) residues and phosphorylation on histone tails is generally considered a mark of transcriptionally active chromatin (e.g. H3K27ac). Additionally, histone tails can be methylated at lysine or arginine residues, however, the consequence of this modification (e.g. activation via H3K4me3 or repression via H3K27me3) depends on the specific residue and broader chromatin context [116]. Modifications at specific residues are numerous and only partially functionally characterized. The latest release (2010) of the human histone modification database includes 43 location specific histone modifications in humans [117]. While context may dictate that not all permutations of these modifications appear in normal histone codes, the amount of information that can be conveyed with these modifications is immense.

Understanding how histone modification abnormalities arise in different cancers begins by identifying the source: histone modifying complexes [118]. Numerous histone modifications require equally numerous histone modifying proteins. According to HIstome, a histone infobase [108], there are currently 13 classes encompassing the roughly 150 known histone modifying enzymes. Proteins that regulate and modify histone PTMs generally fall into one of three broad classes: epigenetic readers, writers and erasers [119,120]. Epigenetic readers are proteins that bear structural domains that recognize and bind specific histone tail PTMs. Examples of histone readers include bromodomain (recognizes acetylated lysines) and chromodomain (recognize methylated lysines) proteins. Epigenetic writers and erasers are, as the monikers imply, enzymes that catalyze the addition and removal of histone PTMs. For example, regarding histone acetylation, histone acetyltransferases (HATs) are the writers and histone deacetylases (HDACs)

are the erasers. Many histone modifying enzymes also have or complex with proteins harboring reading domains, which establishes complex interactions between specific modifications and can also facilitate context-specific lateral elongation of certain histone modifications along the genome [111,119].

In MM many regulators/facilitators of histone modification are known to be abnormally regulated by or directly affected by genomic lesions [57–60,74,121].

Perhaps the most intuitively consequential drivers of histone dysfunction are somatic mutations in the genes that encode the histone proteins. Recent large scale sequencing efforts in MM have identified recurring mutations in HIST1H1B-E, a gene encoding the linker histone H1, at a frequency of up to 6% of cases examined [74]. Mutations in core histones were also detected, albeit at a much lower frequency. These histone H1 mutations were often missense mutations located in the DNA binding domain, which is suggested to be driver mutation in other B-cell malignancies [122,123]. How the disruption of nucleosome structural organization and chromatin dynamics drives malignancy remains largely unclear.

Processes that track genomic DNA, such as transcriptional activation, require structural adjustments of nucleosome occupancy. These events require large ATP-dependent dependent protein complexes known as chromatin remodeling complexes that represent another functional aspect of histone regulation. Two of these complexes, NuRD transcriptional repressive complex and SWI/SNF remodeling complex, have been found to have members that are frequently misregulated in MM [74]. NuRD members CHD2/CHD4(~2% each) and SWI/SNF members ARID1A(1.3%), ARID2(1.3%), ARID4A and ARID5B were shown to be recurrently mutated. SWI/SNF mutations in particular widespread among other forms of cancer with a frequency rivaling TP53 mutations [124]. Notably, mutations in SMARCA4 (a SWI/SNF complex member) are observed in a much higher proportion in cases of MM relapse, suggesting a potential role for driving aggressive disease and drug-resistance [74]. Considered together, NuRD and SWI/SNF complex members are affected by CNVs at a very high rate (~40%) in MM [74]. Chromatin remodeling is inherently much more difficult to study at a systems level than covalent modifications to DNA and histones. For this reason the full scope of how chromatin remodeling

contributes to epigenetic homeostasis remains elusive. Some mechanisms, such as an essential role in facilitating DNA damage repair, are thought to contribute to the oncogenic effects of abnormal chromatin remodeling [124]. Chromatin remodeling is a very attractive target for cancer therapy, however there are currently no therapeutic strategies that can specifically target these complexes.

Histone acetyltransferases (HATs) and deacetylases (HDACs) covalently deposit and remove acetyl groups to histone tail lysine residues [125]. Histone tail acetylation is generally considered to be a chromatin-activating modification. Transfer of acetyl groups from acetyl-CoA to lysine residues on histone tails by HATs neutralizes the highly positive charge of histones and thereby lowering the interaction with negatively charged genomic DNA and de-condensing chromatin. HDACs are a diverse family of enzymes that canonically catalyze the removal of acetyl groups from histone tails [126,127]. There are a total of 18 HDACs divided into four classes based on structural similarity to yeast homologs and sub-cellular localization. Class I, II and IV HDACs are considered the 'classical HDACs' that are zinc-dependent. Class III HDACs on the other hand are known as sirtuins; a family of NAD^+-dependent enzymes that are insensitive to HDAC inhibitors (HDACi's). HDACs lack inherent DNA binding and therefore require coordination with other proteins (e.g. transcription factors) to access and modify DNA. Class I HDACs, consisting of HDAC1, HDAC2, HDAC3 and HDAC8, are ubiquitously expressed, exclusively nuclear HDACs that are responsible for canonical removal of acetyl groups from histone tails. Class II HDACs have limited tissue specific expression and are subdivided into class IIa (HDAC4, HDAC5, HDAC7 and HDAC9) and clad IIb (HDAC6 and HDAC10). Class IIa HDACs can, under the control of regulatory kinases, shuttle between the nucleus and the cytoplasm; a process that governs the non-canonical acetylation of non-histone substrates [127]. Interestingly, this class of HDACs have low catalytic activity that appears to be dispensable for repression of gene expression [127]. Class IIb HDACs are exclusively cytoplasmic, where HDAC6 is the main cytoplasmic deaminase in mammalian cells and very little is known about HDAC10. HDAC6 (unique among HDACs for its two catalytic domains and C-terminal zinc finger) has several known deacetylation targets including cytoskeletal proteins, transmembrane proteins and

chaperones. Class IV of HDACs consists only of HDAC11, about which very little is known beyond its limited tissue-specific expression and cytoplasmic sub-cellular localization [127].

Both HATs and HDACs have described dysregulation in MM. Mutations in genes encoding the HATs EP300 and CREBBP have been described in MM [74] and other B-cell malignancies [128]. Abnormalities in CREBBP are particularly enriched in relapsed MM, suggesting possible impact on drug resistance [74]. Several HDACs including HDAC1, HDAC2, HDAC3 and HDAC6 have been reported to be overexpressed in MM and confer a poor prognosis [129]. The specific targets of MM expressing HDACs/HATs and how they promote disease progression are not certain since these regulators target thousands of genes and thousands of non-histone targets [130]. Many of the known nuclear HDAC/HAT targets are associated with MM pathogenesis including p53, HSP90, NF-κB, RUNX3, STAT-3, E2F1 and MYC [131]. HDAC6 has gained particular interest as a target in MM due to its role in facilitating aggresomal clearance through the lysosome. Inhibiting this process is thought to block a path for MM cells to escape aggresomal buildup generated from proteasome inhibition, a standard-of-care therapy for MM discussed more extensively below. Synergy between HDAC inhibition and proteasome inhibitors has been observed in pre-clinical models of MM [132,133].

Accumulating evidence supporting HDACs as attractive drug-able targets for MM, especially in combination with proteasome inhibition, prompted several clinical evaluations of HDACi's in MM [121]. Panobinostat (Farydak), a pan HDAC inhibitor, demonstrated significant (albeit modest) enhancement of response and prompted the recent FDA approval of panobinostat for patients who have received at least two previous regimens [134–136].

Histone methylation is more complicated that histone acetylation as the functional consequence of methylation can be either repressive or enhancing [120]. Histone lysine methylation was first reported to be involved in transcriptional regulation in the 1960s [137], however it was not until after the turn of the century that the first histone methyltransferase (HMT), SUV39H1, was identified [138]. The catalytic SET domain identified in this first HMT lead to homology searches that illuminated many more HMTs. Turnover of histone lysine methylation was presumed to be extremely slow until the first histone demethylase, LSD1, was discovered

and JmjC domains were described as a key identifying domain for that class of enzymes [139,140]. Histone methylation is unlike histone acetylation in that the controlled addition of one, two or three methyl groups to a lysine residue (mono-, di- and tri-methylated) does not change the electric charge of the amino acid side chain. Therefore histone lysine methylation does not directly affect nucleosome organization but rather serves as a signal for epigenetic readers [120]. Indeed, there are a significant number of domains that recognize these modifications including PHD, chromo, tudor, PWWP, WD40, BAH, ADD, ankyrin repeat, MBT and zn-CW domains [141].

The most well studied histone modifier in MM is so named: multiple myeloma SET domain (MMSET; also known as NSD2/WHSC1). MMSET is a HMT that is overexpressed in MM due to being placed proximal to the IgH strong promotor in t(4;14) translocations that occurs at a frequency of 15-20% [142]. MMSET overexpression directly leads to accumulated methylation of its target (H3K36me2). In other instances, particularly in relapsed MM, MMSET and NSD1 (a related HMT) harbor gain of function mutations that show elevation of H3K36me2 [121,143]. MMSET has also been repeatedly shown to be essential for DNA damage repair pathways. Additionally, cells that overexpress MMSET are exceptionally tolerant of DNA damage; a mechanism that may contribute directly to MM pathogenesis and resistance to chemotherapy [144]. MMSET regulation of transcription seems to modulate several oncogenic pathways that promote malignant progression in many forms of cancer [145]. Overexpression of MMSET has been shown to also have impacts on the global distribution of other histone modifications [146,147], suggesting that MMSET overexpression may lead to pleiotropic dysregulation of other epigenetic pathways. Lastly, MMSET has been shown to complex with the KAP1 corepressor and HDAC1/2 to repress the MYC-targeting microRNA miR-126 [148]. MMSET has long been considered a priority target in MM, especially in cases of t(4;14), however no compounds have been developed that specifically target MMSET.

Methylation of H3K9 is essential for the formation of heterochromatin where it occupies promotors of repressed genes and gene bodies of active genes. H3K9me3 is unique among repressive tri-methyl PTMs in that it occupies both silenced and active genes [149]. HMTs responsible for H3K9 methylation include SUV39H1, SUV39H2, G9a and GLP. Associated

demethylases include KDM3A, KDM3B and LSD1 [120]. Aberrant activity of both H3K9 HMTs and demethylases have been described for MM. Specifically G9a and GLP appear to be overexpressed in MM and KDM3A demethylation upregulates the oncogenic transcription factors IRF-4 and KLF-2 to sustain cell adhesion [150,151].

Tri-methylation of H3K27 is a well characterized repressive mark. Di- and tri-methylation of H3K27 is catalyzed by the HMTs EZH1 and EZH2, with EZH2 having a clear role in MM progression [58]. The relationship between aberrant EZH2 activity and MM progression is discussed extensively in a separate section below.

Further implicating an oncogenic role for H3K27me3, the H3K27 demethylase KDM6A/UTX harbors a recurring loss-of-function mutation in MM [152,153]. KDM6A/UTX complexes with a number of other histone modifying/remodeling complexes including H3K4 (activating) HMTs (KMT2, COMPASS family proteins, HATs (P300) and chromatin remodelers (SWI/SNF) to tightly couple the regulatory switch between chromatin activation (H3K4) and repression (H3K27) [58].

1.4.4 – EZH2 as a Potential Therapeutic Target in Myeloma

Enhancer of zeste homolog 2 (EZH2) is the HMT that catalyzes di- and tri-methylates histone 3 at lysine 27 (H3K27); a mark associated with repressed chromatin. EZH2 is the core catalytic subunit of the polycomb repressive complex 2 (PRC2) [154]. Polycomb complexes (PRC1 and PRC2) are named for the *Drosophila* mutant phenotype displaying improper body segmentation [155,156]. Unlike PRC2, which methylates H3K27, PRC1 monoubiquitylates H2AK119 via its core ubiquitin ligases RING1A and RING1B [154]. It was long thought that the two polycomb complexes interacted through hierarchical recruitment to chromatin, however this model has since been debunked [157].

PRC2 consists of a core catalytic subunit EZH21/EZH2 and additional complex members EED, SUZ12 and RbAp46/48 (also known as RBBP7/4). Unlike most SET-domain (methyltransferase) proteins that remain autonomously active, EZH2 adopts an auto-inhibited conformation when it is independent from its PRC2 partners (an obligate multimeric complex) [158]. EED contains WD-40 repeats that confer high-affinity binding to PCR2's own catalytic

product: H3K27me2/3. This feedback mechanism is thought to confer PRC2's ability to laterally propagate its chromatin modification along adjacent nucleosomes [158].

PRC2's global and focal localization to chromatin is known to be developmentally regulated, however the specific mechanisms that govern context-dependent localization remains elusive [158]. PRC2's affinity for other epigenetic complexes, methylated CpG islands and RNA (seemingly non-specific) have been described and may yet be revealed to play a role in the regulation of PRC2 [158].

EZH2 has also been recently characterized to have several non-canonical functions, broadening the scope of it's regulatory sphere of influence [159]. These non-canonical functions have a range of consequences, however they all ultimately act by regulating transcription. For example, EZH2 methylates transcription factors (i.e. RORα) at a methyl-degron domain. Methylation of the methyl degron sequesters the chromo-domain (monomethyl-lysine binding) harboring DCAF1/DDB1/CUL4 E3 ubiquitin ligase complex for ubiquitination and proteolytic degradation [160]. Another example of non-histone methylation targets includes the recent observation that EZH2 di-methylation of STAT3 at K49 activates IL-6 responsive transcription, an oncogenic pathway known to be exploited by MM [161]. Besides canonical and non-canonical methylation targets, EZH2 has also been recognized to have non-catalytic functions as a co-transcriptional regulator. Non-catalytic activity of EZH2 were first suggested through models demonstrating a growth advantage in cell lines overexpressing catalytic-null EZH2 [162]. Studies identifying more specific mechanisms have also recently highlighted non-catalytic rolls for EZH2 as a co-transcriptional regulator [163,164]. For example, in a breast cancer model EZH2 was also shown to act as a catalytic-independent co-activator of MYC and CCND1/2transcription by coordinating beta-catenin (Wnt pathway) and estrogen receptor alpha at gene promotors [163]. Finally, a novel non-catalytic function for EZH2 was recently described in mice where EZH2 binds and triggers the cleavage of RNA transcribed from B2 SINE retrotransposons in response to heat shock, freeing transcription of stress-response genes [165]. The mechanisms that direct or restrict EZH2 to certain targets remains generally unclear, however, one recent study has

proposed a specific phosphorylation modification on EZH2 may directs its activity towards non-catalytic co-transcriptional activation [166].

Canonically EZH2 is responsible for silencing gene transcription and has been associated with regulating thousands of genes [158]. EZH2 is considered a positive regulator of proliferation and 'stemness.' For example, it is critical for maintaining proliferative capacity during clonal expansion/affinity maturation of germinal center B cells and after which it is gradually silenced preceding terminal differentiation [167]. While the full scope of EZH2's regulatory impact is still unclear, it has become abundantly clear that EZH2 is aberrantly active in many forms of cancer. The first evidence for EZH2's significance in MM came from the observation that EZH2 is overexpressed in aggressive MM despite not being appreciably expressed in plasma cells from heathy donors [168,169]. Following this observation a previous member of our laboratory demonstrated that EZH2 expression is required for the proliferation of growth-factor-independent (IL-6 independent) human myeloma cell lines (HMCLs) harboring a RAS mutation [170]. By demonstrating that knock-down of EZH2 was sufficient to arrest MM cell line growth our laboratory was the first to demonstrate that EZH2 acts as an oncogene in MM. At the time of this observation no chemical inhibitors existed that specifically targeted EZH2 and therefore pre-clinical evaluation of EZH2 ceased.

Since our initial observation that EZH2 promotes MM growth and proliferation, corroborating evidence has continued to accumulate supporting EZH2 as a target in many cancers including MM [159,171–173]. Generally, EZH2 is thought to promote malignant proliferation by silencing expression of tumor suppressor genes [172]. Interest in the oncogenic properties of EZH2 have been of particular interest in lymphomas where an EZH2 suffers a recurring gain of function mutation at frequencies as high as 21% in diffuse large B cell lymphomas [174–176]. In cases of EZH2 gain-of-function mutation an enlargement of the catalytic pocket biases the catalytic activity of mutant EZH2 towards tri-methylation over di-methylation. This mutant allele always appears as a heterozygote as it requires unmodified EZH2 to populate histones with the di-mehtyl mark [177].

In MM several studies have presented additional lines of evidence that EZH2 is aberrantly active in MM [77,152,178–185]. One of the initial studies performed ChIP-seq assays (targeting H3K27me3) on MM patient samples and cell lines. This study observed that genes marked by H3K27me3 were highly enriched within the profile of underexpressed genes in MM. Furthermore, applying a non-specific methyltransferase inhibitor 3-Deazaneplanocin (DZNep), reactivated many of the repressed genes [186]. DZNep was an early tool for studying HMT function but lacked selectivity to draw specific conclusions.

Accumulating evidence suggested that certain cancers (especially those harboring gain-of-function mutations) exploit EZH2 for growth and therefore may be addicted to EZH2 regulation. This ultimately fomented the design of several small compounds that specifically inhibit EZH2 over other HMTs. These small compounds include EPZ-6430 (Tazemetostat, Epizyme), GSK-126 (GSK) and UNC1999 [184,187–189]. UNC1999 has much less selectivity for EZH2 over EZH1 than GSK-126 and EPZ-6438 and is therefore considered a dual inhibitor. It is important to note that no currently published studies have yet demonstrated any significant role for EZH1 in myeloma. In all cases, these compounds inhibit EZH2 catalytic activity by blocking accessibility of the catalytic SET domain. New analogs and unique compounds that target EZH2 or EZH2 and EZH1 together have continued to be developed and tested [159,178,190]

Development of these inhibitors has prompted many studies to evaluate the pre-clinical efficacy of EZH2 inhibitors (EZH2i's) in many cancers including EZH2. These inhibitors provided new specificity in targeting EZH2 and also lacked artifacts seen in the application of DNZep such as the degradation of EZH2 protein itself (not observed with new inhibitors). These inhibitors all demonstrated efficacy in cell lines at doses in the nano-molar to micro-molar range and induced maximal global demethylation of H3K27 after 2-3 days.

Several studies have used these new inhibitors to better understand the transcriptomic footprint of EZH2 in MM. Efforts have been reported to profile both deactivating H3K27me3 and activating H3K4me3 between healthy and malignant plasma cells to identify repressed and bivalent genes unique to MM [182]. These data, when compared to gene expression changes

induced by EZH2 inhibition, demonstrated that EZH2i can reverse repression of genes marked by H3K27me3. This was especially true for genes harboring bivalent histone modifications [182].

Other recent efforts that have tested EZH2i's to MM cell lines have described single agent efficacy in a significant sub-population of myeloma cell lines and *in vivo* models. Several drug-induced effects described by these studies have included apoptosis, de-differentiation, upregulation of tumor suppressors, downregulation of oncogenic pathways, modulation of cell adhesion molecules, cell cycle arrest, targeting of cancer stem cells and selective sensitivity of KMD6A/UTX mutant myelomas [152,178–180,182–185].

Pre-clinical success with EZH2 inhibitors in lymphoid malignancies, namely lymphomas, has prompted the advancement of two EZH2 inhibitors (EPZ-6438: NCT02860286 and GSK-126: NCT02082977) into early-phase clinical trials.

While application of these compounds seems promising, there are still many open areas of inquiry that need to be addressed regarding the specific mechanisms that drive EZH2 to become overexpressed and aberrantly active in MM. Additionally, it remains unclear how predictable EZH2i transcriptomic between different cancers and between different patients of the same cancer.

1.5 - Current Therapeutic Strategies for Management of Newly Diagnosed Myeloma

Treatment strategies for MM have evolved since the 1960s as our understanding of myeloma biology has grown [191]. The last decade in particular has seen a large increase in the number of drugs and therapeutic approaches that are being evaluated in part due to increased understanding of drug resistance mechanisms, high-throughput efforts to test vast quantities of new compounds, personalized medicine approaches to diagnosis/treatment and the advent of new technologies (i.e. gene editing techniques and promising immunotherapies). Additionally attitudes towards treatment have also moved towards a more conscious consideration for quality of life for patients and developing more accurate risk assessments for treatment. MM is still largely considered incurable despite recent advancements that have increased the median survival [3].

Early treatment regimens for MM included alkylating agents and corticosteroids; compounds which are still applied to therapy today [192]. Today, standard-of-care therapy has several options that are largely determined by the level of risk inherent in a particular myelomas genomic classification and other factors including age and health [193]. One option is for patients to undergo autologous stem cell transplant (ASCT) [194,195]. ASCT involves initial cycles of chemotherapy, stem cell collection, ASCT and finally 2+ years of chemotherapeutic maintenance. Traditionally ASCT eligibility have dictated the initial therapies used as more aggressive therapies would decimate the stem cell population needed for harvesting prior to transplant. Today, however, therapies are being changed and optimized to reduce undue hematological toxicity and therefore we are approaching a convergence of treatment options between ASCT-eligible and –ineligible patients.

The list of drugs currently used to treat MM has expanded significantly in recent decades to include proteasome inhibitors (Bortezomib, Carfilzomib and Ixazomib), immunomodulatory drugs (Thalidomide, Lenalidomide and Pomalidomide), monoclonal antibodies (Daratumumab (anti-CD38) and Elotuzumab (anti-SLAMF7)), HDAC inhibitors (Panobinostat), alkylating agents (Melphalan, Cyclophosphamide, Bendamustine) and corticosteroids (Dexamethasone and Prednisone) [191].

Currently, the combination of proteasome inhibitors with immunomodulatory drugs is considered to be the most efficacious treatment strategies to treat newly diagnosed MM. Specifically, bortezomib combined with lenalidomide and dexamethasone (VRD) has become the preferred treatment for patients who can tolerate a three drug cocktail. It is expected that second generation proteasome inhibitors (carfilzomib/ixazomib) will soon replace botezomib due to oral availability. For ASCT ineligible patients, bortezomib and immunomodulatory drugs are often combined with alkylating agents and corticosteroids [191].

Immunotherapy has the potential to revolutionize cancer treatment. Several exciting new anti-MM therapies are currently under development that harness the host immune system to eliminate malignant plasma cells. One example is the momentum behind evaluating PDL inhibitors in MM [196]. The PD-1/PD-L1 pathway is a negative regulator of the immune system

that is exploited by MM to evade the host immune system. Pembrolizumab (an anti-PD1 antibody) has been applied in several ongoing clinical trials. While the therapeutic antibody does not demonstrate strong single agent efficacy in MM, it may work cooperatively with another immune-therapy currently under development for MM: CAR T cells [196]. Chimeric antigen receptor (CAR) T-cell therapy is a very promising strategy for treating MM. Many distinguishing markers/regulators have been identified as specific targets in MM (e.g. MYC or MMSET), yet many lack small compounds that target them. CAR T cell therapy changes this by harvesting T-cells from a patient and engineer them to recognize specific cell surface markers, targeting those cells for intervention by the host immune system. Specifically in MM, CAR T cells are engineered to recognize the B-cell maturation antigen (BCMA) [197]. Adoptive T cell-based therapies have generated a lot of excitement in the field of MM therapy and updates (February, 2018) from an ongoing phase one clinical trial suggest that among patients treated at the highest doses, 94% show complete or partial remissions [198].

1.6 – Proteasome Inhibitors and Drug Resistance

Drug resistant relapse in MM in nearly inevitable. In some cases patients are entirely refractory to initial standard of care therapies. Nearly 25% of MM patients attain only short treatment responses and have a median overall survival of only 3 years [191]. The persistent problem of resistant and refractory MM highlights the need to understand the mechanisms that underpin resistance to the most widely used anti-MM therapies.

1.6.1 – The Ubiquitin Proteasome System and Anti-Myeloma Proteasome Inhibitors

Proteasome inhibitors are among the most widely used therapies to treat newly diagnosed MM. The proteasome is a large barrel shaped holoenzyme that catalyzes the proteolytic degradation of cellular proteins as a component of the ubiquitin proteasome system (UPS) [199,200]. The mammalian UPS comprises of several hundred ubiquitin ligase enzymes (one E1, 50+E2 and 500+ E3 ubiquitin ligases). The diversity of regulatory elements within the ubiquitination ligase system presents a complex regulatory network controlling when and why cellular proteins are targeted for proteolytic turnover. Once ubiquitinated, targeted proteins are

shuttled to the 26S proteasome complex. The 26S proteasome comprises of a 20S core barrel and one or two 19S regulatory subunits. Proteins arriving at the proteasome are bound, de-ubiquitinated and unfolded by a 19S regulatory subunit, after which the protein is processed linearly through the proteolytic core of the proteasome where it is digested by the catalytic ring of beta-subunits. Generally, this process is thought to provide cells with a robust mechanism for maintaining protein homeostasis. The proteasome is a highly conserved complex that senses and controls a myriad of cellular processes [199].

Bortezomib (Bz, Velcade), the most commonly applied proteasome inhibitor used to treat MM. Bz (and second generation proteasome inhibitors) targets the PSMB5 beta subunit of the 20S proteasome core and inhibits it chymotrypsin-like catalytic activity [199].

Malignant plasma cells are thought to be uniquely sensitive to proteasome inhibition for a number of reasons. First, plasma cells function to produce and secrete high quantities of Ig proteins. To accomplish this plasma cells adopt morphological changes that yield a large accentuated endoplasmic reticulum (ER). Such a high degree of protein production in turn yields undue ER-stress from occasionally misfolded proteins. While plasma cells can manage this high degree of turnover, they are uniquely sensitive to any perturbation in their ability to clear misfolded proteins [201]. Additionally MM cells, like other types of cancer, exploit certain signaling cascades to drive and sustain proliferation. Several such pathways require the UPS for turnover to convey a signal. A classic example of this is in the NF-κB pathway where ubiquitination and proteolytic degradation if the IκB are required for nuclear localization of the transcription factors p65/p50 [202]. Other processes and pathways that require proteasome function for complete signaling include cell cycle (p21, cyclins and p27Kip1), oncogenesis (p53 and bax), apoptosis (Bcl-2, XIAP, cIAP), gene expression (c-Jun, E2F1, beta-catenin) and many others [201].

1.6.2 – Proteasome Inhibitor Resistance

Resistance to proteasome inhibitors can be achieved by a great number of mechanisms. Treating a patient with proteasome inhibitors provides the sub-clonally diverse population of malignant plasma cells residing in the bone marrow to undergo a phase of selection. There remains some debate as to whether resistance in some instances is ‘acquired’ *de novo* upon drug

treatment or if selection propagates a minority population harboring 'innate' resistance to the inhibitor, however recent characterization of myelomas diverse sub-clonal architecture increasingly implicates the latter [48]. Furthermore, some recent evidence suggest that drug resistant relapse may arise from an extreme minority population of cancer stem cells that maintain abnormal quiescence while slowly repopulating the bulk tumor with rapidly dividing drug-resistant cells [203].

Regardless of how resistant MM cells arise within the bulk tumor during treatment there are many ways that individual cells can overcome or refract perturbation of the UPS [204]. This most theoretically intuitive mechanism for Bz resistance is a somatic mutation in the targeted PSMB5 subunit, however such mutations are rarely seen in MM cases suggesting that there are much more easily adopted means to resistance [205]. Indeed, resistance to proteasome inhibitors often does not confer a total blockade of drug action but rather elevates the general tolerance for ER-stress. While somatic mutations in proteasome subunits fail to explain recurring resistance there is evidence to suggest that proteasome subunits are altogether upregulated to compensate for the increased ER-stress. For example, the proteasome subunit PSMD4 is frequently amplified in cases of 1q21 amplification or t(4;14) translocation [204]. Another intuitive mechanism for drug resistance are the upregulation of transporters that efflux chemotherapeutics out of target cells to confer multi-drug resistance, however it is unclear the degree to which this occurs in proteasome-inhibitor-resistant MM [206].

An increasingly appreciated mechanism for drug resistance in MM is the relation between malignant plasma cells and their bone marrow microenvironment (BMME) [207]. The BMME contains abundant extracellular matrix proteins (laminin, fibronectin and collagen), soluble factors (growth factors, cytokines, chemokines), and a host of hematopoietic and mesenchymal cells. When providing enough chemical growth agonists the BMME can elevate the survival capacity of MM cells above the level required to survive drug-induced stress. For example, exogenous IL-6 triggers signaling through RAS/MAPK, JAK/STAT3 and PI3K/Akt pathways, all of which drive MM survival. This in turn prompts MM cells to secrete VEGF, a well-known driver of angiogenesis and a hallmark of MM progression [207]. This form of resistance would constitute a form of acquired

resistance where existing MM cells are supported rather than selected. Another mechanism of BMME-coordinated drug resistance is through elevated cell adhesion to bonne marrow stromal cells (termed 'cell-adhesion-mediated drug resistance or CAM-DR). CAM-DR is achieved via a host of adhesion molecules (e.g. integrins, CD44, VCAM-1 or MUC-1) [207]. These interactions then promote enhanced survival signaling in MM cells that are thought to be largely due to epigenetic remodeling [208].

While exogenous factors can drive pro-survival signaling in MM to evade drug resistance, MM cells can also be selected for genomic aberrations that hardwire cell survival and proliferation despite undue stress. Two examples include loss of the tumor suppressor TP53 and the amplification of MYC via secondary translocations [48].

1.7 – Predictive Transcriptomic Profiling in Myeloma

Transcriptomic profiles that predict patient outcomes has been a long-coveted tool in cancer treatment. Originally explored in microarrays, next generation sequencing of cancer transcriptomes is slowly moving towards routine implementation as the need for personalized medicine approaches to cancer treatment becomes more and more apparent. The first predictive profiles in MM were published over 15 years ago by three MM research groups: Arkansas [209], IFM [210] and HOVON [211]. In theory these prognostic, directional gene expression lists could be applied to a patient sample transcriptomic profile to attribute them a level of prognostic risk. The Shaughnessy et al. publication identified a 70-gene signature (GEP70) that binned patients into one of seven risk categories based on gene expression and common cytogenetic abnormalities defined in existing sub-types [209,212]. In a normal patient group these predictions would put roughly 10-15% of patients at high risk. The HOVON and IFM signatures comprise of 92 and 15 genes respectively. While procuring enough RNA for microarray studies proved challenging at the time, new optimization efforts have made this process much more simple and high-throughput. As recently reported [213], the GEP90 signature (now commercialized as 'MyPRS®': Myeloma Prognostic Risk Score) has been applied over 4,700 times since its development in 2006. Here the authors conclude that they have developed a superior technique

to personalize molecular characterization of MM with less subjectivity than cytogenetics/FISH [213]. Using transcriptomics to categorize and stratify risk for newly diagnosed MM could have significant utility.

As suggested by Szalat, Avet-Loiseau and Munshi in a recent review of MM profiling prospects, the ultimate goal of predictive transcriptomics should not only be to offer prognosis but to direct therapy [214]. The current field of MM diagnosis and treatment has yet to adopt a strategy where transcriptomic profiles that distinguish sensitivity and resistance to standard-of-care therapeutics flags likely refractory individuals and directs their therapy accordingly. Furthermore, the recent advent of single cell transcriptomics (a technology still in its infancy), holds immense promise to allow sub-clonal detection of drug resistance to predict innate resistance and likely drug-resistant relapse. Challenges remain for mainstream adoption of these practices due to lack of regulatory oversight, rapidly changing therapies that outdate old gene expression profiles and a lack of consensus among clinicians regarding the utility of transcriptomic profiling [214].

Some efforts to generate sensitivity and resistance profiling have been completed since the publication of original MM prognostic gene expression profiles. Our laboratory recently generated and profiled isogenic cell line pairs (Bz sensitive and resistant via progressive dose escalation) from a Bcl-XL/Myc double transgenic mouse model of MM [215]. The gene expression profile generated to distinguish Bz resistant and sensitive lines (a 23 gene signature) was bioinformatically queried against a host of other anti-cancer-drug-induced transcriptomic profiles. This query accurately predicted secondary therapies that would be uniquely efficacious in Bz resistant cell lines, suggesting that such profiling techniques can be effective and accurate in their predictions [215].

Efforts to mine public cancer cell line gene expression datasets to generate drug sensitivity scores have also recently been attempted [216]. Mining public datasets can be informative, however these studies suffer from a lack of clinical or experimental confirmation.

1.8 – Concluding Thoughts

The above review of MM biology should present an extremely daunting obstacle for therapeutic management. Myeloma's extreme genetic and epigenetic complexity is exemplified by hundreds of recurring mutations, CNVs, translocations and transcriptomic abnormalities. Understanding the highly intricate network of histone PTMs and their writers, readers and erasers presents an entirely different level of oncogenic regulation. Finally, this complex heterogeneity is further exacerbated by the continuous branching, sub-clonal evolution of MM. This seemingly paints a picture of MM where each instance is so distinct that targeting therapies based on all the possible covariates seems impossible.

While some may see these obstacles as unsurmountable, the accumulation of information surrounding MM 'omics' has offered the greatest gift to researchers studying MM. As collecting large amounts of prognostic information (i.e. transcriptomics or whole exome sequence) are more often becoming a routine aspect of MM diagnosis we continue to enhance our understanding of how each of the many MM genomic abnormalities contributes to MM pathology. The new challenge in using this information to manage MM is in the development of new bioinformatics approaches that can accurately use patient data to direct therapies.

As individualizing therapy will help manage MM cases based on distinguishing characteristics, there is also a lot promise in applying strategies that broadly target MM. Aside from the exciting immunotherapies currently being explored, our understanding of MM epigenetics has evolved such that we now recognize broad regulatory mechanisms cancer cells exploit to promote a general state of persistent proliferation.

The subtle nuances of MM biology continue to illuminate an increasingly complex disease. While this does present an immense challenge towards treating MM, these complexities also present a real opportunity to use patient data to accurately recognize specific obstacles and successfully treat individual cases of MM.

1.9 – Statement of Thesis

Multiple myeloma remains an incurable hematological malignancy due to the failure of standard-of-care therapies to broadly target a genetically diverse disease and an inability

overcome inevitable drug-resistant relapse. This thesis will address this outstanding problem of inevitable drug-resistant relapse during MM therapy by combining transcriptomic profiling to predict resistance to proteasome inhibitors and pre-clinical evaluation of epigenetic-targeting therapies to broadly target the myeloma epigenome. This document will describe two studies that each generate/test therapeutic strategies for overcoming heterogeneous drug response across a highly diverse panel of human myeloma cell lines. The first study describes an effort to systematically evaluate the cytotoxic profiles of a large panel of human myeloma cell lines to four proteasome inhibitors. We use gene expression profiles to distinguish the most and least resistant cell lines and from that distinction produce a weighted scoring algorithm that can predict extreme cases of proteasome inhibitor sensitivity or resistance. The second study evaluates new specific inhibitors of EZH2, a histone methyltransferase that is aberrantly active in myeloma. Furthermore we identify a strong synergistic potentiation of HDAC inhibition by EZH2 inhibitor pre-treatment and characterize the transcriptomic changes induced be each drug alone and in combination. These two studies represent two different approaches to overcoming drug-resistance: one by predicting it in advance and the other by broadly targeting a core aspect of myeloma pathology.

CHAPTER 2

A GENE EXPRESSION SIGNATURE DISTINGUISHES INNATE RESPONSE AND RESISTANCE TO PROTEASOME INHIBITORS IN MULTIPLE MYELOMA

Authors:

Amit Kumar Mitra[1], Taylor Harding[1], Ujjal Kumar Mukherjee[2#], JinSung Jang[3], Ying Li[4], Ren HongZheng[5], Jin Jen[3,5], Pieter Sonneveld[6], Shaji Kumar[7], Walter Michael Kuehl[8], Vincent Rajkumar[7], Brian Van Ness1*

[1]Department of Genetics, Cell Biology & Development, University of Minnesota, Minneapolis, MN;

[2]School of Statistics, University of Minnesota, Minneapolis, MN;

[#]Currently, Department of Business Administration, University of Illinois at Urbana-Champaign, Champaign, IL

[3]Genome Analysis Core, Center for Individualized Medicine, Mayo Clinic, Rochester, MN;

[4]Division of Bioinformatics and Biostatistics, Department of Health Science Research, Mayo Clinic, Rochester, MN;

[5]Biomarker Discovery Program, Center for Individualized Medicine, Mayo Clinic, Rochester, MN;

[6]Department of Hematology, Erasmus MC Cancer Institute, Rotterdam, Netherlands

[7]Division of Hematology, Department of Internal Medicine, Mayo Clinic, Rochester, MN;

[8]Genetics Branch, Center for Cancer Research, National Cancer Institute, Bethesda, MD, USA

*Corresponding Author:

DISCLOSURE: Author contributions

This chapter contains work summarized by a paper published in 2017 in Blood Cancer Journal under the same name as this chapter [217]. While I am second author on this publication, the first author, Dr. Amit K. Mitra, has given me explicit permission to use and re-print all of our manuscript in this document.

This disclosure is intended to explicitly outline my contributions to this project: I worked with BVN and AKM to conceive the project and during the entire project I was engaged in discussions regarding interpretation of results and progressing the project. Experimentally I worked collaboratively with AKM to characterize cytotoxic responses of human myeloma cell lines to four proteasome inhibitors. My contribution to the presented data is included in figure 1 of the publication and this chapter. AKM performed all transcriptomic analysis wrote all of the code that underpins the subsequent figures. AKM drafted the manuscript. BVN contributed to writing methods and the entire editing process including edits requested by reviewers of the manuscript. I contributed to the editing of this manuscript during the submission process.

This chapter contains several sections that are transferred verbatim to this document. These include the title, abstract, materials and methods (some supplemental methods merged here) and figures/tables (including descriptions and supplemental materials). I have partially re-written several sections including the introduction, results and discussion for inclusion in this document.

Abstract:

Extensive inter-individual variation in response to chemotherapy is a major stumbling block in achieving desirable efficacy in the treatment of cancers, including multiple myeloma (MM). In this study, our goal was to develop a gene expression signature that predicts response specific to proteasome inhibitors (PI) treatment in MM. Using a well-characterized panel of human myeloma cell lines (HMCLs) representing the biological and genetic heterogeneity of MM, we created an in vitro chemosensitivity profile in response to treatment with the four PIs Bortezomib (Bz), Carfilzomib (Cz), Ixazomib (Ix) and Oprozomib (Opz) as single-agents. Gene expression profiling was performed using next-generation high-throughput RNA-sequencing. Applying machine learning-based computational approaches including the supervised ensemble learning methods Random forest and Random survival forest, we identified a 42-gene expression signature that could not only distinguish good and poor PI-response in the HMCL panel, but could also be successfully applied to four different clinical datasets on MM patients undergoing PI-based chemotherapy to distinguish between extraordinary (good and poor) outcomes. Our results demonstrate the use of in vitro modeling and machine learning-based approaches to establish predictive biomarkers of response and resistance to drugs that may serve to better direct myeloma patient treatment options.

Introduction:

Wide inter-individual variation in response to chemotherapy is a major limitation in achieving consistent therapeutic effect in many cancers, including multiple myeloma (MM), the second-most common hematologic malignancy with an estimated 30 330 new cases (~2% of all new cancer cases) and 12 650 estimated deaths in 2016 (NCI-SEER (The Surveillance, Epidemiology, and End Results program of the National Cancer Institute) Cancer statistics) [218–221]. MM is a complex disease that can be established by a broad spectrum of genomic lesions and diversified by additional genomic/epigenomic abnormalities. The underlying diversity of disease characteristics between patients underpins the observed heterogeneity in response [222–224]. Heterogeneous transcriptomic profiles between patients are one of several factors known to contribute to the inevitable refractory/relapsing resistance to standard-of-care therapies [222]. Deciphering gene expression changes that can distinguish drug-sensitive and drug-resistant myelomas is a promising approach to developing personalized chemotherapeutic regimens that avoids fruitless applications of common therapies.

Proteasome inhibitors (PIs) are among the most commonly applied standard-of-care chemotherapies used to manage MM. PIs are used to treat MM alone or in combination with alkylating agents, corticosteroids, immunomodulatory agents and histone deacetylase inhibitors [224–226]. Bortezomib (Bz/Btz/Velcade) was the first PI to be approved by the US Food and Drug Administration for clinical application in 2003 for the treatment of relapsed and refractory MM [227–229]. The common utilization of Bz for the treatment of MM and other cancers has spurred the development and testing of several second-generation PIs: Carfilzomib (Cz/Cfz/Kyprolis), Oprozomib (Opz) and Ixazomib (Ix/MLN9708/Ninlaro) [224,227,230].

Despite the positive effect Bz has had on MM median survival, MM still remains a mostly incurable disease (5-year survival below 50% according to NCI-SEER cancer statistics). Most patients undergo relapse where even patients with good initial response eventually present chemo-resistant disease [224]. Some recent studies have suggested that some cases of resistance are drug-specific where Bz-resistant MM may still be sensitive to other second-generation PIs [225,231].

Identifying the factors that can drive resistance to PIs is a challenge. In most cases, MM patients receive PIs in combination with other anti-MM agents and therefore patient response data inherently contains diverse covariates. In addition, survival end points in clinical applications are measured in months to years, and hence developing prediction algorithms of response can be a long process.

Despite these challenges we propose that there are transcriptomic signatures that can distinguish different levels of PI sensitivity/resistance. To identify such signatures, we utilized a collection of 50+ human myeloma cell lines (HMCLs) generated through the immortalization of primary MM cells that represent a broad spectrum of the biological and genetic heterogeneity of MM [232]. We used these HMCLs to systematically evaluate the chemo sensitivity of HMCLs to four PIs as single agents: Bz, Cz, Iz and Opz. This systematic evaluation produces a distribution of response. Cell lines that occupy the extremes of this distribution can then be selected for transcriptomic profiling.

Modern transcriptomic profiles contain gene expression data for over twenty thousand human genes. Finding signatures within these profiles that can distinguish categorical outcomes is a problem well suited for machine learning based computational approaches. Generally machine learning approaches are ‘trained’ using large data sets each with known ‘outcomes’. These outcomes (the dependent variable) are either categorical (e.g. resistant or sensitive) or continuous (e.g. on a scale of 0.0-1.0). Training algorithms are numerous and diverse but all essentially randomly interrogate the data to improve correct perdition of the outcome. This prediction is then validated against a test data set (not used in training).

The random forest method is possibly one of the oldest machine learning algorithms [233]. Random forests (RFs), as the moniker implies, are made up of many decision trees. Decision trees are supervised machine learning algorithms where features (tree nodes initiated at the root node) are selected from the data (feature space) and tested/evaluated by some criteria to produce a single outcome (a branch). Eventually a final conclusion/decision is reached at the terminal node. While individual decision trees may not be individually accurate, the consensus generated by all trees in a forest are what gives the random forest algorithm its designation as an

ensemble method for machine learning. In classification models this consensus is the mode of decisions and in regressive models the consensus is the mean. Additional methods can be applied to reduce overfitting (inflated impact of small variations in the test data) such as pruning, boosting and bootstrap aggregating (also known as bagging).

Random forests can also be applied to train models that patient survival data. These data have unique challenges in that they are often right censored (subjects often leave studies early). Random survival forest (RSF) is a prediction method tailored to right censored survival data. It combines the random forest method with propotional hazard based models (e.g. non-parametric Kaplan-Meier or semi-parametric Cox propotional hazard models). Specifically relating to patient survival data, RSF uses Kaplan-Meier estimator for survival data as a decision tree's terminal node.

When applied to gene expression profiling (GEP) data of MM patients from four different PI-based clinical trials, our GEP model of response/resistance to PIs successfully distinguished differences in disease progression and distinguished extraordinary (good and poor) responses. Thus, these results can provide a PI treatment-specific predictor of clinically relevant outcomes that could affect therapeutic choices.

Materials and Methods:

Drugs

Bz (Takeda Pharmaceuticals Inc., Deerfield, IL, USA) was dissolved in serum-free RPMI-1640 (Lonza, Allendale, NJ, USA) and stored at −20 °C. Ix (Takeda), Cz and Opz (Amgen, Thousand Oaks, CA, USA) were dissolved in dimethyl sulfoxide (DMSO; Sigma-Aldrich, St Louis, MO, USA) and stored at −20 °C.

Cell lines

Fifty HMCLs were procured from various institutions, established and characterized, and maintained in HMCL media with interleukin-6 [234]. Supplementary Table S1 provides the cytogenetic characteristics of the HMCLs.

In vitro chemosensitivity assays

Cell cytotoxicity assays were performed on the HMCLs to create a drug sensitivity profile in response to treatment with increasing concentrations of Bz, Cz, Ix and Opz as single agents and half-maximal inhibitory concentration (IC50) values and area under the survival curve (AUSC) were calculated as described earlier [234]. Briefly, cells were counted using Countess automated cell counter (Invitrogen, Carlsbad, CA, USA) and seeded in 96-well plates at a concentration of 4 × 105 cells per ml. After 24 h, cells were treated with increasing concentrations of Bz, Cz, Ix and Opz as single agents. Cell viability assays were performed 48 h post treatment using CellTiter-Glo luminescent cell viability assay (Promega, Madison, WI, USA) according to the manufacturer's instructions using Synergy 2 Microplate Reader (BioTek, Winooski, VT, USA) to generate survival curves. Percent survival values were normalized to untreated controls and IC50 values were determined by calculating the nonlinear regression using sigmoidal dose–response equation (variable slope). AUSC was calculated using trapezoidal rule and log2-transformed for further statistical analysis [234]. Caspase-3/7 activity was evaluated using Caspase-Glo 3/7 Assay kit (Promega) on Synergy 2 Microplate Reader.

Gene expression profiling

RNA was isolated from six most Ix-sensitive and six most Ix-resistant cell lines and RNA sequencing was performed on llumina HiSeq 2000 (Illumina, San Diego, CA, USA) using 50 bp

paired-end protocol with depth of >20 million reads per sample. RNA-sequencing (RNA-seq) data from CD138-selected plasma cells were generated from MM patients enrolled in an ongoing phase-2 Ixazomib clinical trial at Mayo Clinic (Mayo-Ix; NCT01415882) that enrolled patients with relapsed myeloma who had less than six cycles of prior treatment with a Bz-based regimen and were not refractory to Bz [235]. High quality RNA was extracted from HMCLs using QIAshredder and RNeasy kit (Qiagen). RNA concentration and integrity were analyzed using the Nanodrop-8000 and Agilent 2100 Bioanalyzer and stored at -80°C. RNA integrity number/RIN>8 was considered suitable for RNA-seq analysis. RNA-seq library construction was performed using the Illumina TruSeq RNA sample Preparation kit v2. The libraries were size selected to generate inserts of ~200bp and RNA sequencing was performed using llumina's HiSeq 2000 next-generation high-throughput sequencing system using 50bp paired-end protocol with depth of >20million reads-per-sample. Average quality scores were well above Q30 for all libraries in both R1 and R2. Data was normalized and FPKM values were used in further analysis using a combination of Galaxy data analysis software and Partek Genomics Suite. GEP vs *in vitro* chemo-sensitivity data was then used to identify gene expression signatures associated with PI response.

Gene expression data was pre-processed using Galaxy, an open source, web-based platform that provides tools necessary to create and execute RNA-seq analysis. Briefly, an RNA-seq data analysis pipeline was developed using Galaxy that performs quality control (QC) check on the RNA-seq raw reads using FastQC tool, trims the reads to remove base positions that have a low median (or bottom quartile) score and then uses Tophat2 tool to map processed RNA-seq reads to the hg19 human genome build. Estimated insert sizes were derived using Picard's CollectInsertSizeMetrics tool on this initial tophat2 run which was used to calculate mean inner distance between mate pairs (Mean= estimated_insert-size - 2*read_length). Tophat2 was then re-run using correct mean value and finally Cufflinks tool was used on these datasets to assemble the reads into transcripts.

Prior to analysis, the processed transcripts were filtered using the following criteria: genes with variance=0, FPKM<1 and mean FPKM<5 were removed.

Gene expression, treatment arm and outcome data on newly diagnosed myeloma patients enrolled in HOVON65/GMMG-HD4 trial (ISRCTN64455289; n=290) were downloaded from Gene expression omnibus (GEO) (GSE19784) [211]. The APEX data set (GSE9782; n=264) consists of bortezomib-based phase-2 and phase-3 relapsed and/or refractory myeloma clinical trials (The APEX phase-3 trial (039), a companion study (040), the SUMMIT (025) and CREST phase-2 trials (024)) [236]. For both these trials, Affymetrix, Santa Clara, CA, USA gene probe set analysis data (U133-Plus2.0 for HOVON65/GMMG-HD4 and HG-U133A/B for APEX) were available. Pretreatment RNA-seq data, treatment arm and clinical outcome information on CoMMpass (Relating Clinical Outcomes in MM to Personal Assessment of Genetic Profile) trial patients were downloaded from the MMRF (Multiple Myeloma Research Foundation) researcher gateway portal (IA7c release; https://research.themmrf.org). The CoMMpass Trial (NCT0145429), sponsored by MMRF, is a non-registrational, longitudinal study of 1000 newly diagnosed MM patients followed over the course of their disease, up to 8 years.20

Bioinformatics and statistical analysis

All statistical analyses were performed using R software environment (https://www.r-project.org/) version 3.3.1 for statistical computing and graphics, and GraphPad Prism v7.0 (GraphPad Software, Inc., La Jolla, CA, USA). Spearman's rank-order and Pearson's product-moment correlation analyses were performed to compare the PI responses. All tests were two sided and $P<0.05$ was considered statistically significant. Gene expression data were preprocessed, log2-transformed and analyzed using Galaxy and Partek Genomics Suite v6.6 (Partek Inc., St Louis, MO, USA) to perform differential expression testing to identify gene expression signatures PI response (details above). Analysis of variance model or two-sided paired sample t-test was used to evaluate whether each gene is differentially expressed. Heatmaps were generated using unsupervised hierarchical clustering analysis based on the differentially expressed genes.

Supervised machine learning approaches construct algorithms that learn from training data, build models based on properties of training inputs and thus make learned predictions/decisions on new/test samples [233,234]. Random forest, a supervised ensemble

machine learning algorithm, was used to establish the top differentially expressed genes as predictive GEP signatures of PI response [233]. GEP data on top Ix-sensitive vs top Ix-resistant HMCLs (n=12) were used as 'training data set' to build random forest classification models (decision trees) and predict PI resistance of HMCLs (n=44) in the 'test data set', the mRNA-seq data obtained from the Keat's lab repository (http://www.keatslab.org/data-repository). The average bootstrap prediction error was generated using repeated bootstrapping of the train data set with a k-fold cross-validation (k=100). The cross-validation error rate was used to evaluate the accuracy of the method [233,234].

The predictive GEP signature was then applied to the four different PI-based MM clinical trials and random survival forest estimation method for right censored data (randomForestSRC R package), another supervised machine learning decision-tree based algorithm, was used to predict probability of progression/event (0=censored; 1=progression) within the first 3 years for each myeloma patient [237]. The predicted probability values derived using machine learning approaches (random forest and randomForestSRC) were rank-ordered and the predictions for the top (Q3) and bottom quantiles (Q1) were compared with observed PI response using Somers' Dxy rank correlation [238] (see full details in Supplementary Methods available online [217]).

Unsupervised K-means clustering was performed using the algorithm of Hartigan and Wong [239] to identify clinically important K-subgroups based on our PI response GEP signature such that N/K~30 (N=total number of subjects in data set). Kaplan–Meier curves for survival were generated for the extraordinary PI response (good vs poor) clusters by computing progression-free survival (PFS) over time [240] The Kaplan–Meier survival curves were compared statistically using log-rank test and Cox proportion hazard test [241]. Clusters with n<10 were combined for PFS comparisons.

Odds ratios (ORs) between observed clinical responses (available for APEX and CoMMpass data sets) vs extraordinary PI-response K-means clusters were computed using binomial logistic regression analysis (logit model) [242].

Ingenuity pathway analysis

The differentially expressed genes were analyzed using Ingenuity Pathway Analysis (IPA) to identify canonical pathways, downstream effects, upstream regulators and causal networks and to perform predictive toxicology analysis using toxicogenomics approaches (IPA-Tox) [243].

Results:

Wide variability in response to PI treatment

We used a large panel of HMCLs as a model to recapitulate the genomic heterogeneity between MM patients. We systematically measured the *in vitro* sensitivity of 50 HMCLs to four PIs (Bz, Cz, Ix and Opz). Doses were consistent between cell lines and cell viability after 48hrs was measured using a CellTiter-Glo® (Promega) assay. Cytotoxicity in these assays was further confirmed with caspase-3/7 cleavage assays (data not shown). We compared sensitivity across cell lines using two metrics: IC_{50} and area under the survival curve (AUSC). IC_{50} is the dose that produces 50% viability after the specified treatment time (48hrs) and AUSC normalizes the area under the survival curve (trapezoidal method) to a total lack of response (i.e. max dose multiplied by 100% viability). These data identified a distribution of responses to PIs where, as in patient populations, some PIs respond to low doses of PIs while others are relatively resistant (**Figures 1a and 1b**). In some cases AUSC was a better comparative method as some HMCLs displayed PI-resistance to the point of not achieving an IC_{50} value. The summary of cytotoxic analysis across all four PIs (**Table 1**) articulates the magnitude at which responses vary between HMCLs. Generally all four PIs demonstrated similar distributions across the HMCL panel as demonstrated in a correlation matrix between PI IC_{50}'s and AUSCs (**Figure 1c**). Correlation was statistically significant across all four PIs (Holm's method adjusted p-values all <0.001).

We did find some instances where HMCLs showed sensitivity to one PI and resistance to another. This further suggests that some tumors that are refractory to one PI may still respond to another.

Importantly, response was similar between all PIs at the top and bottom of the response distribution (exceptionally high/low response), allowing us to attempt to characterize transcriptomic differences between these extremes.

Deriving a GEP-based signature profile of PI response

We performed differential gene expression analysis between 5 (top 10%) most Ix-sensitive and 5 (bottom 10%) most Ix-resistant cell lines. Notably, these cell lines showed the same relative

sensitivity and resistance to all four proteasome inhibitors. RNA was isolated from these cell lines (untreated) and subjected to RNA-sequencing (RNA-seq) and subsequent data processing and analysis. Prior to analysis, the processed transcripts were filtered using the following criteria: genes with variance=0, FPKM<1 and mean FPKM<5 were removed. Differential gene expression analysis was performed using the remaining 7682 genes to identify GEP signatures that distinguish the highly sensitive from the highly resistant HMCLs. Results showed 506 genes differed significantly between the sensitive and the resistant groups ($P<0.05$; fold change ≠1). In all, 141 genes showed |fold change| >2 and $P<0.05$, whereas 42 genes, listed in **Table 2**, had $P<0.01$ (|fold change| >2) (**Figure 2**). Subsequent analyses used the more stringent highly variable/differentially expressed 42-gene list.

GEP signature of PI response is predictive of in vitro PI chemosensitivity in HMCLs and progression in MM clinical trials

Our experimental approaches yielded a 42-gene signature that distinguished extreme sensitivity and extreme resistance within our HMCL panel. We sought to determine the predictive capacity this signature bears outside this context. We elected to utilize machine-learning computational approaches to further enhance the predictability of our signature using publically available data. Supervised machine learning approaches construct algorithms that learn from training data, build models based on properties of training inputs and thus make learned predictions/decisions on new/test samples. The training data set comprised gene expression profiles of HMCLs that represent extremities of PI responses, whereas the initial validation/test data set was derived from an independent gene expression study on HMCLs (n=44) performed in the Keats laboratory at TGen laboratories (http://www.keatslab.org/data-repository). The final validation data set of human myeloma patients comprised four independent clinical trials (HOVON65/GMMG-HD4 (n=290); APEX (n=264); CoMMpass (n=765); and the Mayo-Ix trial (n=22)).

First, the random forest algorithm for classification was ‘trained’ using mRNA-seq data on the 42-gene signature from 6 most PI-sensitive and 6 most PI-resistant cell lines. The out-of-bag

estimate, which is a measure of mean prediction error of the training model calculated by subsampling the training data set, was computed as 0%. Concurrently, the classification error rate derived from confusion matrix was also 0, thus validating the robustness of the training model. Supplementary Figure S1 provides the gene importance plot representing the most important genes within the 42-gene expression signature influencing PI response based on variable importance (VIMP) measure derived from random forest analysis.

The probability scores of PI resistance were then calculated for each of the HMCLs obtained from the Keatslab data repository ('test' data set). The predicted probabilities of PI resistance were then rank-ordered and Somers' D_{xy} rank correlation analysis was performed between the top quantile (Q3) and bottom quantile (Q1) resistance probability values and observed PI chemosensitivity as a binary outcome (sensitive=0 vs resistance=1). Results revealed high positive Somers D_{xy} rank correlation for the PI drug cytotoxicity parameters (IC_{50} and AUSC) (**Table 3**), indicating that our 42-gene GEP signature validated quite well in an independent data set of HMCLs.

As the classification model was generated using HMCLs with top-6+bottom-6 Ix IC50 values as training data set, the test data set for Ix IC_{50} prediction included RNA-seq data on the remaining 32 cells lines only from an independent data set obtained from the Keatslab repository. Among these, Somers' c value for correlation between observed Ix IC50 and response probabilities of the top 6 predicted Ix-resistant cell lines was 0.667 whereas it was 1.0 for the top 6 predicted Ix-sensitive lines. Somers' c for the combined set of 12 predicted sensitive+resistant HMCLs was 0.743. Thus, the independent cell line test set showed very good correlation with the signature-derived predictor.

Although the training set showed good prediction capabilities in an independent set of HMCLs, we were particularly interested to determine whether it is able to stratify patient outcomes in multiple clinical trials. Four different PI-treating trials were examined (treatment details provided in Materials and Methods). Microarray gene expression data from clinical trials was mean-centered and scaled before analysis. The standardized transcriptomic profiling data from APEX trial was used as a training data set to perform random survival forest analysis to

predict the percent probability of a progression/event within 3 years in the HOVON-GMMG-HD4, CoMMpass and Mayo-Ix clinical trials (test data sets). Somers' D_{xy} rank correlation analysis between the top and bottom quantiles of predicted percentage values from random survival forest model on test data and the progression index of the test data sets showed consistent positive values for the HOVON-GMMG-HD4, CoMMpass and Mayo-Ix clinical trials revealing high prediction accuracy of the random survival forest-based prediction model [237,238] (**Table 4**). Somers' c for the training data set (APEX) was=0.852.

As we were particularly interested in our signature's drug response performance, we chose to look at progression as one measure of response/nonresponse as well as associations that distinguish clinical definition of response, complete response versus nonresponse [244]. K-means clustering is a computational method for clustering datasets (e.g. patient sample transcriptomes) into a user defined number of clusters. K-means clustering was performed on 188 MM patients from the Bz treatment arm of the APEX data set19 to partition the samples into clusters/subgroups based on the expression of the 42 genes comprising the GEP signature of PI response. Results show significant differences in PFS between the signature-derived poor PI-response and good PI-response groups (hazard ratio (HR)=2.346; P=0.0076; **Figure 3a**). Conversely, no difference in PFS is observed between the K-means clusters when the 42-gene model was applied to the expression data of 76 patients in the dexamethasone arm of APEX phase-3 trial that compared single-agent Bz with high-dose dexamethasone (HR=1.1; P=0.732; **Figure 3a**), showing our GEP signature is drug-specific. Concurrently, statistically significant association is observed between the K-means clusters and clinical response in the Bz arm (ORresponder vs nonresponder=5.813; 95% confidence interval=1.833–20.007; POR=0.0036) but not in the Dex arm (ORresponder vs nonresponder=2.139; 95% confidence interval=0.753–6.326; POR=0.158) of the APEX data set.

When applied to the gene expression data from HOVON-GMMG-HD4 clinical trial (n=290) that implemented a Bz-based drug regimen [211], the 42-gene signature shows statistically significant differences in PFS among K-means clusters representing good vs poor PI response in the Bz-treated PAD (bortezomib, doxorubicin and dexamethasone) arm (HR=2.161;

P=0.024), whereas no difference in PFS is observed in the VAD (vincristine, doxorubicin and dexamethasone) arm (HR=1.282; P=0.437; Figure 3b). What is particularly striking is that within the first 1.5 years the predicted good response group in the PI-containing therapy had no progression events, whereas 35% of the predicted poor response group had progression events.

Clinical data were available on 765 patients from the CoMMpass study. A total of 253 patients used Bz as first-line therapy, alone or in combinations. Of these, 128 had RNA-seq and PFS data available. K-means clustering based on the expression of the 42 genes distinguishes between good and poor PFS subgroups of myeloma patients (HR=2.556; P=0.0277; **Figure 3c**). In addition, the K-means clusters are also found associated with clinical response (OR=5.20; 95% confidence interval=1.22 36.077; POR=0.0453). In contrast, among the 96 patients using Lenalidomide (an immuno-modulatory drug) as first-line therapy, no association was observed between the good and poor K-means clusters and PFS (P=0.49; Figure 3c). Our results thus further validate the PI response specificity of our method.

Finally, we applied our algorithm based on the our 42-gene PI response signature to an ongoing clinical trial at Mayo Clinic that uses Ix-containing drug regimen. Interestingly, even with small numbers of patients available, our GEP-based PI response classifier distinguishes between the top (medium PFS=22.42 months) and bottom responders (medium PFS=12 155 months) in this Ix trial (risk ratio=2.5) (Figure 3d). Notably, all 10 patients in the good performance group were alive at the latest point of the interim analysis, whereas 4 out of 9 patients in the poor PI response cluster died (inset of **Figure 3d**).

Ingenuity pathway analysis

We subjected our 42-genes to network analysis to determine if this signature was particularly enriched for any specific biological pathways. Ingenuity Pathway Analysis (IPA)[245] is a network analysis platform that can be queried with gene expression changes and return enriched network information from the QIAGEN knowledge base. Out of the 42 genes, 12 overlapped with the top IPA network obtained from the analysis of direct and indirect relationships (score=26), as represented in **Supplementary Figure S2a**. Genes/molecules in this network include the 26s proteasome complex. Furthermore, when we used the IPA upstream regulator

analysis, TFEB and CCND1 were identified as the top hits/factors that may control the genes and pathways highlighted by network analysis (**Supplementary Figure S2b**). The functional significance is discussed further in the Discussion.

Discussion:

MM remains an incurable disease primarily due to the inability of current standard-of-care to treat effectively treat MM. Patients who are not already refractory to anti-MM chemotherapies will almost always develop drug-resistant relapse. This strongly supports the need for predictive methods that identify cases of extreme innate drug-resistance.

Differential gene expression signatures have been developed for MM [211,232,246], however these signatures were designed to stratify patients based on prognosis and none of those signatures were treatment specific. Furthermore, no study thus far has made use of the vast array of HMCLs as model system to generate drug chemosensitivity profile as a representation of the response variation in patient subtypes that may be used to derive a PI-specific GEP signature predictive of resistance and treatment outcomes.

In this study, we successfully used a panel of 50 HMCLs to model heterogeneous response to PIs within a gnomically diverse population. All four PIs had distributions of sensitivity that was highly correlated across the panel. Some outliers were noted. Interestingly, several cell lines with intermediate response to Bz or Ix were found highly responsive to Cz treatment. However, in general the ranked correlation with response was very similar among all four PIs, particularly those lines that were collectively the most responsive and least responsive to all four PIs (extraordinary responders). Further characterization of the outliers may reveal important features that better direct which PI is most effective.

Having established this chemosensitivity distribution among HMCLs we focused on identifying common transcriptomic differences between highly sensitive and highly resistant HMCLs. RNA-seq analysis and stringent thresholding produced our 42-gene signature that represents those transcriptomic differences. Importantly, this signature was not applied across the full range of responses, but was very effective in identifying extraordinary (good versus poor) response.

Several of the genes identified in our GEP have known connections to the ubiquitin proteasome system and endoplasmic reticulum (ER) stress. IPA WFS1, a cation-selective ion channel embedded in the ER, plays a role in ER stress (a direct consequence of inhibiting protein

turnover at the proteasome) [247]. Furthermore, WFS1 is downstream from the transcription factor XBP-1, which is also noted to be directly involved in ER-stress induced apoptosis [248]. This may be, in part, why high XBP-1 expression is a good prognostic marker for MM [248,249]. Interestingly, we found that the unspliced transcript of XBP1 (Xbp1u) had ~1.5 times lower expression in Ix-resistant cell lines when compared with Ix-sensitive cell lines. The transcription factor EB (TFEB) is a master gene for lysosomal biogenesis that ultimately facilitates autophagy cell death. While this may be a path to cell-death in MM it is also notable that lysosomal clearance of aggresomes is a means to tolerate PI-induced ER stress [250]. RNF170 encodes an ER membrane ubiquitin ligase that mediates ubiquitination and degradation and plays a key role in cell signaling [251].

While many of these genes seemingly have no connection to the proteasome and its related pathways, several genes included in our GEP signature have been previously implicated with prognosis and disease progression in myeloma. For example, CCND1, the gene encoding cell cycle regulator cyclin D1, is frequently misregulated in MM. CCND1 has additionally been reported to be a strong prognostic indicator [232,234]. HSPA1B is an NRF2-mediated oxidative stress response gene that was also identified in a previous study of ours screening for transcriptomic markers of Bz sensitivity/resistance in a *murine* model of MM [215]. Gla, a metabolic enzyme, has been shown to play a role in regulating bone resorption in MM [252].

We used this 42-gene signature to train ensemble machine learning methods, thereby further assessing the predictability of this signature outside the context in which it was generated. We first used RF methods to train models using our HMCL transcriptomic data and test with transcriptomic data generated in a separate laboratory.

While the number of cell lines used to generate our 42-gene signature was relatively small, when applied to clinical trial data, it was remarkably predictive of extraordinary PI sensitivity/resistance. RSF methods, when trained using clinical trial data demonstrated consistent correlations with outcomes in test data sets. Using our signature to K-means cluster clinical trial cohort's accurately segregated patients treated with PIs into different outcomes.

Encouragingly, this was not observed in clinical trial arms that did not contain PIs in the treatment regimen.

Earlier, we demonstrated that gene expression signatures may be used to identify secondary therapies in PI-resistant MM using in silico predictions that were confirmed *in vitro* [215,253]. In 2014, the NCI initiated the Exceptional Responders Initiative to understand the molecular basis of exceptional response to chemotherapy in cancer patients enrolled in clinical trials [254]. The primary goal of the study is to identify molecular features in malignant tissue that may aid to predict response to same or similar drugs. On similar lines, our work should serve as resource to use machine learning-based approaches for the personalized prediction of exceptional chemoresistance and to eventually identify signatures of drug combination regimens that may effectively reverse drug resistance by predicting drugs for various subpopulations/subclones of tumors based on pharmacogenomic signature profiles.

Acknowledgments:

This work was supported by a grant from the Minnesota Partnership for Biotechnology and Medical Genomics to BVN and SK. AKM was supported by a grant from the International Myeloma Foundation. We are thankful to Professor Leif Bergsagel at Mayo Clinic, Scottsdale, and Professor Jonathan Keats at The Translational Genomics Research Institute (TGen) Phoenix, AZ, for their gracious help in obtaining the cell lines and the link to their expression profiles. We thankfully acknowledge the University of Minnesota Genomics Center, Minnesota Supercomputing Institute and the members of the Mayo Clinic Genome Analysis Core for technical support with RNA-seq profiling and analysis. The CoMMpass trial is sponsored by MMRF.

Competing interests

The authors declare no conflict of interest.

Figure Legends:

Figure 1. *In vitro* chemo-sensitivity profiles of human myeloma cell lines following proteasome inhibitor treatment.

a) Plots show survival compared to untreated control versus increasing concentration of bortezomib, oprozomib, ixazomib, carfilzomib. In b) the Area Under the Survival Curve (AUSC) was normalized and expressed as percentage of the largest value for each drug, shown for all cell lines treated with the four proteasome inhibitors. In c) the Scatterplot matrix is shown as a pairwise correlation of the natural log (Ln) of IC_{50} and AUSC values for the response to each PI drug. Scatterplot matrix was generated using the R graphing package ggplot2.

Figure 2. Heat map representing differential gene expression between PI-sensitive vs PI-resistant myeloma cell lines.

Gene expression was z-score normalized (standardized: shifted to mean of 0 and scaled to standard deviation of 1) and compared among the 5 most Ix-responsive and 5 least Ix-responsive cell lines. Heatmap was generated using the top 42 differentially expressed genes (|fold-difference|>2; $p<0.01$). Columns are ordered by Ix IC_{50} of cell; genes are ordered by fold-difference. Color indicates fold-change between Ix-resistant vs Ix-sensitive cell lines.

Figure 3. Plots showing stratification in progression-free survival (PFS) among MM patients on PI-based clinical trials in which the 42-gene model was used to assign extraordinary (good and poor) PI-response.

Kaplan-Meier survival curves in a) APEX dataset: bortezomib arm shows significant separation of PFS between clusters representing good vs poor outcomes; whereas the dexamethasone arm shows no stratification; b) patients in the HOVON-GMMG-HD4 trial (Bz-treated/PAD and VAD

arms) were assigned good versus poor PI-response based on the 42 gene model. PFS curves for the interim analysis of the c) CoMMpass trial (NCT0145429) patients administered Bz or Lenalidomide (Len) as first line of therapy, and d) the Mayo Clinic Ix-trial (NCT01415882). Patients were assigned good versus poor response based on the 42-gene model. Inset of 3d) shows survival of each patient considered. Dashed line represents end of year 1 (365.25 days from randomization).

Figure S1: Gene importance plot derived from Variable/ Feature selection using machine learning on the training dataset.

MeanDecreaseGini is the measure of gene importance for training dataset.

Figure S2. Ingenuity Pathway analysis showing the prediction of the a) top network and b) top upstream regulator based on the 42-gene signature of PI-response.

Gene nodes are displayed using various shapes denoting the functional class of the gene product. Green symbolizes downregulation of gene expression, while red represents upregulation of gene expression. The significance of up/down-regulation is represented by color intensity.

Table 1. Numerical summaries of chemo-sensitivity parameters in HMCLs

Proteasome inhibitor	Mean (nM)	Minimum (nM)	Median (nM)	Maximum (nM)
Bortezomib_ IC_{50}	17.1	2.8	11.7	124.3
Carfilzomib_ IC_{50}	10.9	0.7	7.1	55.3
Ixazomib_ IC_{50}	155.3	15.1	42.1	4757.9
Oprozomib_ IC_{50}	45.8	7.6	23.7	776.0
Bortezomib_ AUSC	2700.1	319.6	1524.0	38974.0
Carfilzomib_ AUSC	3503.4	375.5	1448.5	19097.0
Ixazomib_ AUSC	10030.0	1702.0	6456.0	46494.0
Oprozomib_ AUSC	5017.0	1050.0	2885.0	59917.0

Table 2. List of genes most significantly associated with PI resistance (|Fold-difference| > 2; p < 0.01)

Differential gene expression analysis was performed to compare gene expression profiles of 5 (Top 10%) most Ix-sensitive and 5 (Bottom 10%) most Ix-resistant cell lines. These 42 genes were used as GEP signature of PI resistance to stratify PI response in test datasets (in vitro and among patients).

#	Gene ID	p-value	Fold-difference (Sensitive vs. Resistant)	Fold-difference (Description)
1	SLC1A4	0.00004	2.695	Sensitive up vs Resistant
2	NEK3	0.00006	-2.544	Sensitive down vs Resistant
3	GLA	0.00007	2.073	Sensitive up vs Resistant
4	AKNA	0.00020	4.043	Sensitive up vs Resistant
5	ARHGAP27	0.00035	3.599	Sensitive up vs Resistant
6	LY96	0.00045	3.796	Sensitive up vs Resistant
7	DLST	0.00070	-2.001	Sensitive down vs Resistant
8	MSL3	0.00132	2.237	Sensitive up vs Resistant
9	SQRDL	0.00134	3.906	Sensitive up vs Resistant
10	NCAPH2	0.00206	2.129	Sensitive up vs Resistant
11	PLK1S1	0.00262	-2.035	Sensitive down vs Resistant
12	MRI1	0.00284	2.448	Sensitive up vs Resistant
13	TARS2	0.00294	-2.083	Sensitive down vs Resistant
14	OBFC2A	0.00307	3.756	Sensitive up vs Resistant
15	RAB8A	0.00319	2.097	Sensitive up vs Resistant
16	ABHD2	0.00363	2.475	Sensitive up vs Resistant
17	LMF2	0.00364	2.558	Sensitive up vs Resistant
18	C6orf48	0.00367	-2.462	Sensitive down vs Resistant
19	TUBA4A	0.00400	2.189	Sensitive up vs Resistant
20	HSPA1B	0.00467	-2.335	Sensitive down vs Resistant
21	TFEB	0.00471	-2.302	Sensitive down vs Resistant
22	RNF170	0.00504	-2.34	Sensitive down vs Resistant
23	SOX12	0.00569	-2.281	Sensitive down vs Resistant
24	ZNFX1-AS1	0.00604	-2.482	Sensitive down vs Resistant
25	C2orf69	0.00622	2.038	Sensitive up vs Resistant

26	PTPN18	0.00634	2.635	Sensitive up vs Resistant
27	PRKD2	0.00641	3.5	Sensitive up vs Resistant
28	KHK	0.00662	2.484	Sensitive up vs Resistant
29	PAQR6	0.00710	-3.645	Sensitive down vs Resistant
30	HIST1H2BD	0.00763	-4.514	Sensitive down vs Resistant
31	CERK	0.00776	2.481	Sensitive up vs Resistant
32	UBE2K	0.00806	-2.048	Sensitive down vs Resistant
33	LYSMD1	0.00814	-2.379	Sensitive down vs Resistant
34	GPSM3	0.00832	5.309	Sensitive up vs Resistant
35	MNAT1	0.00906	-2.144	Sensitive down vs Resistant
36	WFS1	0.00911	2.397	Sensitive up vs Resistant
37	MYH9	0.00923	2.011	Sensitive up vs Resistant
38	CYTIP	0.00925	2.855	Sensitive up vs Resistant
39	SVIP	0.00928	2.148	Sensitive up vs Resistant
40	ARSA	0.00931	3.3	Sensitive up vs Resistant
41	SFMBT2	0.00947	2.111	Sensitive up vs Resistant
42	POLR3GL	0.00958	-2.251	Sensitive down vs Resistant

Table 3. Summary of correlation between predicted probabilities of PI-resistance vs observed PI cytotoxicity values

Random forest classification model was generated using HMCLs with top-6 + bottom-6 Ix-IC50 values as training dataset. Predicted probability values of HMCLs in the test dataset were rank-ordered and Somers' Dxy rank correlation analysis was performed between the top quantile/Q3 and bottom quantile/Q1 resistance probability values observed PI-chemosensitivity as a binary outcome (sensitive=0 vs resistance=1). Spearman rank-ordered correlation was performed in cell lines representing Q3 and Q1 probabilities of resistance and corresponding cytotoxicity values.

	Somers' c			**Spearman's rho**	
	c_{Q3}	**c_{Q1}**	**C_{Q3+Q1}**	**$Spearman_{Q3+Q1}$**	**P**
Bz_IC50	0.643	0.786	0.852	0.748	0.00036
Cz_IC50	0.714	0.524	0.750	0.563	0.00981
Opz_IC50	0.667	0.944	0.802	0.626	0.00548
Bz_AUSC	0.643	0.786	0.852	0.736	0.00050
Cz_AUSC	0.595	0.667	0.712	0.601	0.00507
Ix_AUSC	0.857	0.889	0.927	0.765	0.00009
Opz_AUSC	0.667	0.786	0.813	0.630	0.00509

Table 4. Summary of Somers' Dxy rank correlation analysis between predicted probability values of progression (derived from random survival forest model) and the progression index of MM patients from PI-based clinical trials (test datasets)

Transcriptomic profiling data from APEX trials was used as training dataset.

	Somers' c		
	c_{Q3}	**c_{Q1}**	**C_{Q3+Q1}**
HOVON-GMMG-HD4 (PAD Arm)	0.596	0.599	0.561
CoMMpass – Bz First-line therapy	0.705	0.469	0.595
CoMMpass – Len First-line therapy	0.320	0.203	0.262
Mayo-Ix	0.500	0.833	0.680
APEX-Dex Arm	0.365	0.467	0.431

Table S1. List of Human Myeloma Cell Lines (HMCLs) included in this study

Translocations and cyclin D expression (TC)-based classification system- 4=4;14 translocation involving MMSET/FGFR3; 11/6/12=Cyclin D1/3/2 IgH translocation; M = MAF.IgH; M.L,M.K &M.0=rearrangement with IgL,IgK, or no Ig; D2 = CYCLIN D2 expression without primary IgH TLC; 0 = no Ig TLC; low expression of all 3 Cyclin D genes

Cell lines	Number of Chromosomes	Translocations and cyclin D expression (TC)-based classification system	TC Group code
H929	45	4;14 translocation involving MMSET/FGFR3	4
JIM3	61	4;14 translocation involving MMSET/FGFR3	4
Kas6/1	70	4;14 translocation involving MMSET/FGFR3	4
KMS18	74	4;14 translocation involving MMSET/FGFR3	4
KMS26	75	4;14 translocation involving MMSET/FGFR3	4
KMS28PE	43	4;14 translocation involving MMSET/FGFR3	4
KMS34	71	4;14 translocation involving MMSET/FGFR3	4
LP1	80	4;14 translocation involving MMSET/FGFR3	4
OPM1	74	4;14 translocation involving MMSET/FGFR3	4
OPM2	74	4;14 translocation involving MMSET/FGFR3	4
PE2	72	4;14 translocation involving MMSET/FGFR3	4
UTMC2	77	4;14 translocation involving MMSET/FGFR3	4
XG7	43	4;14 translocation involving MMSET/FGFR3	4
KMM1	80	Cyclin D3 IgH translocation	6
FLAM76	42	Cyclin D1 IgH translocation	11
H1112	46	Cyclin D1 IgH translocation	11
Karpas620	68	Cyclin D1 IgH translocation	11
KMS12BM	77	Cyclin D1 IgH translocation	11
KMS12PE	77	Cyclin D1 IgH translocation	11
MMM1	47	Cyclin D1 IgH translocation	11
MOLP8	86	Cyclin D1 IgH translocation	11
OCIMY7	78	Cyclin D1 IgH translocation	11
SKMM2	37	Cyclin D1 IgH translocation	11
U266P/VR	39	Cyclin D1 IgH translocation	11
XG1	44	Cyclin D1 IgH translocation	11
AMO1	75	Cyclin D2 IgH translocation	12
DELTA47	45	CYCLIN D2 expression without primary IgH TLC	D2
FR4	100	CYCLIN D2 expression without primary IgH TLC	D2
JK6L	50	CYCLIN D2 expression without primary IgH TLC	D2
KHM1B	59	CYCLIN D2 expression without primary IgH TLC	D2
KMS20	41	CYCLIN D2 expression without primary IgH TLC	D2
KP6	47	CYCLIN D2 expression without primary IgH TLC	D2

MOLP2	NA	CYCLIN D2 expression without primary IgH TLC	D2
OCIMY1	49	CYCLIN D2 expression without primary IgH TLC	D2
ANBL6	82	MAF.IgH translocation	M
ARD	48	MAF.IgH translocation	M
ARP1	48	MAF.IgH translocation	M
ARP11c	48	MAF.IgH translocation	M
JJN3	60	MAF.IgH translocation	M
MM1S/VR	44	MAF.IgH translocation	M
OCIMY5	46	MAF.IgH translocation	M
SACHI	42	MAF.IgH translocation	M
SKMM1	79	MAF.IgH translocation	M
L363	46	No Ig rearrangement	M_0
KMS11	70	MAF.IgH translocation; 4;14 translocation involving MMSET/FGFR3	M_4
RPMI8226	60	rearrangement with IgL,	M_L
XG2	49	rearrangement with IgL,	M_L
XG6	77	rearrangement with IgL,	M_L

FIGURE 1

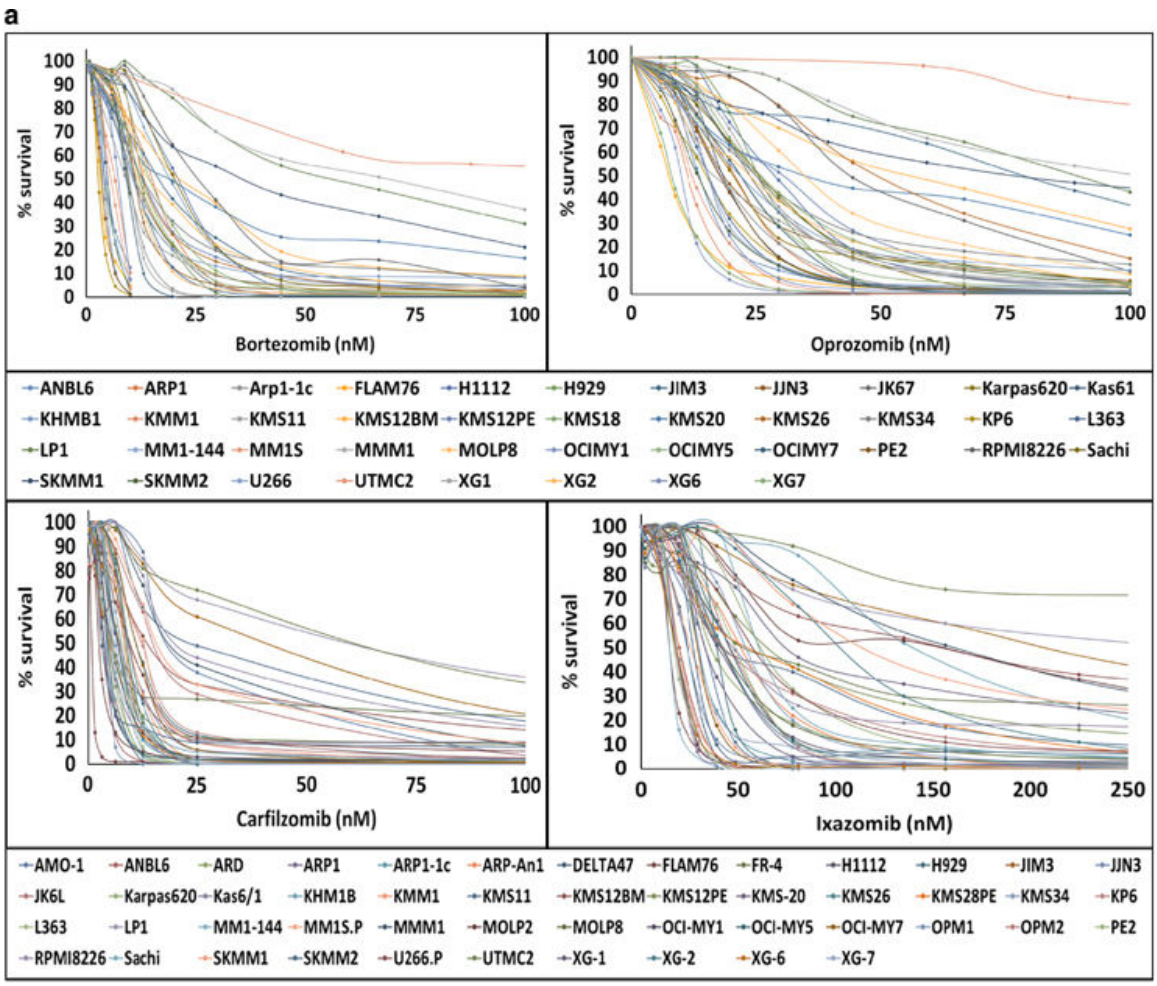
a
% survival
Bortezomib (nM)
Oprozomib (nM)
Carfilzomib (nM)
Ixazomib (nM)
ANBL6 ARP1 Arp1-1c FLAM76 H1112 H929 JIM3 JJN3 JK67 Karpas620 Kas61
KHMB1 KMM1 KMS11 KMS12BM KMS12PE KMS18 KMS20 KMS26 KMS34 KP6 L363
LP1 MM1-144 MM1S MMM1 MOLP8 OCIMY1 OCIMY5 OCIMY7 PE2 RPMI8226 Sachi
SKMM1 SKMM2 U266 UTMC2 XG1 XG2 XG6 XG7
AMO-1 ANBL6 ARD ARP1 ARP1-1c ARP-An1 DELTA47 FLAM76 FR-4 H1112 H929 JIM3 JJN3
JK6L Karpas620 Kas6/1 KHM1B KMM1 KMS11 KMS12BM KMS12PE KMS-20 KMS26 KMS28PE KMS34 KP6
L363 LP1 MM1-144 MM1S.P MMM1 MOLP2 MOLP8 OCI-MY1 OCI-MY5 OCI-MY7 OPM1 OPM2 PE2
RPMI8226 Sachi SKMM1 SKMM2 U266.P UTMC2 XG-1 XG-2 XG-6 XG-7

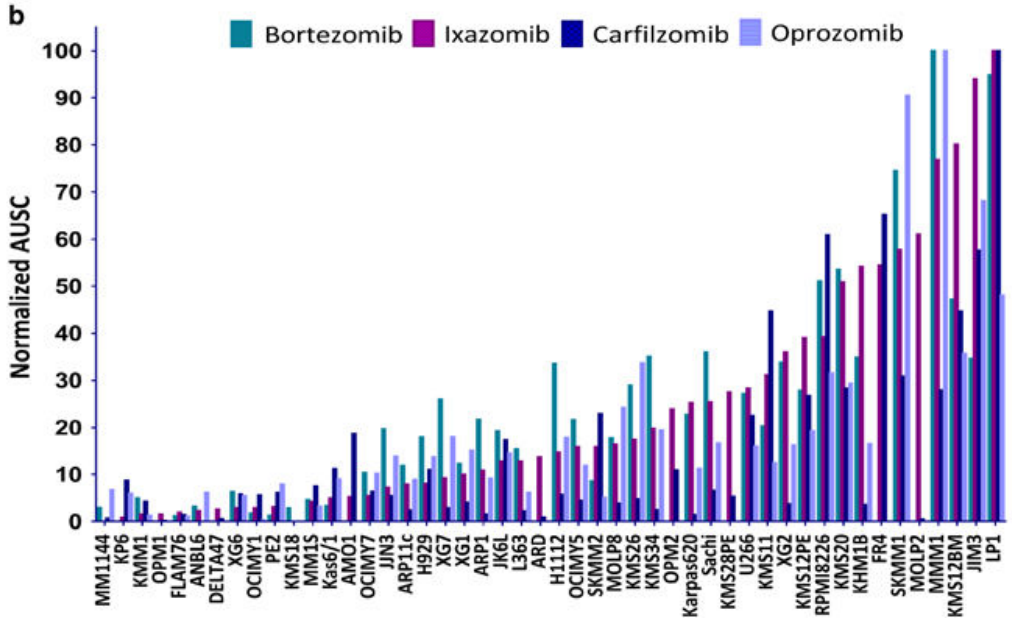
b
Bortezomib
Ixazomib
Carfilzomib
Oprozomib
Normalized AUSC
MM1144 KP6 KMM1 OPM1 FLAM76 ANBL6 DELTA47 XG6 OCIMY1 PE2 KMS18 MM1S Kas6/1 AMO1 OCIMY7 JJN3 ARP11c H929 XG7 XG1 ARP1 JK6L L363 ARD H1112 OCIMY5 SKMM2 MOLP8 KMS26 KMS34 OPM2 Karpas620 Sachi KMS28PE U266 KMS11 XG2 KMS12PE RPMI8226 KMS20 KHM1B FR4 SKMM1 MOLP2 MMM1 KMS12BM JIM3 LP1

FIGURE 1 continued

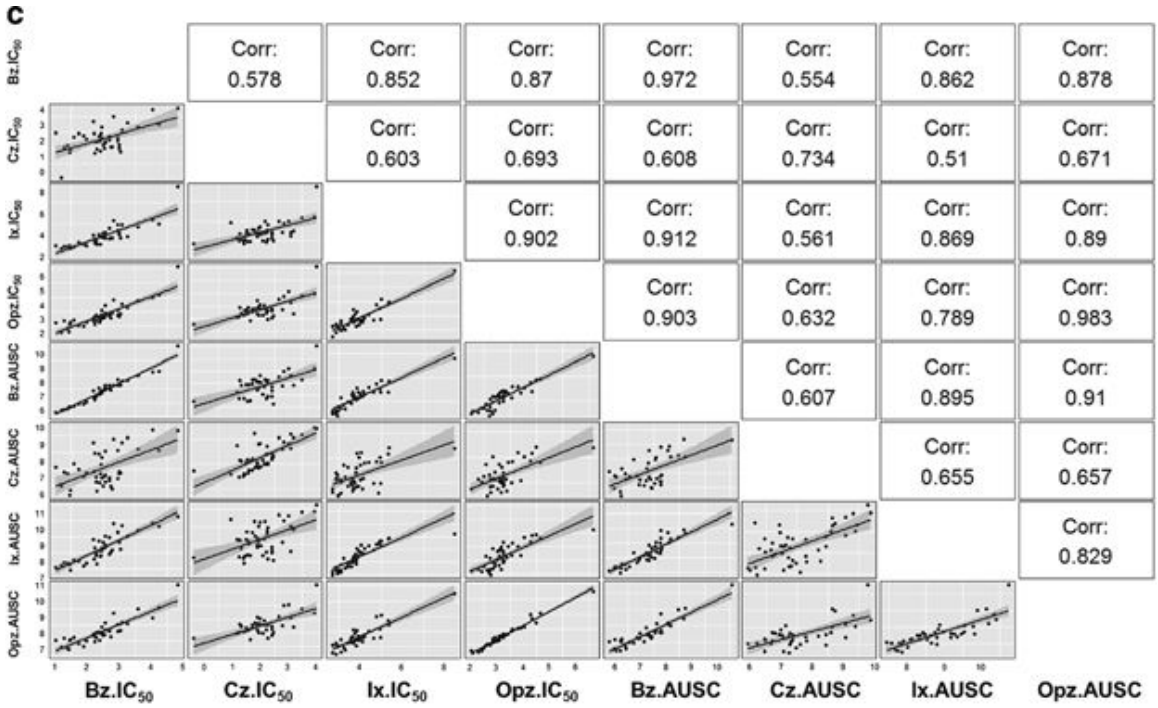

FIGURE 2

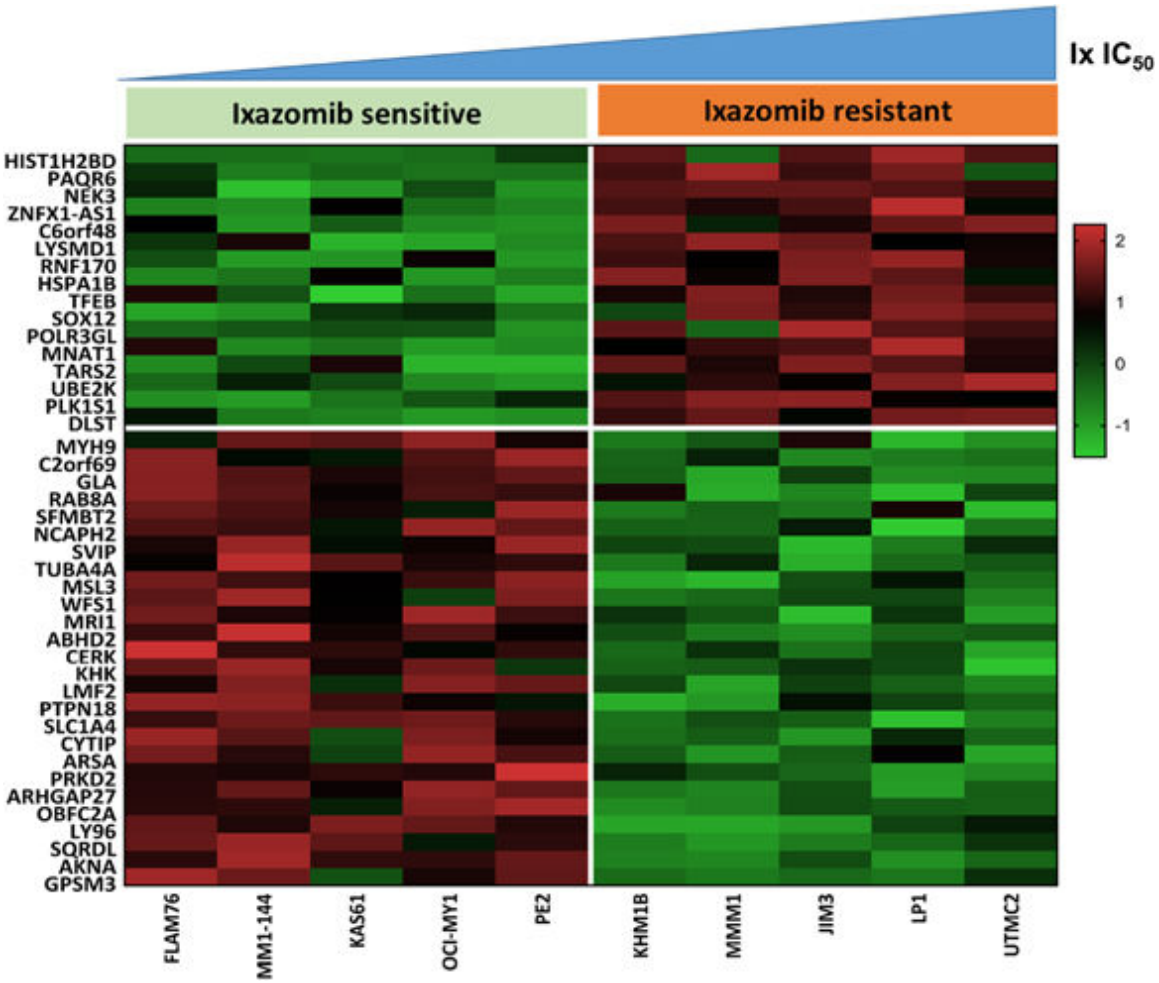
Ix IC50
Ixazomib sensitive
Ixazomib resistant
HIST1H2BD
PAQR6
NEK3
ZNFX1-AS1
C6orf48
LYSMD1
RNF170
HSPA1B
TFEB
SOX12
POLR3GL
MNAT1
TARS2
UBE2K
PLK1S1
DLST
MYH9
C2orf69
GLA
RAB8A
SFMBT2
NCAPH2
SVIP
TUBA4A
MSL3
WFS1
MRI1
ABHD2
CERK
KHK
LMF2
PTPN18
SLC1A4
CYTIP
ARSA
PRKD2
ARHGAP27
OBFC2A
LY96
SQRDL
AKNA
GPSM3
2
1
0
-1
FLAM76
MM1-144
KAS61
OCI-MY1
PE2
KHM1B
MMM1
JIM3
LP1
UTMC2

FIGURE 3

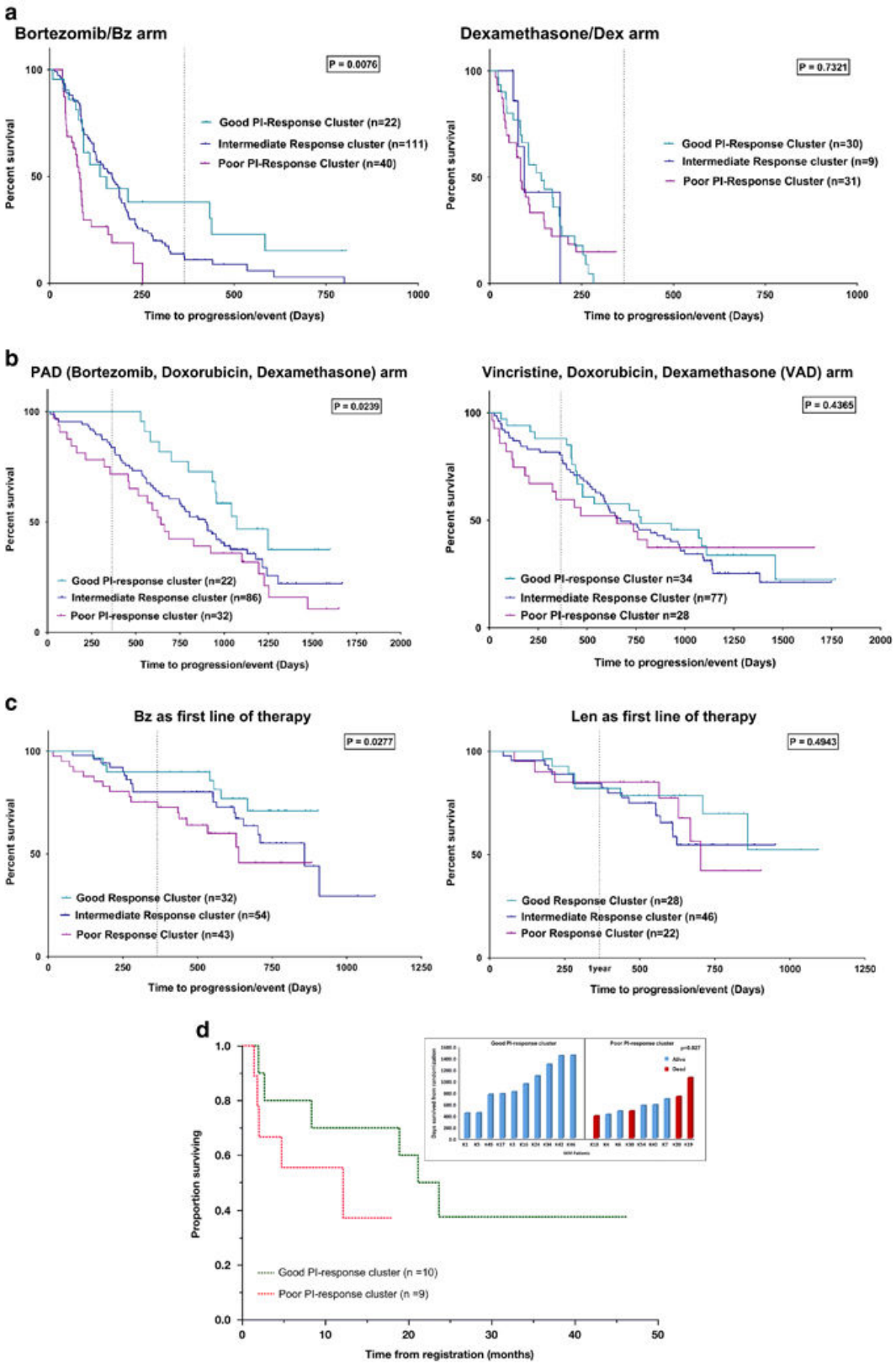
a
Bortezomib/Bz arm
P = 0.0076
Good PI-Response Cluster (n=22)
Intermediate Response cluster (n=111)
Poor PI-Response Cluster (n=40)
Percent survival
Time to progression/event (Days)
Dexamethasone/Dex arm
P = 0.7321
Good PI-Response Cluster (n=30)
Intermediate Response cluster (n=9)
Poor PI-Response Cluster (n=31)
b
PAD (Bortezomib, Doxorubicin, Dexamethasone) arm
P = 0.0239
Good PI-response cluster (n=22)
Intermediate Response cluster (n=86)
Poor PI-response cluster (n=32)
Vincristine, Doxorubicin, Dexamethasone (VAD) arm
P = 0.4365
Good PI-response Cluster n=34
Intermediate Response Cluster (n=77)
Poor PI-response Cluster n=28
c
Bz as first line of therapy
P = 0.0277
Good Response Cluster (n=32)
Intermediate Response cluster (n=54)
Poor Response Cluster (n=43)
Len as first line of therapy
P = 0.4943
Good Response Cluster (n=28)
Intermediate Response cluster (n=46)
Poor Response Cluster (n=22)
1year
d
Proportion surviving
Good PI-response cluster (n =10)
Poor PI-response cluster (n =9)
Time from registration (months)

FIGURE S1

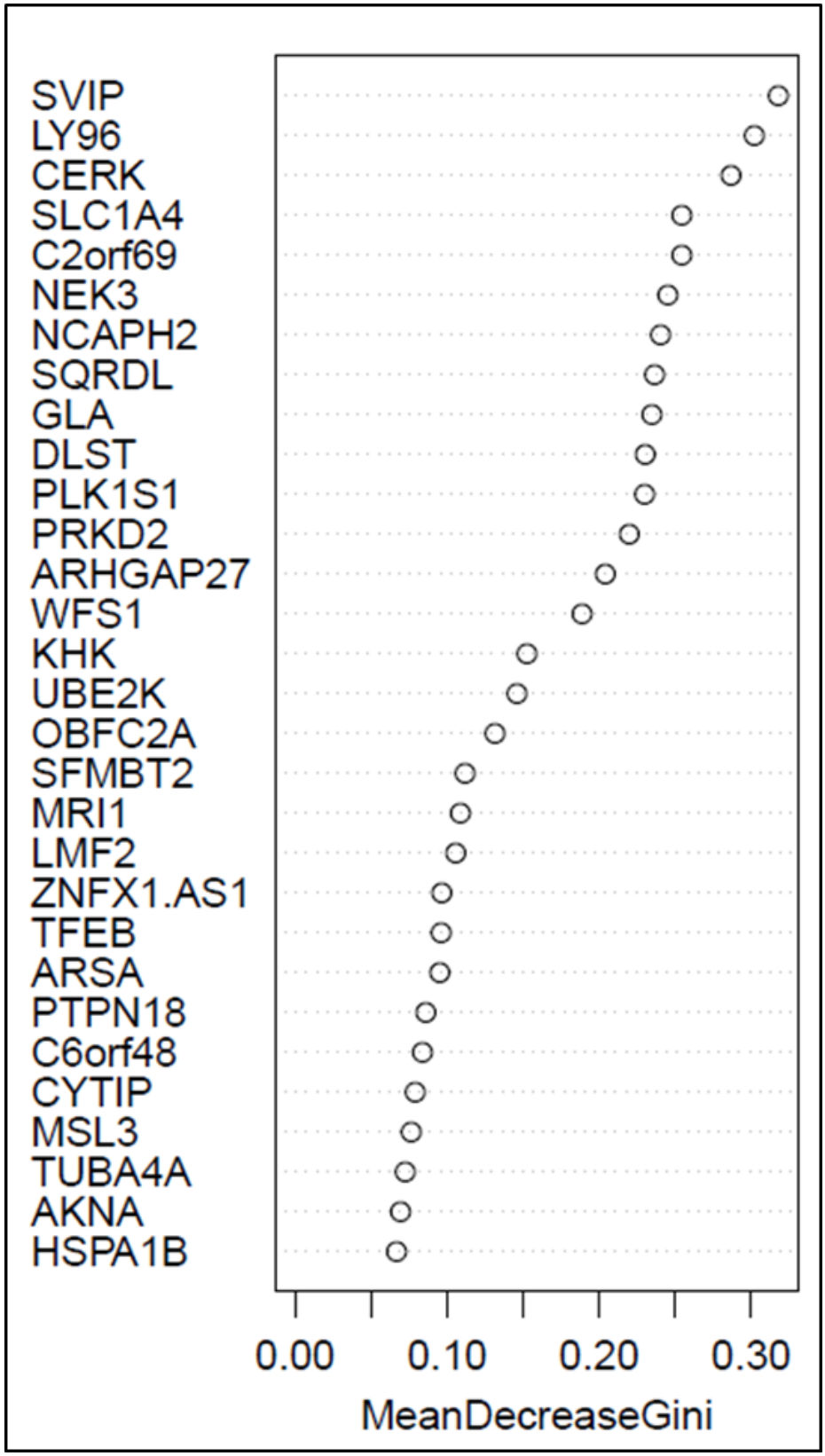
SVIP
LY96
CERK
SLC1A4
C2orf69
NEK3
NCAPH2
SQRDL
GLA
DLST
PLK1S1
PRKD2
ARHGAP27
WFS1
KHK
UBE2K
OBFC2A
SFMBT2
MRI1
LMF2
ZNFX1.AS1
TFEB
ARSA
PTPN18
C6orf48
CYTIP
MSL3
TUBA4A
AKNA
HSPA1B
0.00
0.10
0.20
0.30
MeanDecreaseGini

FIGURE S2

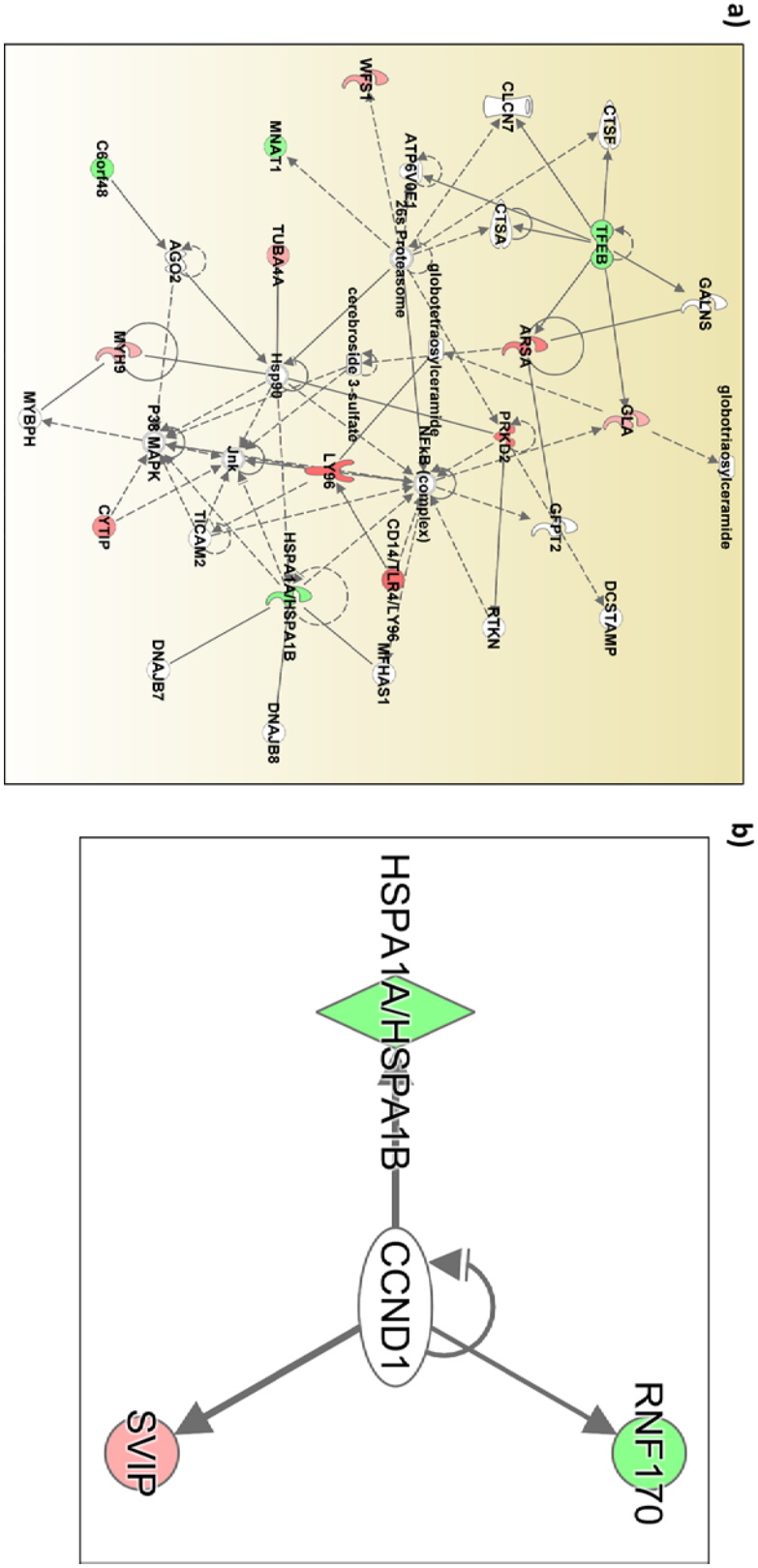
a)
WFS1
CLCN7
CTSF
ATP6V0E1
C6orf48
MNAT1
CTSA
TFEB
GALNS
26s Proteasome
globotetraosylceramide
AGO2
TUBA4A
ARSA
cerebroside 3-sulfate
MYH9
Hsp90
GLA
globotriaosylceramide
MYBPH
P38 MAPK
NFκB (complex)
PRKD2
Jnk
LY96
GFPT2
CYTIP
TICAM2
CD14/TLR4/LY96
DCSTAMP
HSPA1A/HSPA1B
RTKN
MFHAS1
DNAJB7
DNAJB8
b)
HSPA1A/HSPA1B
CCND1
RNF170
SVIP

CHAPTER 3

EZH2 INHIBITORS SENSITIZE MYELOMA CELL LINES TO PANOBINOSTAT RESULTING IN UNIQUE COMBINATORIAL TRANSCRIPTOMIC CHANGES

Authors:

Taylor Harding[1], Jessica Swanson[1], Brian Van Ness[1]*

1 Department of Genetics, Cell Biology & Development, University of Minnesota, Minneapolis, MN

*Corresponding Author

Conflict of Interest:

The authors have no conflicts of interest to disclose.

Author Contributions:

TH, JS and BVN conceived the study. TH conceived experiments, performed experiments, analyzed data and wrote the manuscript. JS collected preliminary data, performed some western blot experiments and analyzed data (Figure 1) under direct supervision of TH. BVN advised the study. JS and BVN contributed to editing of the manuscript.

Abstract:

Multiple myeloma (MM) remains a largely incurable hematologic cancer due to an inability to broadly target inevitable drug-resistant relapse. Epigenetic abnormalities are abundantly present in multiple myeloma and have increasingly demonstrated critical roles for tumor development and relapse to standard therapies. Accumulating evidence suggests that the histone methyltransferase EZH2 is aberrantly active in MM. We tested the efficacy of EZH2 specific inhibitors in a large panel of human MM cell lines (HMCLs) and found that only a subset of HMCLs demonstrate single agent sensitivity despite ubiquitous global H3K27 demethylation. Pre-treatment with EZH2 inhibitors greatly enhanced the sensitivity of HMCLs to the pan-HDAC inhibitor panobinostat in nearly all cases regardless of single agent EZH2 inhibitor sensitivity. Transcriptomic profiling revealed large-scale transcriptomic alteration by EZH2 inhibition highly enriched for cancer-related pathways. Combination treatment greatly increased the scale of gene expression change with a large portion of differentially expressed genes being unique to the combination. Transcriptomic analysis demonstrated that combination treatment further perturbed oncogenic pathways and signaling nodes consistent with an antiproliferative/pro-apoptotic state. We conclude that combined inhibition of HDAC and EZH2 inhibitors is a promising therapeutic strategy to broadly target the epigenetic landscape of aggressive MM.

Introduction:

Multiple myeloma (MM), a hematopoietic malignancy with over 30,000 new cases each year in the United States, is characterized by clonal expansion of malignant post-germinal-center B-cell-derived plasma cells within the bone marrow [3]. While current therapies including proteasome inhibitors and immunomodulatory drugs have improved disease management, MM remains largely incurable [231]. Heterogeneous patient response to therapy and the inevitable emergence of drug-resistant relapse impede long-term therapeutic efficacy. This illustrates the need for new therapeutic strategies that improve the efficacy of current compounds and more broadly target malignant plasma cells.

Epigenetic abnormalities are abundantly present in multiple myeloma (MM) and have increasingly demonstrated critical roles for tumor development and resistance to therapy [77,57,255,58,256]. Therapeutic strategies that target epigenetic modifiers have recently gained momentum in many cancers including recent FDA approval for the pan-HDAC inhibitor panobinostat (PAN) in MM [257,134,136].

Enhancer of zeste homolog 2 (EZH2), the catalytic subunit of the polycomb repressive complex 2 (PRC2), regulates the expression of thousands of genes to control developmental programs, maintain proliferative capacity and repress tumor suppressors in many forms of cancer [190,59,172,171,258–260]. EZH2's canonical function is to repress gene expression via methylation of H3K27, however, EZH2 has recently been shown to have several additional catalytic and non-catalytic functions that regulate transcription factor complexes and non-coding RNAs [171,160,162–165].

Following the initial observation that EZH2 is over expressed in aggressive myelomas [168,169], we demonstrated that EZH2 expression is driven by IL-6 and is required for the proliferation of growth-factor-independent human myeloma cell lines (HMCLs) harboring a *ras* mutation [170]. Since publishing these findings, corroborating evidence has accumulated suggesting that EZH2 is aberrantly active in MM and implicating EZH2 as a putative therapeutic target [186,147,185,183,182,179,184,180,152,261]. Characterization of recurring EZH2 activating mutations in lymphomas [174] has driven the recent development of several EZH2-specific

inhibitors (EZH2i's: e.g. EPZ6438, GSK126 and UNC1999) which avoid the off-target effects of non-specific histone methyl-transferases inhibitors (i.e. DZNep) previously used to study EZH2 [181,188,187,262,189,178].

Recent efforts to evaluate the efficacy of EZH2 inhibitors in MM have further described a complex EZH2-mediated regulatory network that modulates the expression of many functionally significant miRNAs, MM-associated oncogenes and cell adhesion pathways [183,179,184,152]. Despite these findings, specific mechanisms of EZH2i-mediated cytotoxicity in HMCLs and biomarkers that distinguish EZH2i-sensitive myelomas remain elusive. Further, it is not clear that EZH2 inhibition is an effective treatment strategy in all myelomas.

In the present study, we profile a large panel of HMCLs for EZH2i efficacy. We found that only a subset of HMCLs respond to single agent EZH2i, but all HMCLs respond to combination treatment with added HDAC inhibition. Additionally, comprehensive transcriptomic profiling of combination treatment reveals substantial changes in oncogenic pathways.

Materials and Methods:

Drugs:

Panobinostat/LBH-589(Novartis; Basel, Switzerland), GSK-126(GlaxoSmithKline; Brentford, U.K.) and Tazemetostat/EPZ-6438(Epizyme; Cambridge, MA) were purchased from Selleckchem (Panobinostat and EPZ-6438) and Cayman Chemical (GSK-126). All drugs were dissolved in DMSO (Sigma-Aldrich; St. Louis, MO) and stored at −20 °C.

Cell culture and viability assays:

Cell culture conditions for HMCLs used are previously described [263]. HMCLs were seeded at $4x10^5$ cells per ml in 96-well plates and were treated with the primary drug (EZH2i) after 24hrs. Secondary treatment (panobinostat) was added at a small volume (32x) to minimize dilution of the primary treatment. Cell viability was measured using a CellTiter-Glo luminescent viability assay (Promega; Madison, WI) and a Synergy 2 Microplate Reader (BioTek; Winooski, VT). For propidium iodine exclusion assays, plated HMCLs were transferred to round bottom 96-well plates (125µl/well), pelleted, resuspended in 200µl PBS containing 2µg propidium iodine, and propidium iodine staining was quantified using a BD FACSCantoII RUO Flow Cytometer (BD Biosciences; Franklin Lakes, NJ). Area under the survival curve (AUSC) was calculated using the trapezoidal method. Before AUSCs were compared to measure synergy each curve was individually normalized to the zero panobinostat condition. All viability data is normalized to untreated (i.e. media-treated) controls.

Histone analysis

Histones were isolated using a Histone Extraction Kit (Abcam; Cambridge, U.K.: ab113476). Extracted histone were western blotted for total H3 (CST; Danvers, MA: 96C10) and H3K27Me3 (CST: C36B11). Fluorescently labelled secondary antibodies (LICORE; Lincoln, NE: IRDye® 680RD and 800CW) were quantified with a LI-COR® fluorescence imager and densitometry was quantified in Image J (NIH).

Transcriptomic profiling and analysis

RNA was extracted (RNeasy Kit; QIAGEN) and stored in RNAlater™ (Invitrogen; Carlsbad, CA) at -80°C. Biological triplicates were subjected to RNA-sequencing (RNA-seq) on a

HiSeq 2000 (Illumina; San Diego, CA) using 50bp single-end reads at a depth of >10 million reads per replicate. Sequencing data was processed and analyzed for differential expression using Galaxy [264] downstream analysis was conducted using the R programing language and Ingenuity Pathway Analysis (IPA; QIAGEN; Venlo, Netherlands). Differential expression was considered significant with an FDR<0.05 and FPKM values ≥ 1 for at least one value (control or treated).

Results:

EZH2 inhibition reduces viability in a subset of human myeloma cell lines.

To evaluate the single agent efficacy of EZH2 inhibition as an anti-MM therapeutic strategy we treated a panel of 14 human myeloma cell lines (HMCLs) with the selective EZH2 inhibitors (EZH2i's) EPZ-6438 and GSK-126. Treatment with these compounds for 4 days or less was insufficient to induce substantial reduction in viability measured via CellTiter-Glo®. After 9 days of treatment, both compounds produced a consistent single agent response in a subset of cell lines (Figure 1a). These EZH2i sensitive cell lines demonstrated sensitivity at doses in the low micromolar range within a timeline consistent with others' observations [187]. We also tested the EZH1/2 dual inhibitor UNC1999 in many of these HMCLs and observed very similar cytotoxic responses compared with EPZ-6438 and GSK-126 and no added sensitivity in EZH2i resistant cell lines upon dual inhibition (data not shown).

To determine whether the lack of response in some HMCLs was due to a lack of target inhibition we extracted histones from treated cell lines to measure the relative abundance of global tri-methylated H3K27; a histone modification sufficient to measure global EZH2 catalytic activity [265]. Western blotting was performed on histones extracted from HMCLs treated with EZH2i's for 6 days. Dual fluorescent labelling of total H3 and H3K27me3 (Figure 1b) allowed us to quantify (Figure 1c) the relative change in H3K27 de-methylation at different doses relative to an untreated control. Both EZH2i-resistant HMCLs (MMM1 and H929) and EZH2i–sensitive HMCLs (FLAM76 and SKMM2) showed a large decrease in the relative abundance of H3K27me3 at doses well below 1μM, regardless of the effect on viability. Flam76 is a particularly sensitive cell line that is among the fastest to demonstrate viability loss after EZH2i treatment. This loss in viability explains the apparent decrease in detection of total H3 at higher EPZ-6438 doses. It is interesting to note that this loss of H3 detection occurs at higher doses (100-500nM) than doses required to reduce relative H3K27me3 (10-100nM).

EZH2 inhibitor pre-treatment synergistically enhances sensitivity to the pan-HDAC inhibitor panobinostat.

Despite heterogeneous HMCL response to EZH2i's, consistent changes in global H3K27 methylation led us to consider that global epigenetic changes induced by EZH2i's may sensitize HMCLs to other anti-MM compounds regardless of EZH2i single-agent response. To test this, we treated HMCLs with EZH2i's in combination with several classes of compounds including proteasome inhibitors, immunomodulatory compounds and glucocorticoid receptor agonists, all of which failed to demonstrate consistent synergistic toxicity with EZH2i's (data not shown). The pan-HDAC inhibitor panobinostat (Novartis), however, did consistently demonstrate a synergistic effect on HMCL viability. Initially, we found that simultaneously treating HMCLs with panobinostat and EZH2 inhibitors had little synergistic effect (Figure 2a). Pre-treating HMCLs with EZH2i's for several days, however, strongly enhanced the cytotoxicity of panobinostat (Figure 2b). This was evident even in cases where the single agent EZH2i had no significant effect on viability. We further confirmed that relative loss in viability was cytotoxicity by measuring viability after combination treatment using CellTiter-Glo® in tandem with propidium iodine exclusion staining and flow cytometry (Figure S1).

Many HMCLs lack a single agent response to EZH2i's and therefore we were unable to quantitatively compare this synergistic interaction across a panel of HMCLs using the common Chou-Talalay method for generating combination index plots [266]. We chose instead to compare synergy by calculating the relative drop in the area under the survival curve (AUSC) between dose response curves of panobinostat alone and panobinostat combined with a fixed dose of EZH2i (each curve normalized to untreated or EZH2i-only controls) (Figure 2a,b). We systematically evaluated the normalized panobinostat AUSC decrease produced by pre-treatment with either EPZ-6438 or GSK-126 across a panel of 24 HMCLs (Figure 2c). We found that pre-treatment with EZH2i's strongly enhance the toxicity of panobinostat in almost all cases with consistent results between the two EZH2i's. We additionally compared the effects of simultaneous EPZ-6438 treatment vs EPZ-6438 pre-treatment on panobinostat toxicity in the same HMCL panel (Figure S2). Pre-treatment with EZH2i's was nearly always more effective. One drawback to the AUSC decrease metric is that in a few cases where the EZH2i single agent response is particularly strong, normalization can exaggerate the change in the shape of the

curve and therefore exaggerate the AUSC change or suggest antagonism (i.e. SKMM2 and FLAM76). Despite this, it was clear that pre-treatment with EZH2i's had a strong dose-dependent effect (Figure 2d) on panobinostat efficacy regardless of EZH2i single agent toxicity across nearly all HMCLs tested.

Having evaluated EZH2i sensitivity in several panel experiments we identified the following HMCLs as having demonstrated consistent EZH2i single agent sensitivity: SKMM2, FLAM76, KMS12BM, L363, MOLP8, MM1-144, KAS61, MM1.S P and MM1.S VR. Overall our data did not suggest any trends between EZH2i sensitive and resistant HMCLs based on characterized genomic lesions including t(4;14), RAS mutation status and UTX/KDM6A mutation status (**Table S1**).

EPZ-6438 induces robust transcriptomic change as a single agent and in combination with panobinostat.

EZH2 and HDACs are both epigenetic regulators known to affect the expression of thousands of genes. We sought to determine if the enhanced cytotoxic response of the EZH2i/panobinostat combination is due to enhanced changes in the expression of a shared set of genes or if the combination produced a large set of gene expression changes that are unique to the combination. We selected 6 HMCLs to sample and screen for the ideal conditions to quantify transcriptomic changes via RNA-sequencing (RNA-seq): MMM1, SACHI, SKMM2, KMS20, KARPAS620 and FLAM76. These HMCLs were selected to represent EZH2i-sensitivity (SKMM2 & FLAM76) and EZH2i-resistance (MMM1, KARPAS620, KMS20 and SACHI). Samples were collected during days 0, 1, 2, 3, 4, 5.5 and 7 during treatment where EPZ-6438 (500nM or 5μM) or media was added at day 0 and panobinostat (two sub-IC50 concentrations per line experimentally determined during EZH2i pre-treatment) was added at day 4 as a single agent or as a combination with EPZ-6438 pre-treatment. We systematically evaluated these samples for viability and relative H3K27me3 levels (Figure S3) to identify the optimal doses and time points to submit paired samples for RNA-seq. Our results showed that demethylation of H3K27 was complete within the first three days regardless of EPZ-6438 dose. At that time SKMM2 and

FLAM76 also began to show a cytotoxic response to EPZ-6438. We chose to submit replicates for sequencing from MMM1 and FLAM76. We chose days 1, 4 and 5.5 that were treated with 5μM for EPZ-6438 and 3nM/20nM panobinostat (FLAM76/MMM1 respectively).

RNA-seq revealed large transcriptomic changes induced by EPZ-6438 (Figure 3a,b). Full differential expression data for each condition is provided as a supplemental file (File S1). Transcriptomic changes were minimal after one day of EZH2i treatment. This was expected given the time required for EZH2i-induced histone demethylation. 4 Days of treatment with EPZ-6438 produced much more substantial gene expression changes with a clear bias towards global upregulation of gene expression in both HMCLs, which was expected following inhibition of a negative regulator of transcription. Gene expression changes that appeared on day 5.5 of treatment were roughly between two and three times the number of differentially expressed genes seen at Day 4. The magnitude of this continued change was surprising, as we did not expect additional deregulation to occur days after the global H3K27me3 levels had reached a minimum. To confirm the specificity of our sequencing between different time points we compared the number of genes conserved between different EPZ-6438 single agent treatment times and found that most of the genes identified in an earlier time point also appeared at the following time point (Figure 3b).

Unfortunately, at the doses used, panobinostat only induced substantial gene expression changes in MMM1. While FLAM76 demonstrated little to no transcriptomic perturbation from panobinostat alone, the combination roughly doubled the number of differentially expressed genes measured from EPZ-6438 alone (758 to 1534 genes with at least a 2-fold expression change). MMM1 additionally demonstrated a very large increase in the number of genes effected by the combination over the two single agents. Comparing the overlap between the two single agent conditions with the combination it is clear that a large portion of differentially expressed genes identified in the combination are unique to the combination (Figure 3c). In both cell lines, at a fold change threshold of ±2 roughly 2/3 of differentially expressed genes in the combination condition were unique to the combination.

We were surprised at the low degree of overlap (consistently below 20-25%) between the two cell lines at all conditions examined. The 758 (FLAM76) and 510 (MMM1) differentially expressed genes at day 5.5 of EPZ-6438 single agent treatment only had 92 overlapping genes. Additionally, there were only 183 genes shared between the 1891(FLAM76) and 1063(MMM1) genes unique to the combination. Another recent study using microarray transcriptomic analysis profiling different MM cell lines in response to EZH2 inhibition also noted little consistency in the magnitude and content of transcriptomic response [183]. It may be that the substantial epigenetic heterogeneity between patient tumors may not yield a predictable gene expression profile in response to EZH2 inhibition.

Network analysis of EZH2i/HDACi transcriptomic profiles reveals highly enriched cancer-related pathways and regulators.

The magnitude of transcriptomic change in HMCLs treated with EPZ-6438, panobinostat and the combination required network analysis to identify higher order changes in established molecular pathways and functions. Ingenuity Pathway Analysis (IPA) [245] is a network analysis platform that can be queried with gene expression changes and return enriched network information from the QIAGEN knowledge base. Specifically, we considered significant enrichment of predicted upstream regulators (genes, groups or complexes), diseases/biological functions, and canonical pathways. We submitted filtered gene expression profiles (FDR<0.05 and |FC|>2) for all differential expression measurements and have included catalogs of all significant ($p<0.05$) hits returned (supplemental files S2-4). We compiled many of the top, contextually relevant hits into heat maps for each of the three analysis categories mentioned above (Figure 4a-c).

It has been proposed that EZH2 promotes MM development by regulating the expression of numerous oncogenes and tumor suppressors [183,182,179,180]. Consistent with this, we observed that many of the upstream regulators predicted from our transcriptomic profiling are key in promoting MM development. For example, CCND1, a core regulator of cell cycle progression, has recurrent mutations in MM and is a highly enriched as a predicted upstream regulator in our transcriptomic profiles. MYC, an aberrantly expressed transcription factor in many cancers

including MM [267], is enriched in most of our transcriptomic profiles, has significantly lowered expression(Figure 4d) upon treatment with single agent EPZ-6438/combination in both HMCLs, and is strongly predicted to be deactivated upon combination treatment in both lines. Several additional hits have also been previously proposed to directly or indirectly interact with EZH2 including NFKB [268], STAT1 [269], MYC [270,271], TP53 [258,268] and SMARCA4 [272]. IRF4, a late B-cell transcription factor, has recently been shown to facilitate EZH2i-sensitivity through BCL6-mediated downregulation in HMCLs harboring a UTX/KDM6A mutant background [152]. BCL6 is consistently enriched as a predicted upstream regulator in our data and IRF4 expression is downregulated upon combination treatment in both cell lines. It may be possible that the enhanced cytotoxicity of the combination treatment is due, at least in part, to synergistic regulation of key transcription factors such as IRF4 and MYC. Neither FLAM76 nor MMM1 have any known UTX/KDM6A mutations (J. Keats, personal communication) (**Table S1**).

Several upstream regulator hits had a strong prediction of activation/deactivation. For example TP53, TNF, IFNA, IFNG, STAT1 and EIF2AK2 were all predicted as being strongly activated in most conditions suggesting a decreased oncogenic state and increased sensitivity to pro-apoptotic signaling. Examples of regulators with predicted deactivation included BTK, MAPK1 and IRF4. BTK, a kinase critical for B-cell development, is a putative target in several cancers and BTK inhibitors have been shown to act synergistically with HDAC inhibitors in pre-clinical models of lymphoma [273]. While the modulation of these regulators may not be enough to drive cytotoxicity alone, they suggest a general reduction of the pro-growth/anti-apoptotic state of malignant plasma cells.

The diseases and biological functions output from IPA highlighted gene ontology enrichment in many expected areas including hematologic cancers and cell death. Many key genes involved in cell death had some of the highest fold-change expression differences and suggested an increased pro-apoptotic state in single agent EPZ-6438 and to an even higher degree in the combination. These genes included the upregulation of PMAIP1 (NOXA), XAF1 and CDKN1A (p21) and the downregulation of BCL2 and XBP1(Figure 4d). Terms related to cell

adhesion and movement were highly represented. Modulation of cell adhesion has previously been shown to be a consequence of EZH2 inhibition in MM [183].

Canonical pathway analysis yielded many results that reflected some of the same genes enriched in upstream regulators. Some of the strongest and most consistent enrichments included the interferon signaling pathway and the antigen presentation pathway, both of which were enriched after EPZ-6438 single agent treatment and the combination and have been shown to be directly modulated by EZH2 [269]. The interferon pathway has long been considered a target for therapeutic activation in MM [274]. Enrichment of this pathway was centered on the upregulation of STAT1 and most of its downstream promotor targets. The antigen presentation pathway showed a consistent increase in the upstream transcriptional coactivator CIITA and downstream MHC class II genes (Figure 4d). MHCII genes were among others enriched in the B-cell development pathway where other B-cell markers were upregulated.

While there were many consistent enrichments observed with EPZ-6438 single-agent treatment between lines there were few similarities when genes unique to the combination were submitted to IPA. A few exceptions to this include the predicted upregulation of the 'sirtuin signaling pathway' and enrichment of the 'Endoplasmic Reticulum Stress Pathway', 'Mitochondrial Dysfunction' and 'tRNA Charging' pathways. Another consistency between both unique-to-combination genes was the strong predicted activation of cell death and apoptosis related ontology terms.

In general, network analysis of EZH2i-induced gene expression changes revealed a consistent modulation of cancer-related pathways in a manner suggesting a less growth-promoting state. The combination with panobinostat indicated strong predictions of cell-stress/death in addition to further perturbation of the pathways identified in the single agents. While many of these factors were previously known to be downstream of EZH2 inhibition, the combination with panobinostat illuminated an enhanced augmentation of tumor-promoting pathways as well as several enriched results unique to the combination.

Discussion:

Recent development of EZH2-specific inhibitors has prompted several studies evaluating the efficacy of EZH2 inhibition in HMCLs. Several of these studies have identified significant pathways and regulators that are modulated in HMCLs upon EZH2 inhibition including contextually relevant oncogenes/tumor suppressors [183,179,184,152], novel miRNAs [179], cell-to-cell adhesion/mobility [183] and dysregulation of cell cycle control [180]. Our evaluation of a large panel of HMCLs for single agent cytotoxic response to EPZ-6438 and GSK-126 recapitulated previously described dose and temporal thresholds for cytotoxicity in HMCLs. Other studies that have evaluated EZH2i's in HMCLs have measured baseline EZH2 protein levels and did not demonstrate a correlation with single agent sensitivity [183,180]. Some recent studies have proposed that certain subsets of MM are sensitive to EZH2 inhibition such as MM cases harboring recurring UTX/KDM6A loss-of-function mutations or recurring t(4:14) translocation, both of which are known to directly impact modification EZH2's target residue and alter EZH2 distribution respectively [152]. The relative sensitivity and resistance for HMCLs that were shared between our evaluation and that of others was generally consistent. In HMCLs not examined by others, predictions of sensitivity based on subtype were consistent in some cases (sensitivity in UTX mutant KMS12, L363 and t(4:14) containing KAS61) and inconsistent in others (resistance in t(4:14) containing OPM2, PE2, H929, JIM3 as well as UTMC2 that contains both t(4:14) and UTX lesions) (**Table S1**). As speculated by others [152], these specific lesion may be sufficient to distinguish sensitivity in certain genomic/epigenomic contexts, however other factors clearly play a role in effecting single agent sensitivity.

To our knowledge, we are the first to report enhancement of HMCL sensitivity to panobinostat via EZH2i pre-treatment. Panobinostat has recently been approved for use in refractory MM, however its therapeutic benefit has been modest [134]. Therefore, combination therapies that enhance HDACi efficacy could have great therapeutic benefit. We found that this synergistic interaction did not require EZH2i single agent sensitivity. This synergistic interaction has been explored in other cancer contexts [275–277] however the combination has yet to be applied in any clinical trials. Encouragingly, one study found that combining panobinostat with a

non-specific inhibitor of methyltransferase activity (DZNep) was tolerated in a murine xenograft model of AML [278] suggesting that EZH2i/panobinostat combination may not produce undue *in vivo* toxicity.

We were surprised by how many EPZ-6438-induced transcriptomic changes were observed well after global H3K27 levels had reached a minimum. Extensive global/temporal profiling of chromatin will be required to determine if these final expression changes are direct effects of EZH2i or if they are rather pleiotropic fallout from the substantial epigenetic modification. We have postulated that upregulating the expression of so many genes may result in some non-specific toxicity. This could, in part, explain consistent toxicity of the combination treatment despite an apparent lack of overlap between differentially expressed genes. With a more lenient 1.5 fold-change threshold, combination treatment in FLAM76 and MMM1 showed as much as a roughly 15% and 22% significant differential expression of the queried genome. While the contribution of non-specific transcriptomic stress remains speculative, it is clear is that the combination of the two inhibitors upregulated a large set of genes that were unique to the combination. This suggests that PRC2 and HDACs likely cooperate to silence a large portion of the genome and that this cooperation may be essential for the survival of myelomas that exploit aberrant PRC2 activity.

Our network analysis largely corroborated findings that EZH2 inhibition leads to a robust upregulation of tumor suppressors and concomitant downregulation of oncogenic pathways. These pathways included key regulators of cell-to-cell interaction, antigen presentation, differentiation, apoptosis, cell cycle progression, metabolism and central signaling nodes such as MYC and TP53. MYC, a classic anti-cancer target for which there is no selective small compound inhibitor, seems to be particularly implicated in recent literature describing the anti-cancer effects of EZH2 inhibition [258,179,152,270,271]. It remains unclear if these factors and pathways directly induce cytotoxicity in combination treatment or if the combined transcriptomic change pushes HMCLs towards a more apoptosis-permissive state that is perturbed by the direct toxicity of panobinostat.

The magnitude of transcriptomic change and network analysis hits, both shared and distinct between the two lines, in addition to the low degree of overlap between the two lines presents a challenge in discerning definitive biomarkers for EZH2i sensitivity. Any attempt to define a consistent consensus EZH2i gene expression profile in HMCLs or to identify biomarkers for sensitivity would require a much more exhaustive transcriptomic profiling of a large panel of HMCLs. Even in that case, we speculate, as others have [183], that identifying a predictive signature or single sensitivity biomarker for a highly networked regulator targeting thousands of genes in an extremely epigenetically heterogeneous disease background is a dubious prospect. Despite these challenges towards defining the scope of PRC2/HDAC interaction specific to MM, accumulating evidence suggests a generalized effect including downregulation of oncogenic pathways and upregulation of tumor suppressors. This leads to either direct cytotoxicity or sensitization of HMCLs to combination therapies in a targeted manner.

In conclusion, our data suggests that while only a subset of human myeloma cell lines respond to EZH2 inhibition, nearly all lines tested were effectively targeted for cell death through a synergistic combination of panobinostat and EZH2 inhibitor pre-treatment. This combination was effective at lowering the therapeutic threshold of panobinostat even in cases where there was no single agent EZH2 inhibitor response. Transcriptomic analysis of single agents and combination treatments corroborates the regulation of many oncogenic pathways towards a less growth-promoting state and reveals a large transcriptomic response unique to the drug combination. These data support the further evaluation of therapeutic combination to broadly target aggressive MM in *in vivo* and clinical contexts.

Acknowledgements:

We gratefully acknowledge the expert technical support provided by the University of Minnesota Genomics Center. We gratefully acknowledge the laboratory of Jonathan Keats, Ph.D. for information provided regarding human myeloma cell line mutation/translocation statuses.

Conflicts of Interest

None

Supplementary information:

Supplemental figures and tables appear below. Supplementary data files are included with the submission of this thesis:

Supplemental file descriptions:

- **File S1**(.xlsx): Full differential expression results from RNA-seq experiments in both cell lines. Each differential expression condition (treatment vs untreated control) is on its own tab. In each tab genes with no detectable expression in either control or treatment have been removed. Infinite (positive or negative) 'log2.fold.change' values are represented by '#NUM!' in .xlsx format.
- **File S2**(.xlsx): Full catalog of Ingenuity Pathway Analysis (QIAGEN) results: canonical pathway analysis. Each differential expression condition (treatment vs untreated control) is on its own tab. Activation z-scores absent when not provided by IPA.
- **File S3**(.xlsx): Full catalog of Ingenuity Pathway Analysis (QIAGEN) results: upstream regulator analysis. Each differential expression condition (treatment vs untreated control) is on its own tab. Activation z -scores absent when not provided by IPA.
- **File S4**(.xlsx): Full catalog of Ingenuity Pathway Analysis (QIAGEN) results: disease and biological functions analysis. Each differential expression condition (treatment vs untreated control) is on its own tab. Activation z -scores absent when not provided by IPA.

Figure legends:

Figure 1: EZH2 inhibition induces H3K27 demethylation in all HMCLs and decreases viability in a subset of HMCLs.

(**a**) A panel of 14 HMCLs were treated with a concentration range of EZH2 inhibitors EPZ-6438 and GSK-126 for either 4 or 9 days. Viability was measured with CellTiter-Glo® (Promega) assays and normalized to untreated controls. (**b**) H3K27 demethylation was quantified after a 6 day treatment with a range of EZH2 inhibitors in two EZH2i-sensitive (FLAM76 and SKMM2) and two EZH2i-resistant (MMM1 and H929) HMCLs. H3K27me3 was quantified by western blot where total histone 3 (mouse anti-H3; CST#3638) and H3K27me3 (rabbit anti-H3K27me3; CST#9733) were simultaneously quantified via a LI-COR® fluorescence reader. Relative densitometry (**c**) was calculated for each EZH2i concentration and normalized to the untreated control. All error bars represent SEM between biological replicates.

Figure 2: EZH2 inhibitor pre-treatment sensitizes HMCLs to panobinostat in a dose-dependent manner.

HMCLs were treated with a combination of the pan-HDAC inhibitor panobinostat and EZH2 inhibitors GSK-126 or EPZ-6438. Viability was measured via CellTiter-Glo® and normalized to untreated controls. Two treatment schedules (represented by schematics in (**a**) and (**b**)) were applied and data is represented in the HMCL UTMC2 where EPZ-6438 was either combined with panobinostat simultaneously (**a**) or 5 days prior to panobinostat (**b**). Bar plots represent a measurement of synergy quantified by the decrease in the area under the survival curve (AUSC) between panobinostat single agent treatment and combination treatment (where AUSC of each EZH2i+pan/CTRL+pan dose response curve is normalized separately to isolate the shape of the curve from single agent EZH2i toxicity). (**c**) A panel of HMCLs (n = 24) were treated with panobinostat for 48hrs after a 4-day pre-treatment with either GSK-126 or EPZ-6438. The resulting synergy is represented as decrease in normalized AUSC across the HMCL panel. (**d**) Three HMCLs representing three levels of EZH2i sensitivity (none, minimal and strong) were pre-

treated with a range of EPZ-6438 concentrations for 7 days followed by treatment with a constant range of panobinostat for 48hrs. Viability was measured via CellTiter-Glo®. All error bars represent SEM between biological replicates.

Figure 3: Transcriptomic profiling of EPZ-6438/Panobinostat single agents and combination.

(**a**) All significant (FDR<0.05, FPKM≥1) gene expression changes for two HMCLs (FLAM76 & MMM1) treated with EPZ-6438 (5μM for 1,4 or 5.5 days) and/or panobinostat (FLAM76-3nM;MMM1-20nM for 1.5 days after 4 days EPZ-6438/media pre-treatment). Infinite/negative-infinite fold change values (i.e. 0 FPKM relative to 10 FPKM) display the same color saturation as the finite minimum or maximum fold change value. (**b**) Pie charts each representing the total number (center) of upregulated (red) and downregulated (green) genes (FDR<0.05, FPKM≥1) for each treatment condition. At each condition two fold change thresholds are displayed (|FC|≥2 above and |FC|≥2 below) for both HMCLs as well as for the overlap in significant gene expression changes for each condition/threshold between the two HMCLs. Arrowed lines between sampling days display the number of upregulated (red arrow) and downregulated (green arrow) genes shared between the three different EPZ-6438 single agent sampling times. (**c**) Venn Diagrams displaying genes shared between the day 5.5 EPZ-6438, panobinostat and combo differential expression conditions as well as the genes unique to the combination. The dotted arrow/number represent genes unique to the combination that are shared between the two HMCLs.

Figure 4: Ingenuity Pathway Analysis of EPZ-6438-, panobinostat-, and combination-induced gene expression changes.

Filtered differential gene expression profiles (FPKM≥1, |FC|≥2,FDR<0.05) for two HMCLs (FLAM76 & MMM1) treated with EPZ-6438(μM), panobinostat(FLAM76-3nM;MMM1-20nM) or the combination (relative to time-matched untreated control) were subjected to Ingenuity Pathway Analysis (IPA). Heat maps represent selected top results from different types of IPA analysis: (**a**) predicted upstream regulators (genes, groups or complexes), (**b**) enriched disease and biological functions and (**c**) enriched canonical pathways. Each differential expression condition is

represented by two columns. The left column displays the –log10(p-value) returned by IPA for enrichment and the right column displays the predicted activation z-score (when applicable; not all predictions have activation directionality). Analysis of unique-to-combination (UTC) genes subsetted from the combination condition for each line is also displayed. White heat map cells represent a lack of significant enrichment/prediction ($p>0.05$ and $|z|<2$ respectively). Grey heat map cells represent missing activation z-scores when p-values are significant. (d) differential expression (RNA-seq: log2 fold change) across all conditions for selected genes pertinent to top IPA hits and discussed in text. Only gene expression changes significant at FDR<0.05 and |fc|>1.5 are displayed.

Figure S1: Cytotoxicity of EZH2i and Panobinostat combination is confirmed via propidium iodine exclusion assay.

Four HMCLs seeded in 96-well plates were treated for 48hrs with either panobinostat or the protesome inhibitor bortezomib (Takeda). These treatments were preceded by a 5-day treatment with either 5μM EPZ-6438 (panobinostat only) or media. After the 48hr secondary treatment plates were sampled and assayed for viability by both CellTiter-Glo® (**a**) and propidium iodine (PI) staining followed by flow cytometry (**b**) in tandem. All error bars represent SEM between biological replicates.

Figure S2: EPZ-6438 sensitizing of HMCLs to panobinostat is consistently more effective as a pre-treatment across an HMCL panel.

24 HMCLs were either pre-treated with EPZ-6438 for 5 days followed by a 48hr panobinostat treatment (“pre-treated”) or they were pre-treated with media for 5 days followed by a 48hr simultaneous treatment with EPZ-6438 and panobinostat. In both cases two doses of EPZ-6438 were evaluated (0.5μM & 5μM). Viability was measured via CellTiter-Glo® and synergy is represented by the decrease in normalized AUSC between single agent panobinostat and the combination treatment. Negative values represent an increase in normalized AUSC.

Figure S3: Time-course measurement of H3K37 demethylation and cell viability after treatment with EPZ-6438, panobinostat and the combination in 6 HMCLs.

6 HMCLs (MMM1, SACHI, SKMM2, KMS20, KARPAS620 and FLAM76) were sampled at 0, 1, 2, 3, 4, 5.5 and 7 days post-treatment with 500nM EPZ-6438, 5μM EPZ-6438 or media (untreated control). Cells additionally treated with panobinostat (single agent and combined with EPZ-6438 4 day pre-treatment) on day 4 in this sampling schedule were harvested on days 5.5 and 7. Samples were either (**a**) immediately measured for viability via CellTiter-Glo® (normalized to time-matched untreated control) or subjected to histone-purification and storage at -80^{o}C. Frozen histone preparations were later western blotted and quantified (**b**) for H3K27me3 abundance (each sampling day normalized to total H3).

Table S1: List of human myeloma cell lines used in this study with annotated UTX/KDM6A, RAS and t(4;14) status

'ND' = no data. 'WT' = wild type. Zygosity is not specified in every case. HMCL status data is sourced from the Keat's lab repository (http://www.keatslab.org/data-repository) and recently published data [152]. HMCLs demonstrating consistent sensitivity to EZH2 inhibition in our experiments appear below in red.

MM cell line	UTX/KDM6A status	RAS status	t(4;14)
ARD	Homozygous mutation	ND	No
ARP1-1C	WT	WT	No
DELTA97	WT	WT	No
FLAM76	WT	WT	No
H929	WT	NRAS mutation	Yes
JIM3	WT	KRAS mutation	Yes
KARPAS620	WT	KRAS mutation	No
KAS61	WT	WT	Yes
KMS12BM	mutation	WT	No
KMS20	WT	KRAS mutation	No
KMS28PE	Homozygous mutation	KRAS heterozygous mutation	Yes
L363	mutation	NRAS mutation	No
MM1.S	WT	KRAS mutation	No
MM1.S VR	WT	KRAS mutation	No
MM1-144	ND	ND	ND
MMM1	WT	NRAS mutation	No
MOLP8	WT	NRAS mutation	No
OCIMY1	WT	KRAS mutation	No
OPM2	WT	FGFR3 mutation	Yes
PE2	WT	NRAS mutation	Yes
SACHI	WT	WT	No
SKMM1	WT	NRAS mutation	No
SKMM2	WT	WT	No
U266	WT	BRAF mutation	No
U266 VR	WT	BRAF mutation	No
UTMC2	Homozygous mutation	WT	Yes

FIGURE 1

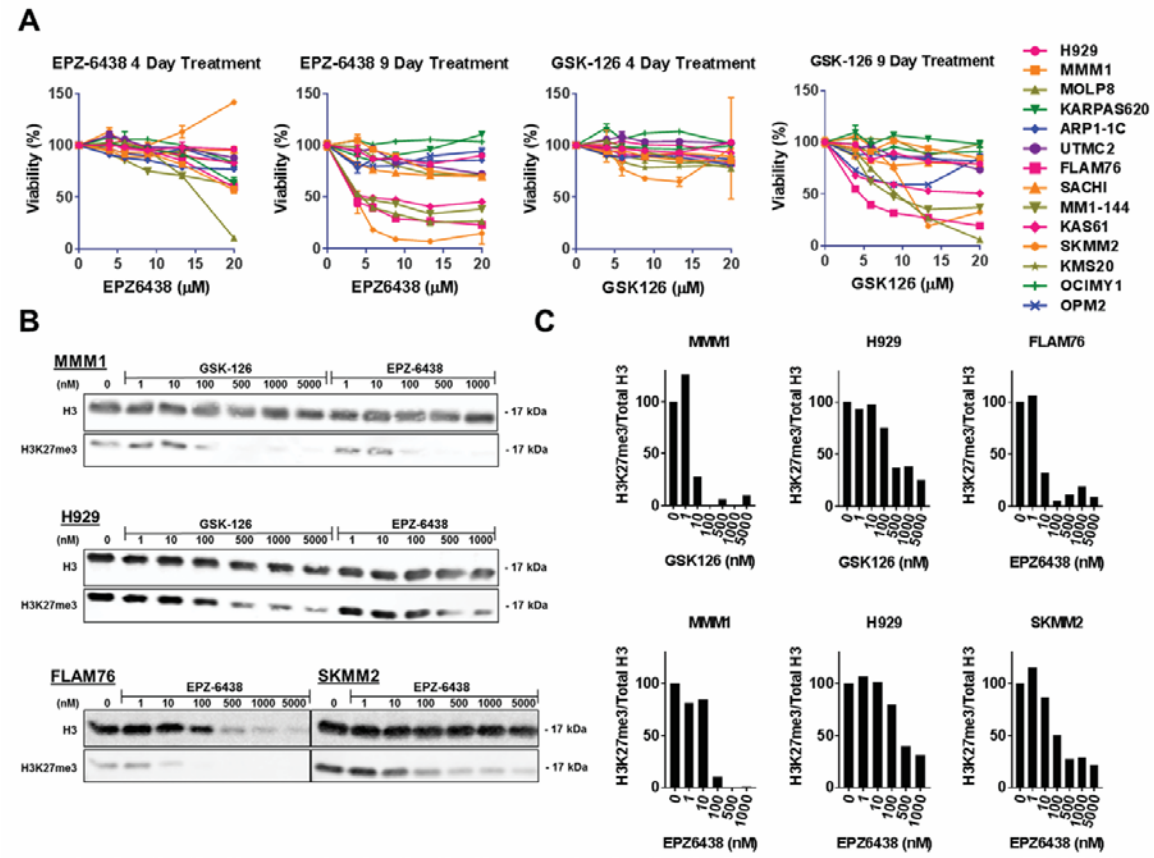
A
EPZ-6438 4 Day Treatment
EPZ-6438 9 Day Treatment
GSK-126 4 Day Treatment
GSK-126 9 Day Treatment
Viability (%)
EPZ6438 (μM)
GSK126 (μM)
H929
MMM1
MOLP8
KARPAS620
ARP1-1C
UTMC2
FLAM76
SACHI
MM1-144
KAS61
SKMM2
KMS20
OCIMY1
OPM2
B
MMM1
H929
FLAM76
SKMM2
GSK-126
EPZ-6438
(nM)
H3
H3K27me3
- 17 kDa
C
MMM1
H929
FLAM76
SKMM2
H3K27me3/Total H3
GSK126 (nM)
EPZ6438 (nM)

FIGURE 2

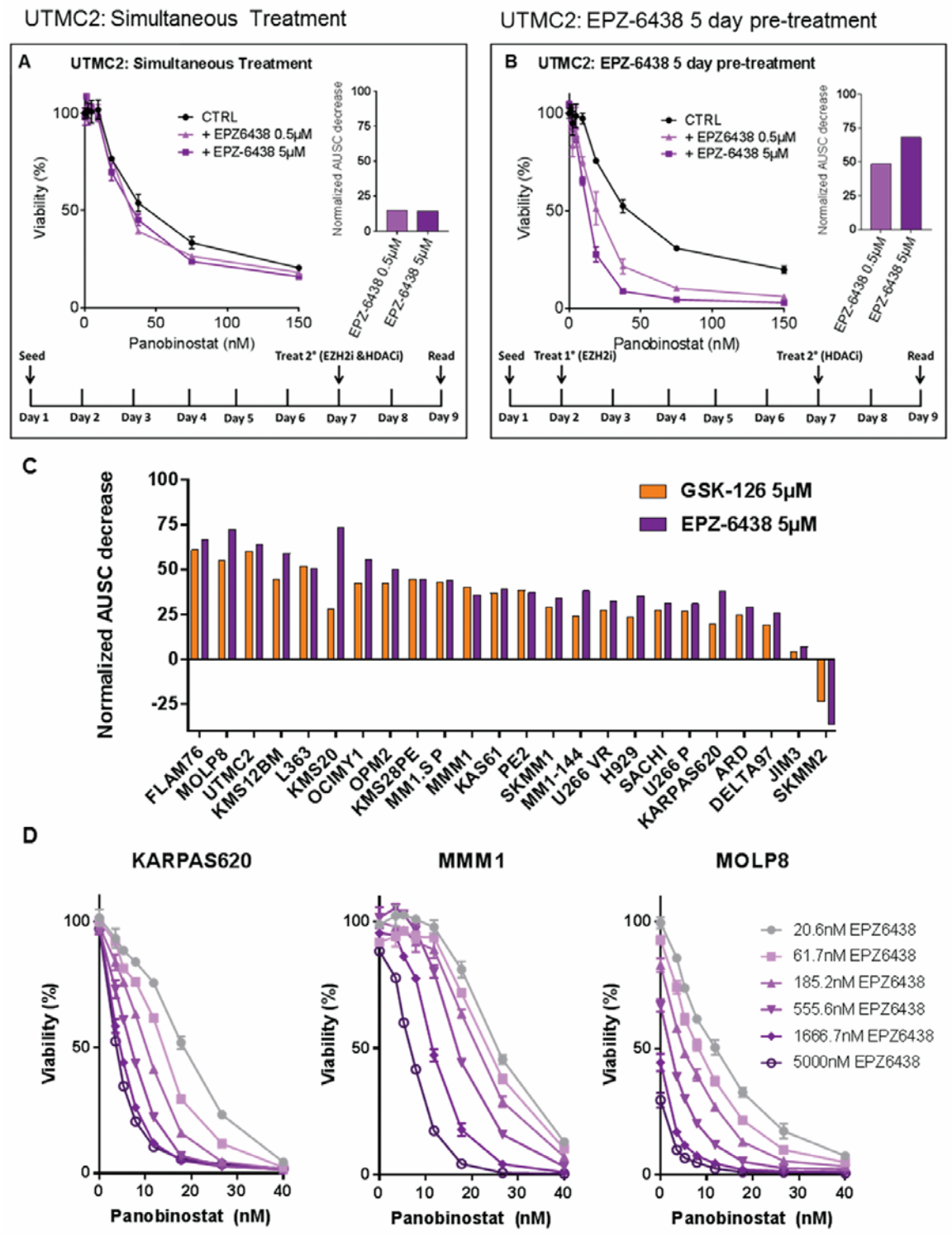
UTMC2: Simultaneous Treatment
UTMC2: EPZ-6438 5 day pre-treatment
A
UTMC2: Simultaneous Treatment
CTRL
+ EPZ6438 0.5μM
+ EPZ-6438 5μM
Viability (%)
Panobinostat (nM)
Normalized AUSC decrease
EPZ-6438 0.5μM
EPZ-6438 5μM
Seed
Treat 2° (EZH2i &HDACi)
Read
Day 1
Day 2
Day 3
Day 4
Day 5
Day 6
Day 7
Day 8
Day 9
B
UTMC2: EPZ-6438 5 day pre-treatment
Treat 1° (EZH2i)
Treat 2° (HDACi)
C
Normalized AUSC decrease
GSK-126 5μM
EPZ-6438 5μM
FLAM76
MOLP8
UTMC2
KMS12BM
L363
KMS20
OCIMY1
OPM2
KMS28PE
MM1.S P
MMM1
KAS61
PE2
SKMM1
MM1-144
U266 VR
H929
SACHI
U266 P
KARPAS620
ARD
DELTA97
JIM3
SKMM2
D
KARPAS620
MMM1
MOLP8
20.6nM EPZ6438
61.7nM EPZ6438
185.2nM EPZ6438
555.6nM EPZ6438
1666.7nM EPZ6438
5000nM EPZ6438

FIGURE 3

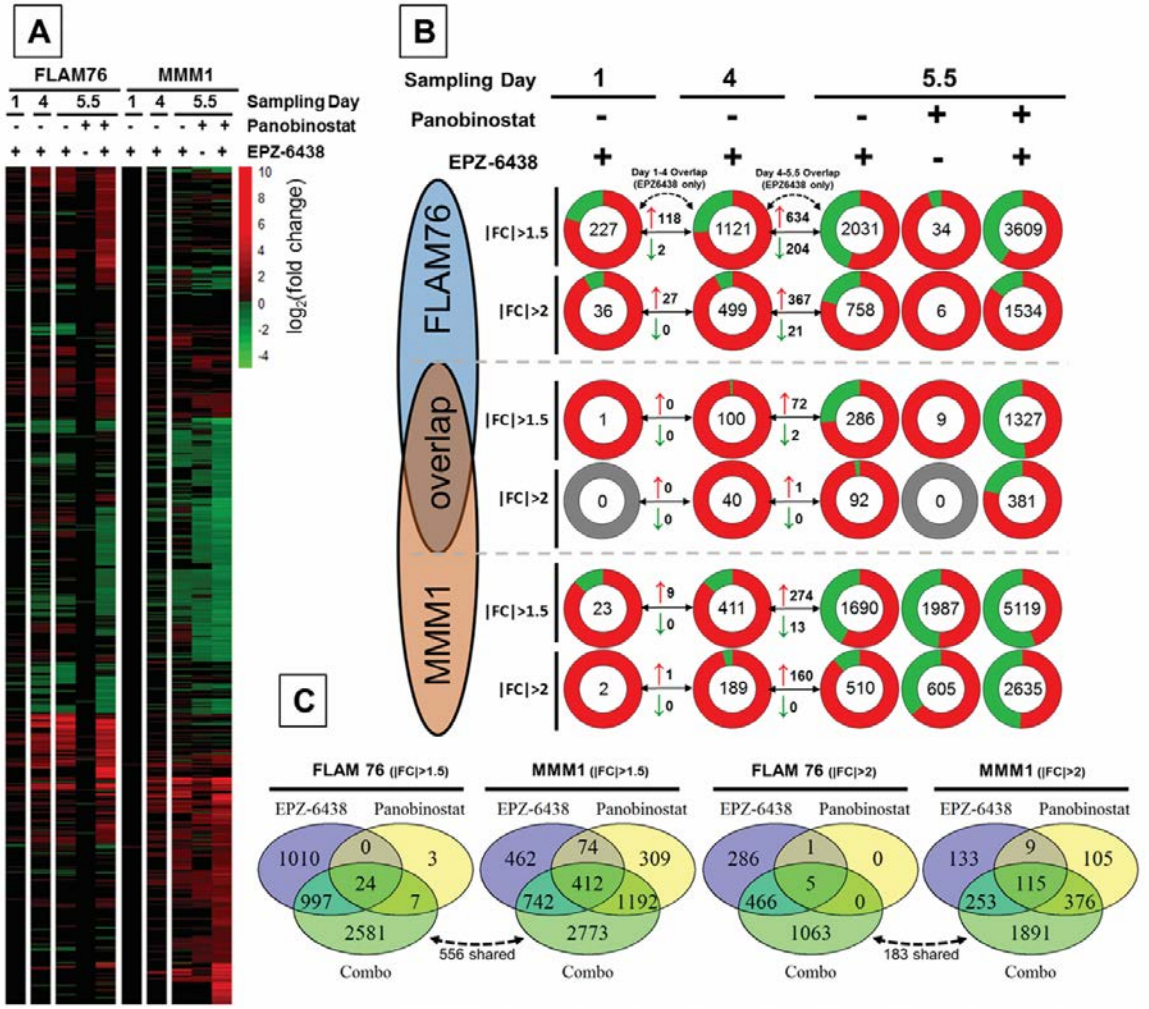
A
FLAM76
MMM1
Sampling Day
Panobinostat
EPZ-6438
log2(fold change)
B
Sampling Day
Panobinostat
EPZ-6438
Day 1-4 Overlap (EPZ6438 only)
Day 4-5.5 Overlap (EPZ6438 only)
FLAM76
overlap
MMM1
|FC|>1.5
|FC|>2
C
FLAM 76 (|FC|>1.5)
MMM1 (|FC|>1.5)
FLAM 76 (|FC|>2)
MMM1 (|FC|>2)
EPZ-6438
Panobinostat
Combo
556 shared
183 shared

FIGURE 4

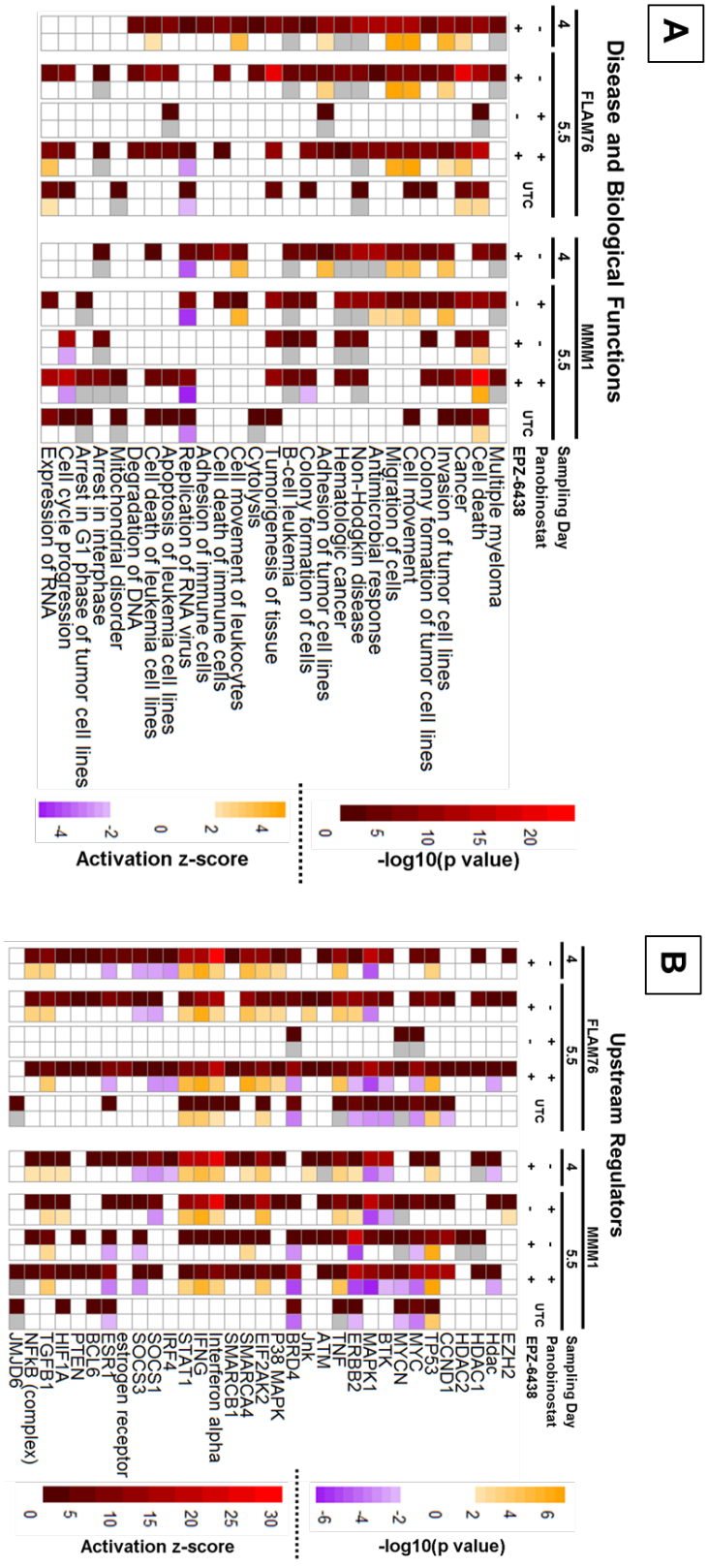
A
Disease and Biological Functions
FLAM76
MMM1
Sampling Day
Panobinostat
EPZ-6438
UTC
Multiple myeloma
Cell death
Cancer
Invasion of tumor cell lines
Colony formation of tumor cell lines
Cell movement
Migration of cells
Antimicrobial response
Non-Hodgkin disease
Hematologic cancer
Adhesion of tumor cell lines
Colony formation of cells
B-cell leukemia
Tumorigenesis of tissue
Cytolysis
Cell movement of leukocytes
Cell death of immune cells
Adhesion of immune cells
Replication of RNA virus
Apoptosis of leukemia cell lines
Cell death of leukemia cell lines
Degradation of DNA
Mitochondrial disorder
Arrest in interphase
Arrest in G1 phase of tumor cell lines
Cell cycle progression
Expression of RNA
-log10(p value)
Activation z-score
B
Upstream Regulators
EZH2
Hdac
HDAC1
HDAC2
CCND1
TP53
MYC
MYCN
BTK
MAPK1
ERBB2
TNF
ATM
Jnk
BRD4
P38 MAPK
EIF2AK2
SMARCA4
SMARCB1
Interferon alpha
IFNG
STAT1
IRF4
SOCS1
SOCS3
estrogen receptor
ESR1
BCL6
PTEN
HIF1A
TGFB1
NFkB (complex)
JMJD6
-log10(p value)
Activation z-score

FIGURE 4 continued

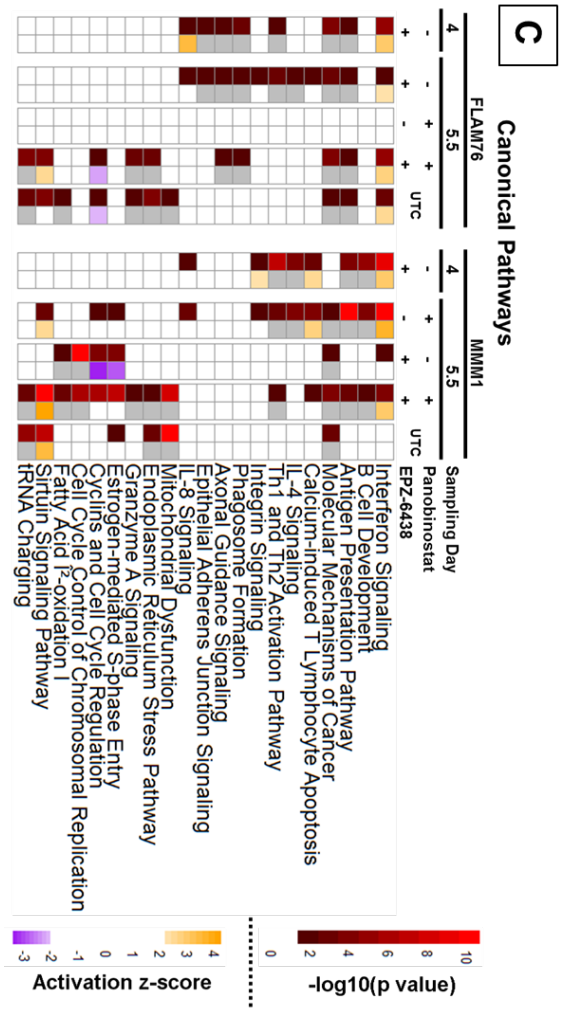

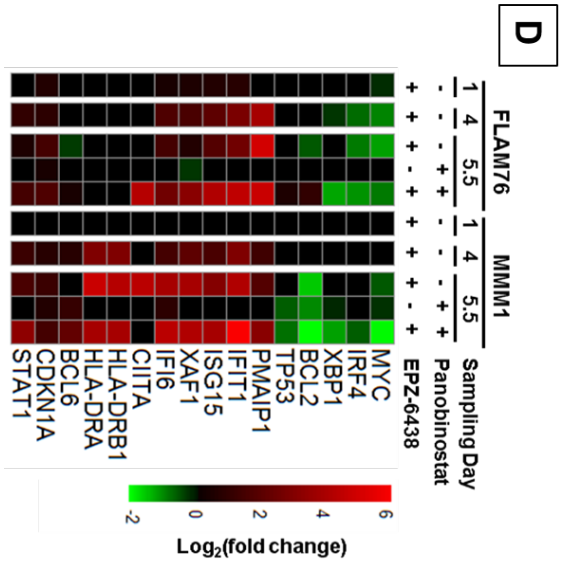

FIGURE S1

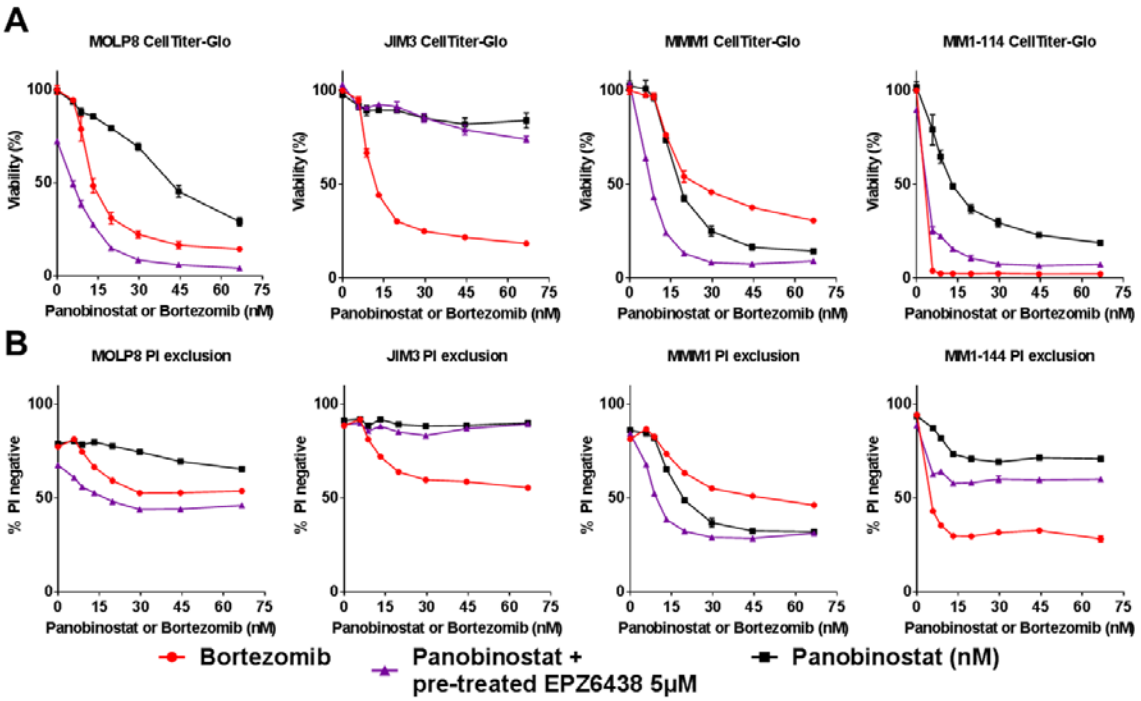
A
MOLP8 CellTiter-Glo
JIM3 CellTiter-Glo
MM1 CellTiter-Glo
MM1-114 CellTiter-Glo
Viability (%)
Panobinostat or Bortezomib (nM)
B
MOLP8 PI exclusion
JIM3 PI exclusion
MM1 PI exclusion
MM1-144 PI exclusion
% PI negative
Panobinostat or Bortezomib (nM)
Bortezomib
Panobinostat + pre-treated EPZ6438 5μM
Panobinostat (nM)

FIGURE S2

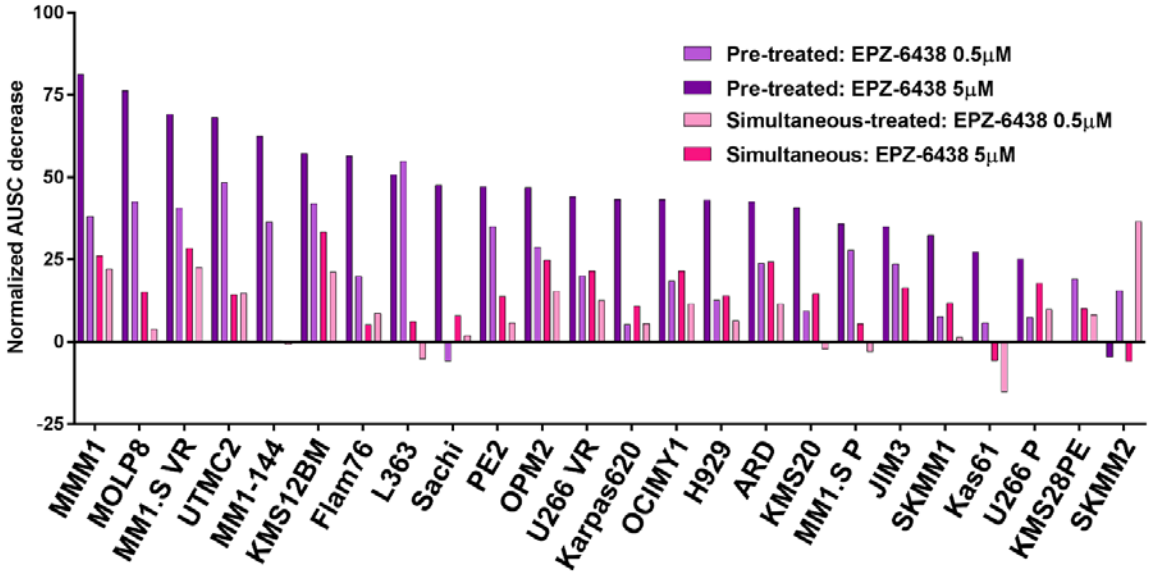
Normalized AUSC decrease
100
75
50
25
0
-25
Pre-treated: EPZ-6438 0.5μM
Pre-treated: EPZ-6438 5μM
Simultaneous-treated: EPZ-6438 0.5μM
Simultaneous: EPZ-6438 5μM
MMM1
MOLP8
MM1.S VR
UTMC2
MM1-144
KMS12BM
Flam76
L363
Sachi
PE2
OPM2
U266 VR
Karpas620
OCIMY1
H929
ARD
KMS20
MM1.S P
JIM3
SKMM1
Kas61
U266 P
KMS28PE
SKMM2

FIGURE S3

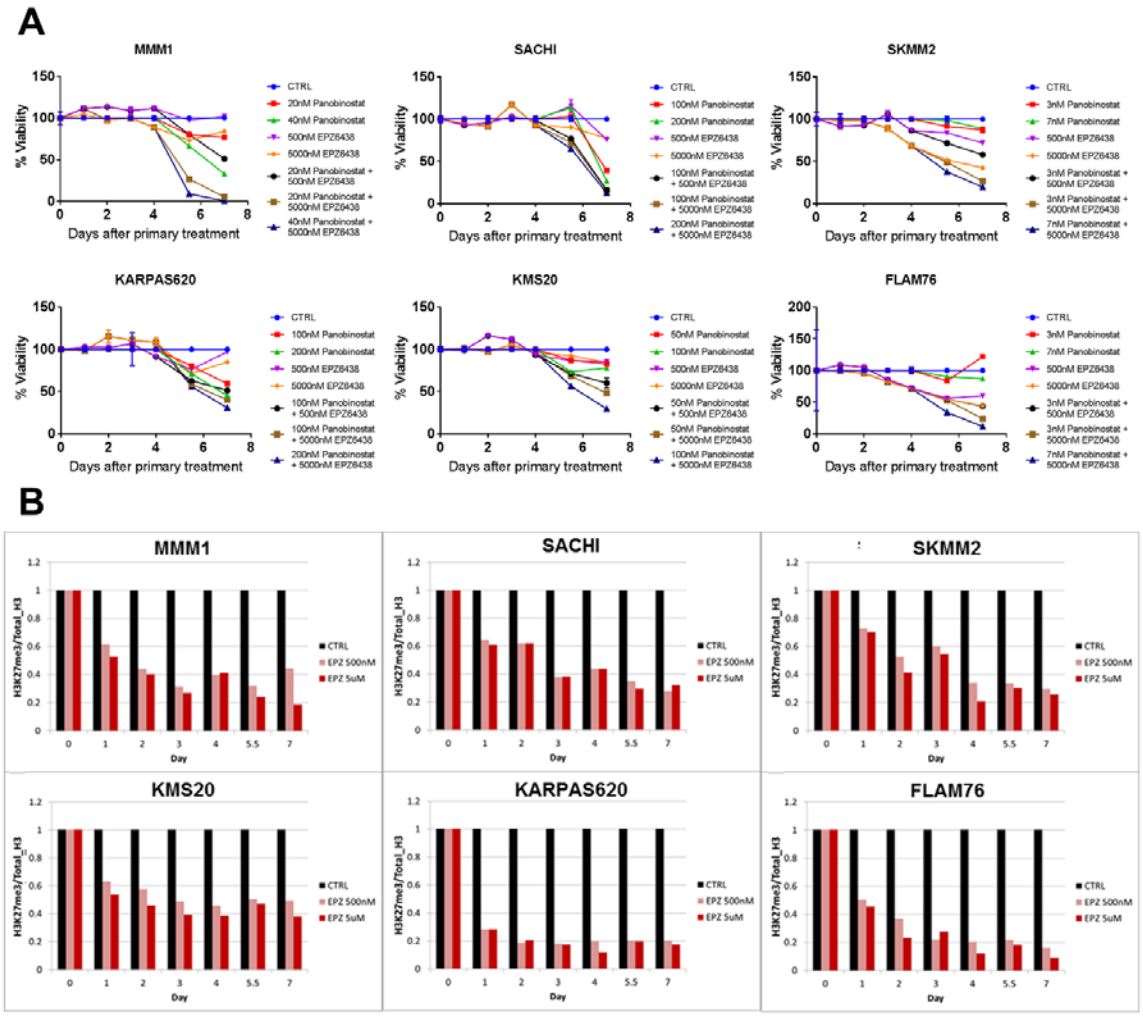
A
MMM1
SACHI
SKMM2
KARPAS620
KMS20
FLAM76
% Viability
Days after primary treatment
CTRL
20nM Panobinostat
40nM Panobinostat
500nM EPZ6438
5000nM EPZ6438
20nM Panobinostat + 500nM EPZ6438
20nM Panobinostat + 5000nM EPZ6438
40nM Panobinostat + 5000nM EPZ6438
100nM Panobinostat
200nM Panobinostat
100nM Panobinostat + 500nM EPZ6438
100nM Panobinostat + 5000nM EPZ6438
200nM Panobinostat + 5000nM EPZ6438
3nM Panobinostat
7nM Panobinostat
3nM Panobinostat + 500nM EPZ6438
3nM Panobinostat + 5000nM EPZ6438
7nM Panobinostat + 5000nM EPZ6438
50nM Panobinostat
50nM Panobinostat + 500nM EPZ6438
50nM Panobinostat + 5000nM EPZ6438
B
MMM1
SACHI
SKMM2
KMS20
KARPAS620
FLAM76
H3K27me3/Total_H3
Day
CTRL
EPZ 500nM
EPZ 5uM

CHAPTER 4

SUPPLEMENTAL CHAPTER: UNPUBLISHED FINDINGS RELATING TO COMBINED TREATMENT OF EZH2 AND HDAC INHIBITORS IN HUMAN MYELOMA CELL LINES

This supplementary chapter expands on the study outlined in Chapter 3. Specifically, this chapter contains additional data that was either alluded to in the previous chapter or was not included in submissions for publication.

Chapter 3 outlined evaluation of efficacy of two EZH2 inhibitors against a panel of HMCLs: EPZ-6438 and GSK-126. These two inhibitors specifically target EZH2. Some interest has also been generated around dual inhibitors that target EZH2 and EZH1, a related HMT that can replace EZH2 as the core catalytic subunit of the polycomb repressive complex 2 (PRC2). Little to nothing is described in the literature regarding EZH1's activity or expression in MM, however, some studies in other cancers and MM suggest an added benefit of using EZH1/2 dual inhibitors [279,280].

To test the efficacy of dual inhibition in tandem with EZH2i, we treated 12 HMCLs with all three inhibitors: EZH2-specific inhibitors EPZ-6438, GSK-126 and dual inhibitor UNC1999 [189] (**Figure 1**). All three drugs were applied with the same concentration gradient and viability was read after 4,6,10 and 18 days post treatment. UNC1999 did demonstrate 100% kill at 30μM in all HMCLs and time points, however this is similar to high-dose toxicity observed in GSK-126 (data not shown). In both of those instances this high does toxicity was markedly more rapid than the timeline required for lower dose response and latent sensitivity in some lines was achieved at much lower (up to an entire order of magnitude) doses. Together this suggests an off-target effect of extreme doses.

There was no general trend towards selective sensitivity to the dual inhibitor. In many instances UNC1999 kill curves mirrored EPZ-6438, however there were instances of lower dose sensitivity in MOLP8. It would be interesting to follow up this finding by measuring EZH1 expression levels in MOLP8 compared to other HMCLs.

In Chapter 3 synergy between EZH2i's and panobinostat was assessed by comparing changes in the area under the survival curve (AUSC). This metric was useful for condensing the

data into a manuscript. The individual kill curves used to generate Figure 2c in Chapter 3 are included as **Figure 2** in this chapter.

Panobinostat is a pan-HDAC inhibitor. We sought to determine if certain broad classes of HDADs are specifically responsible for the synergy observed between EZH2i's and panobinostat. As overviewed in the introduction, HDACs are a large family of enzymes that are segregated into classes based on homology to yeast HDACs. HDAC6, a class IIb HDAC is exclusively cytoplasmic and, as discussed in Chapter 1, is of particular interest in MM. We sought to determine if Inhibition of HDAC6 via tubacin and nexturastat A would recapitulate panobinostat's synergy with EZH2i-pre-treatment in four HMCLs that had demonstrated consistent and strong synergy. Conversely, we also applied inhibitors that target all other HDACs (classes I,IIa and IV): sodium butyrate and valproic acid (**Figure 3**). Interestingly, synergy was observed to nearly recapitulate AUSC changes seen with panobinostat, with the exception of tubacin which did demonstrated relatively mild synergy. These data suggest that EZH2i pre-treatment may be sufficient to potentiate sensitivity to both broad types of HDACs. This suggests that either synergy seen in panobinostat is due to several different synergistic mechanisms or that this synergistic toxicity may be non-specific.

We were intrigued by the large number of unique-to-combination (UTC) genes identified in our transcriptomic analysis of HMCLs treated with both EPZ-6438 and panobinostat. This clearly suggested to us that EZH2 cooperates with HDACs to silence thousands of genes that cannot be freed from repression by inhibition of either alone. We were further surprised that UTC genes, when subjected to network analysis via IPA, did not demonstrate additional enrichment of terms (vs. EZH2i or panobinostat alone) commensurate with the nearly two thirds of genes identified at the combination that were UTC. This led us to postulate that these genes may not represent a controlled epigenetic network as is suggested for EZH2i-induced GEPs (presumably cells never abolish activities of all HDACs in any viable context). Rather, these genes are non-specifically overexpressed, which we have postulated could, at that magnitude, produce non-specific transcriptomic stress where transcription machinery is overloaded. When we looked at the most highly expressed genes that were significantly differentially expressed in the

combination condition in both HMCLs there seemed to be a strong bias towards downregulation. To examine this trend globally we visualized our drug induced (individual and combination) GEPs in a plot similar to a volcano plot except that the x-axis represents ranked expression of genes (filtered for significant differential expression) in the control condition (untreated) and the y-axis represents the change in expression for each gene (log_2(1+FPKM_change)). This allows one to view trends in gene expression changes with even density across the data (**Figure 4**). While less consistent/clear in earlier time points or single agents, the bias towards downregulation of highly expressed genes was clearer in combination conditions in both HMCLs. It is important to note that these differences could represent compression of the transcriptomic data. That is to say that upregulation of so many low expressed genes may cause the highly expressed genes to become less frequently represented in raw reads. Indeed, if this were to be the case, one would expect that the mean FPKM change per gene would be close to 0 as it is in FLAM76 (mean FPKM_change/gene = 3.69). In MMM1 however this mean change per gene is -17.27 showing a clearer bias towards downregulation. This is far from a conclusive evidence of transcriptomic stress as a mechanism for cytotoxicity. It would be interesting to test if titrating down transcriptomic capacity with transcription inhibitors would demonstrate significant synergy with either EZH2 inhibitors or HDAC inhibitors.

Figure Legends

Figure 1: EZH2 inhibition yields similar efficacy to dual inhibition of EZH2 and EZH1.

A panel of 12 HMCLs were treated with a concentration gradient of two EZH2 inhibitors EPZ-6438 and GSK-126 and one EZH2/1 dual inhibitor UNC1999. Viability was measured (resampling) after treatment for 4, 6, 10 and 12 days. Viability was measured with CellTiter-Glo® (Promega) assays and normalized to untreated controls. All error bars represent SEM between biological replicates.

Figure 2: Combination of EZH2 inhibition and panobinostat across a panel of 24 HMCLs

A panel of HMCLs (n = 24) were treated with panobinostat for 48hrs after a 4-day pre-treatment with either GSK-126 or EPZ-6438. Viability was measured with CellTiter-Glo® (Promega) assays and normalized to untreated controls. All error bars represent SEM between biological replicates.

Figure 3: HDAC inhibitors either targeting class IIb HDACs or all other HDACs both demonstrate synergy with EZH2i pre-treatment.

Each HMCL (arranged vertically) is represented by two plots both showing HMCLs treated with three drugs (control (solid) and EPZ-6438 pre-treated (dotted)), one of which is panobinostat. Plots on the left show treatment with HDAC6-specific inhibitors nexturastat A and tubacin. Plots on the right show treatment with sodium butyrate and valproic acid. Viability was measured via CellTiter-Glo® and normalized to untreated controls. Bar plots represent a measurement of synergy quantified by the decrease in the area under the survival curve (AUSC) between panobinostat single agent treatment and combination treatment (where AUSC of each EZH2i+pan/CTRL+pan dose response curve is normalized separately to isolate the shape of the curve from single agent EZH2i toxicity). All error bars represent SEM between biological replicates.

Figure 4: Transcriptomic analysis suggests potential biases in the direction of gene expression changes.

Each scatter plot (generated using the ggplot2 R package) represents all of the differentially expreassed genes for a particular differential expression experiment in either MMM1 (a-e) and FLAM76 (f-j). The x-axis in these plots is rank order for expression (FPKM) values in the untreated condition while the y-axis represents the change in expression observed in the differential expression measurement ($\log_2$(1+FPKM_change). The trend-line indicates a smoothed mean expression change along the x-axis. The text appearing in the bottom left displays calculated average FPKM changes for all, upregulated and downregulated genes. Blue lines indicate control FPKM values at increasing orders of magnitude (starting at FPKM = 10 on the left).

FIGURE 1

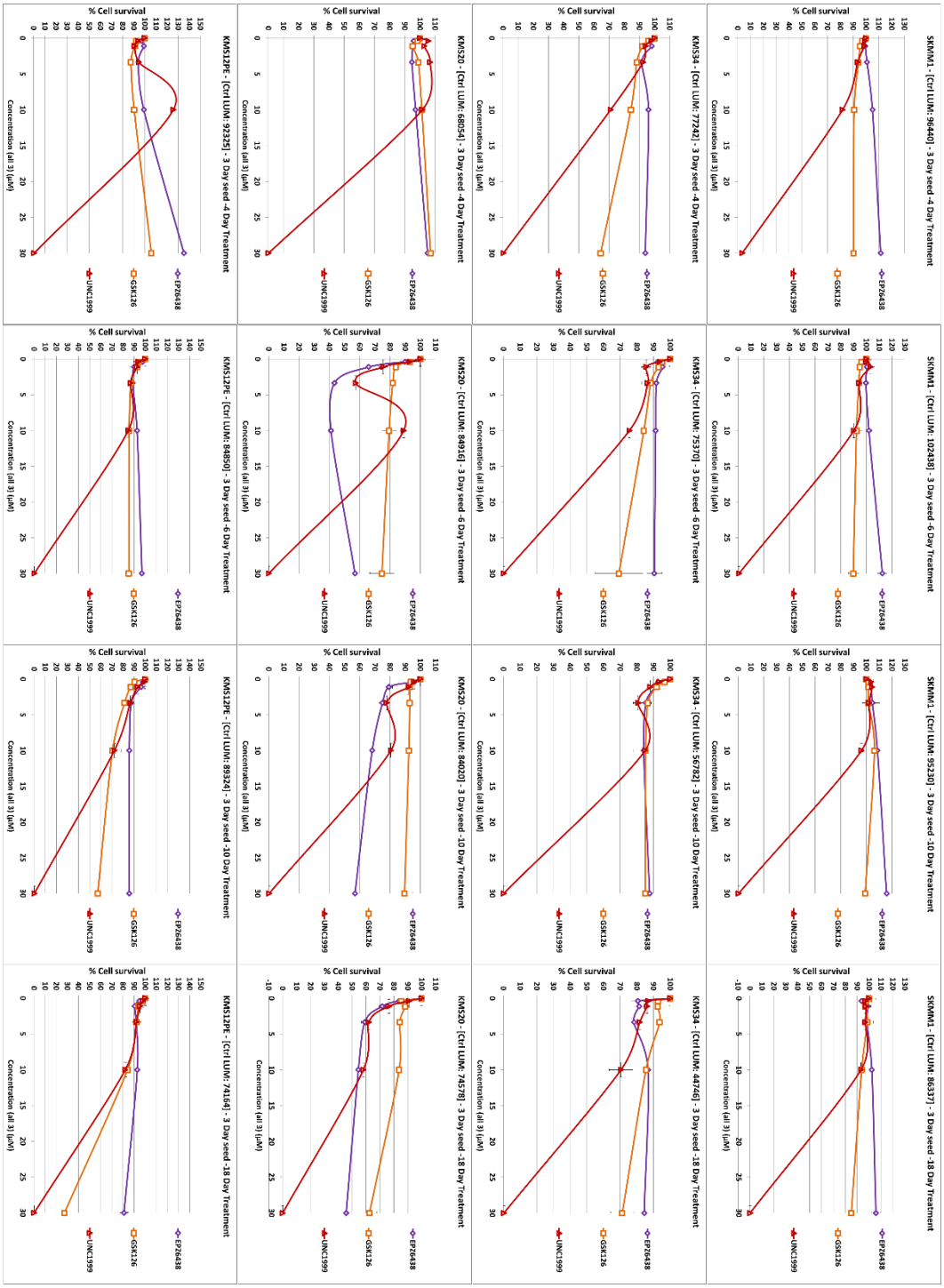
SKMM1 - [Ctrl LUM: 96440] - 3 Day seed -4 Day Treatment
SKMM1 - [Ctrl LUM: 102438] - 3 Day seed -6 Day Treatment
SKMM1 - [Ctrl LUM: 95230] - 3 Day seed -10 Day Treatment
SKMM1 - [Ctrl LUM: 86337] - 3 Day seed -18 Day Treatment
KMS34 - [Ctrl LUM: 77242] - 3 Day seed -4 Day Treatment
KMS34 - [Ctrl LUM: 75370] - 3 Day seed -6 Day Treatment
KMS34 - [Ctrl LUM: 56782] - 3 Day seed -10 Day Treatment
KMS34 - [Ctrl LUM: 44746] - 3 Day seed -18 Day Treatment
KMS20 - [Ctrl LUM: 68054] - 3 Day seed -4 Day Treatment
KMS20 - [Ctrl LUM: 84916] - 3 Day seed -6 Day Treatment
KMS20 - [Ctrl LUM: 84020] - 3 Day seed -10 Day Treatment
KMS20 - [Ctrl LUM: 74578] - 3 Day seed -18 Day Treatment
KMS12PE - [Ctrl LUM: 92325] - 3 Day seed -4 Day Treatment
KMS12PE - [Ctrl LUM: 84850] - 3 Day seed -6 Day Treatment
KMS12PE - [Ctrl LUM: 89924] - 3 Day seed -10 Day Treatment
KMS12PE - [Ctrl LUM: 74164] - 3 Day seed -18 Day Treatment
% Cell survival
Concentration (all 3) (μM)
EPZ6438
GSK126
UNC1999

FIGURE 1 continued

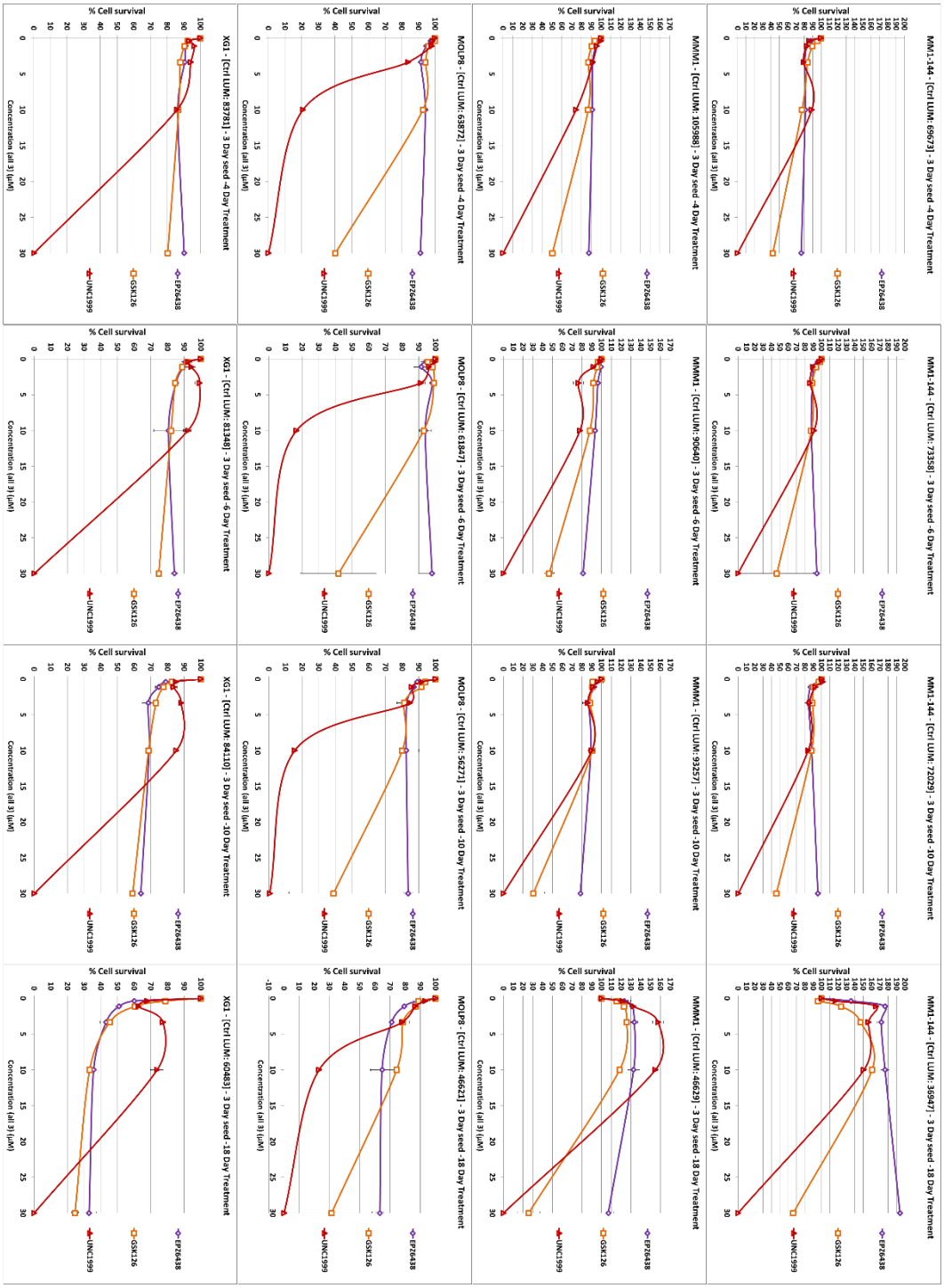

FIGURE 1 continued

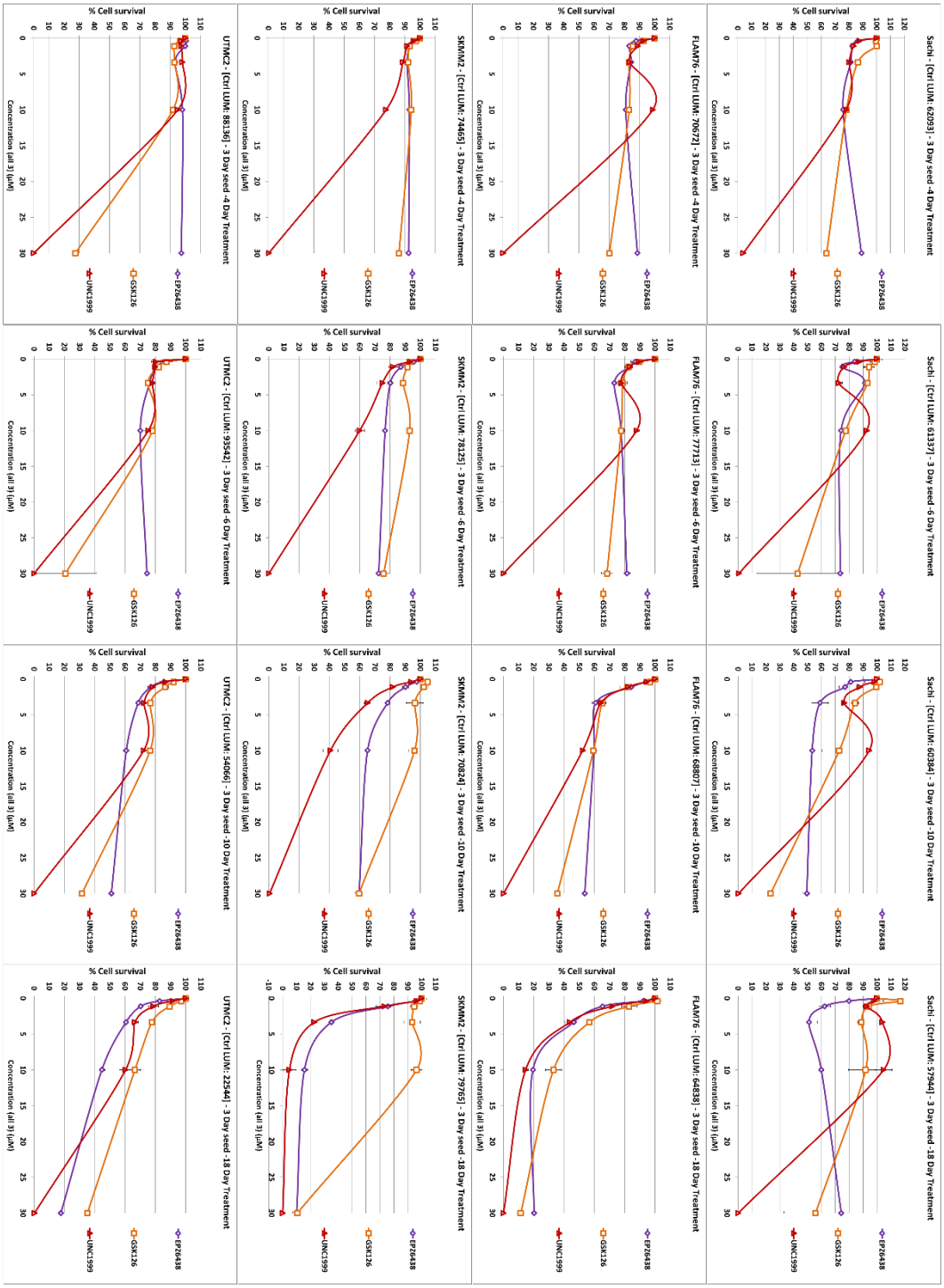

FIGURE 2

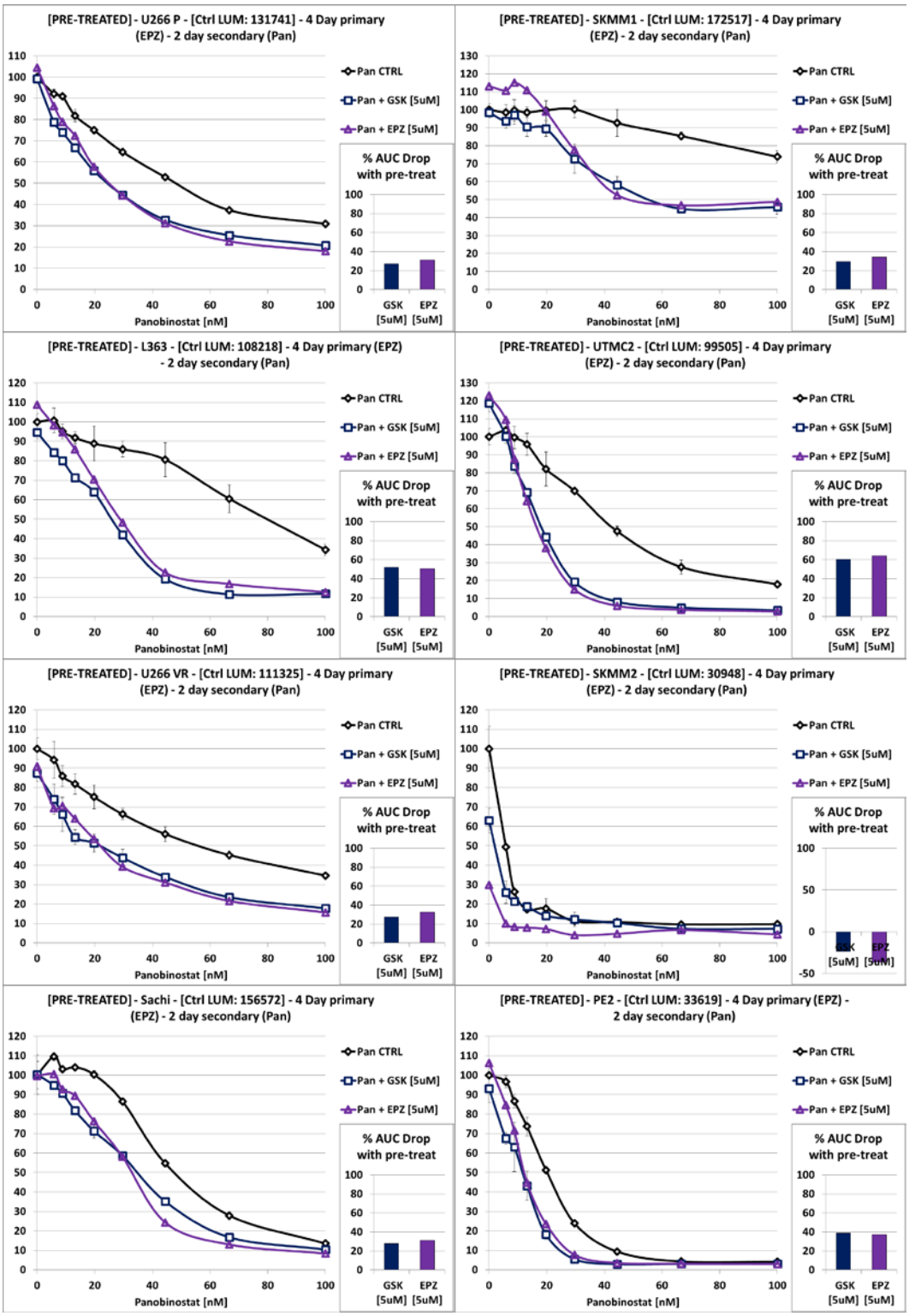
[PRE-TREATED] - U266 P - [Ctrl LUM: 131741] - 4 Day primary (EPZ) - 2 day secondary (Pan)
[PRE-TREATED] - SKMM1 - [Ctrl LUM: 172517] - 4 Day primary (EPZ) - 2 day secondary (Pan)
[PRE-TREATED] - L363 - [Ctrl LUM: 108218] - 4 Day primary (EPZ) - 2 day secondary (Pan)
[PRE-TREATED] - UTMC2 - [Ctrl LUM: 99505] - 4 Day primary (EPZ) - 2 day secondary (Pan)
[PRE-TREATED] - U266 VR - [Ctrl LUM: 111325] - 4 Day primary (EPZ) - 2 day secondary (Pan)
[PRE-TREATED] - SKMM2 - [Ctrl LUM: 30948] - 4 Day primary (EPZ) - 2 day secondary (Pan)
[PRE-TREATED] - Sachi - [Ctrl LUM: 156572] - 4 Day primary (EPZ) - 2 day secondary (Pan)
[PRE-TREATED] - PE2 - [Ctrl LUM: 33619] - 4 Day primary (EPZ) - 2 day secondary (Pan)
Pan CTRL
Pan + GSK [5uM]
Pan + EPZ [5uM]
% AUC Drop with pre-treat
GSK [5uM]
EPZ [5uM]
Panobinostat [nM]

FIGURE 2 continued

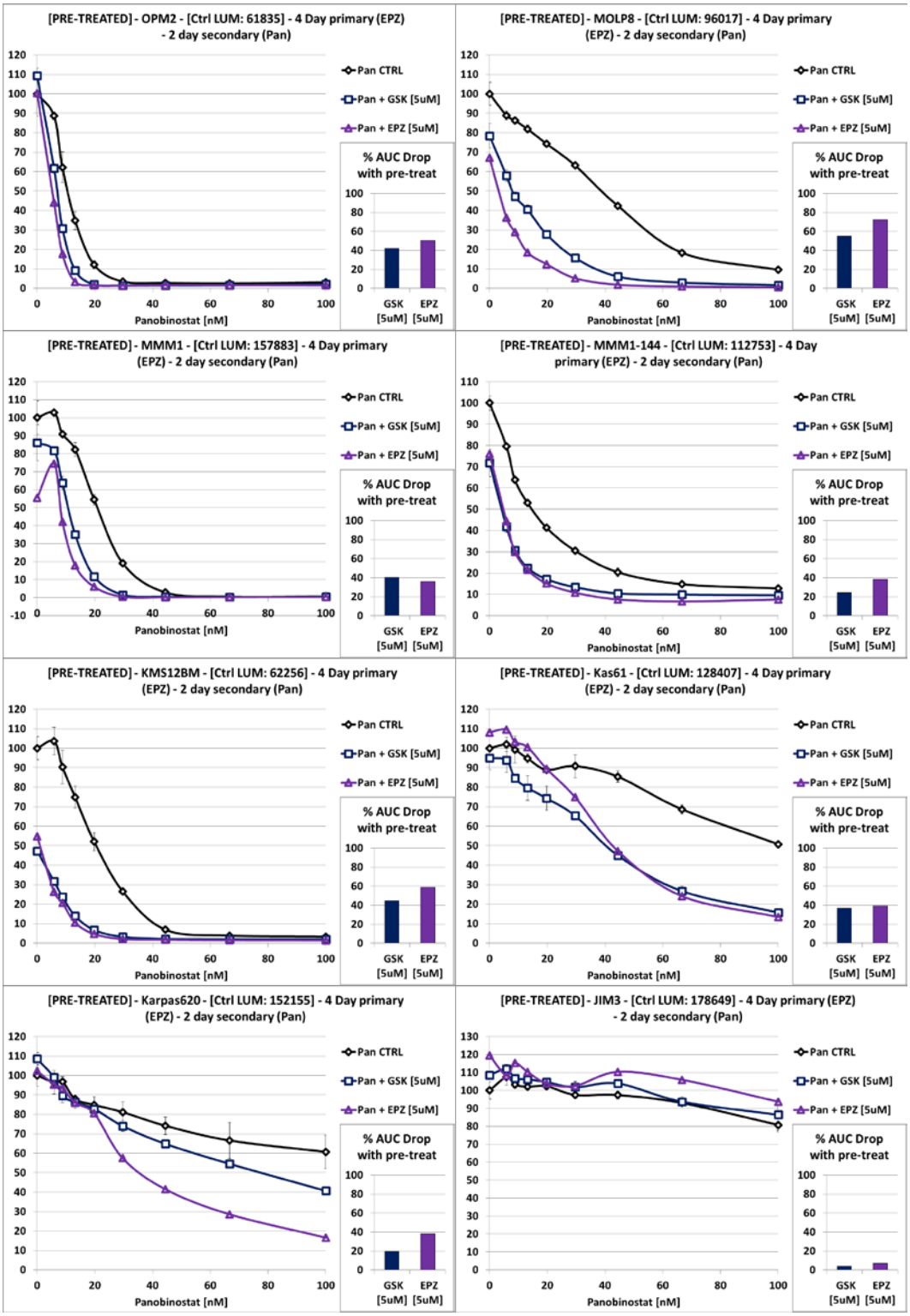

FIGURE 2 continued

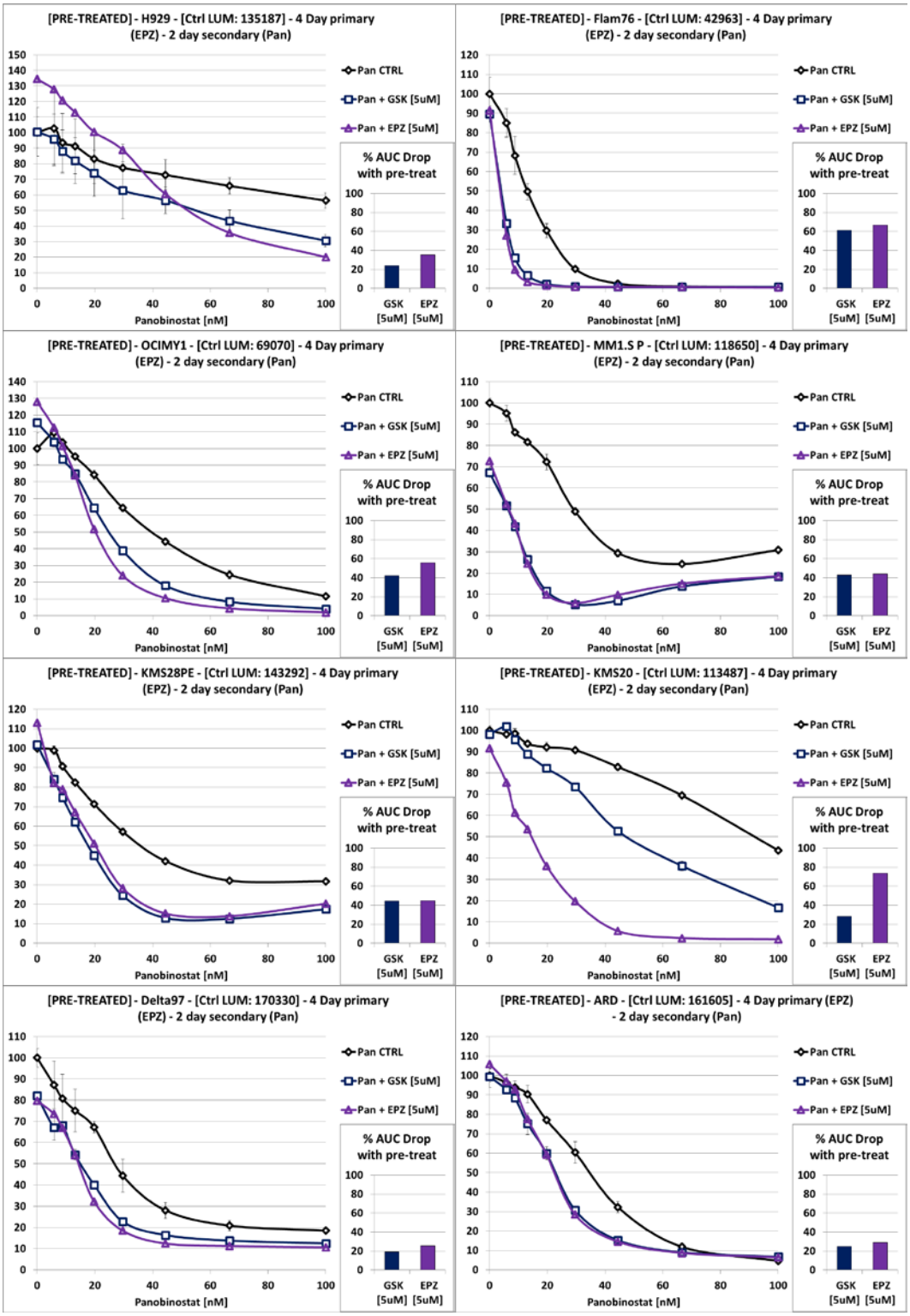

FIGURE 3

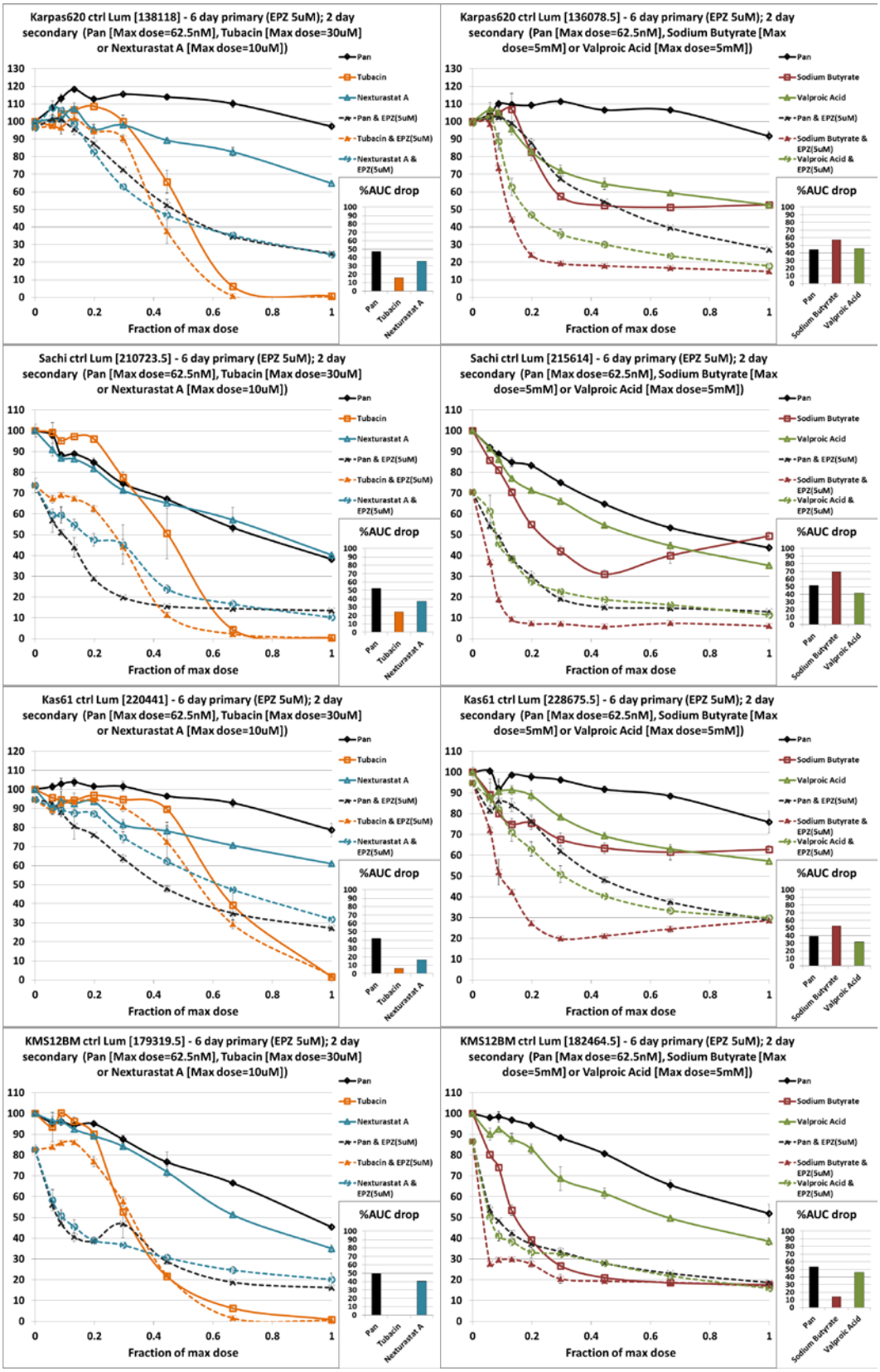
Karpas620 ctrl Lum [138118] - 6 day primary (EPZ 5uM); 2 day secondary (Pan [Max dose=62.5nM], Tubacin [Max dose=30uM] or Nexturastat A [Max dose=10uM])
Karpas620 ctrl Lum [136078.5] - 6 day primary (EPZ 5uM); 2 day secondary (Pan [Max dose=62.5nM], Sodium Butyrate [Max dose=5mM] or Valproic Acid [Max dose=5mM])
Sachi ctrl Lum [210723.5] - 6 day primary (EPZ 5uM); 2 day secondary (Pan [Max dose=62.5nM], Tubacin [Max dose=30uM] or Nexturastat A [Max dose=10uM])
Sachi ctrl Lum [215614] - 6 day primary (EPZ 5uM); 2 day secondary (Pan [Max dose=62.5nM], Sodium Butyrate [Max dose=5mM] or Valproic Acid [Max dose=5mM])
Kas61 ctrl Lum [220441] - 6 day primary (EPZ 5uM); 2 day secondary (Pan [Max dose=62.5nM], Tubacin [Max dose=30uM] or Nexturastat A [Max dose=10uM])
Kas61 ctrl Lum [228675.5] - 6 day primary (EPZ 5uM); 2 day secondary (Pan [Max dose=62.5nM], Sodium Butyrate [Max dose=5mM] or Valproic Acid [Max dose=5mM])
KMS12BM ctrl Lum [179319.5] - 6 day primary (EPZ 5uM); 2 day secondary (Pan [Max dose=62.5nM], Tubacin [Max dose=30uM] or Nexturastat A [Max dose=10uM])
KMS12BM ctrl Lum [182464.5] - 6 day primary (EPZ 5uM); 2 day secondary (Pan [Max dose=62.5nM], Sodium Butyrate [Max dose=5mM] or Valproic Acid [Max dose=5mM])
Fraction of max dose
Pan
Tubacin
Nexturastat A
Pan & EPZ(5uM)
Tubacin & EPZ(5uM)
Nexturastat A & EPZ(5uM)
Sodium Butyrate
Valproic Acid
Sodium Butyrate & EPZ(5uM)
Valproic Acid & EPZ(5uM)
%AUC drop

Figure 4a (MMM1 - Day 1 - EPZ-6438)

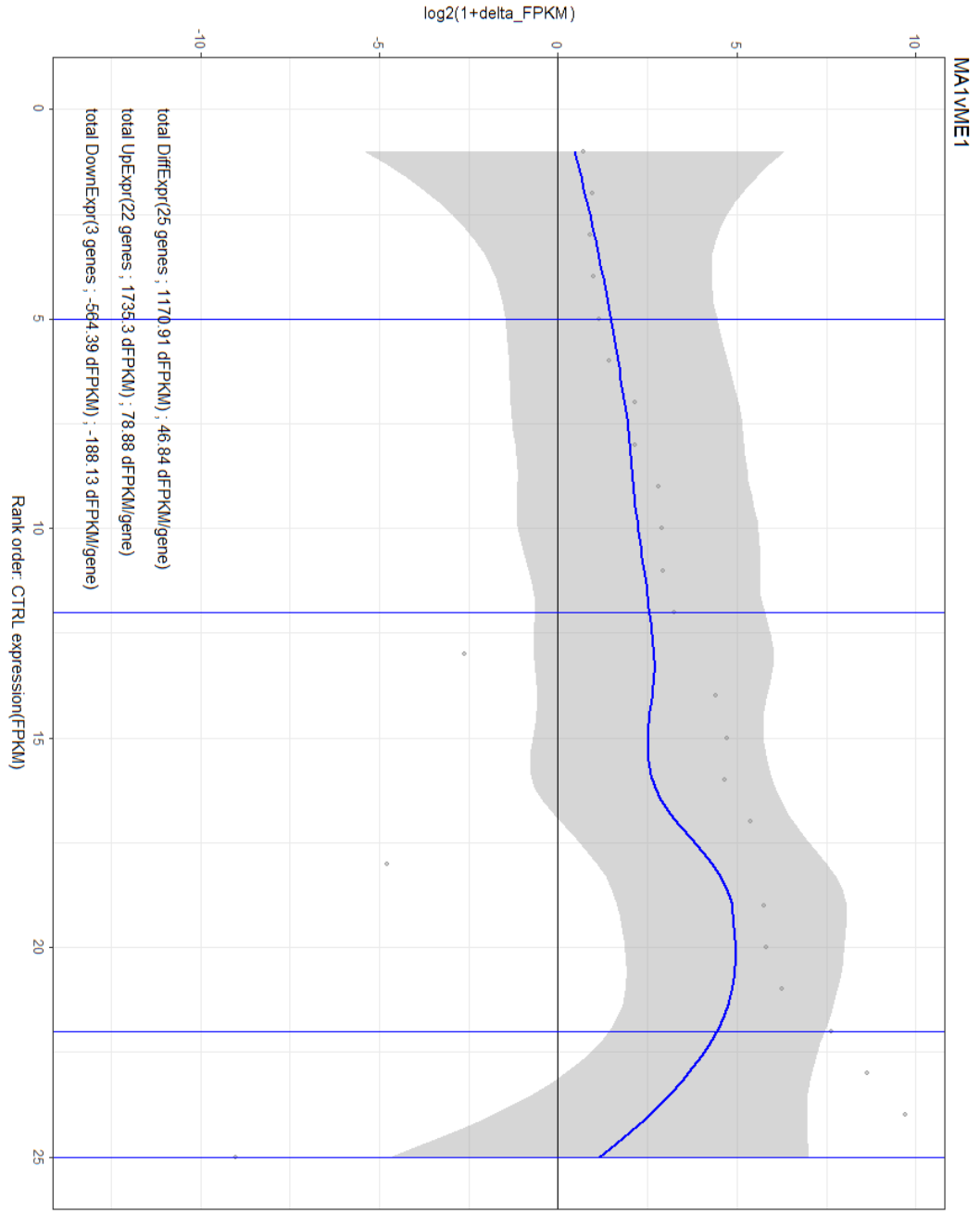

Figure 4b (MMM1 - Day 4 - EPZ-6438)

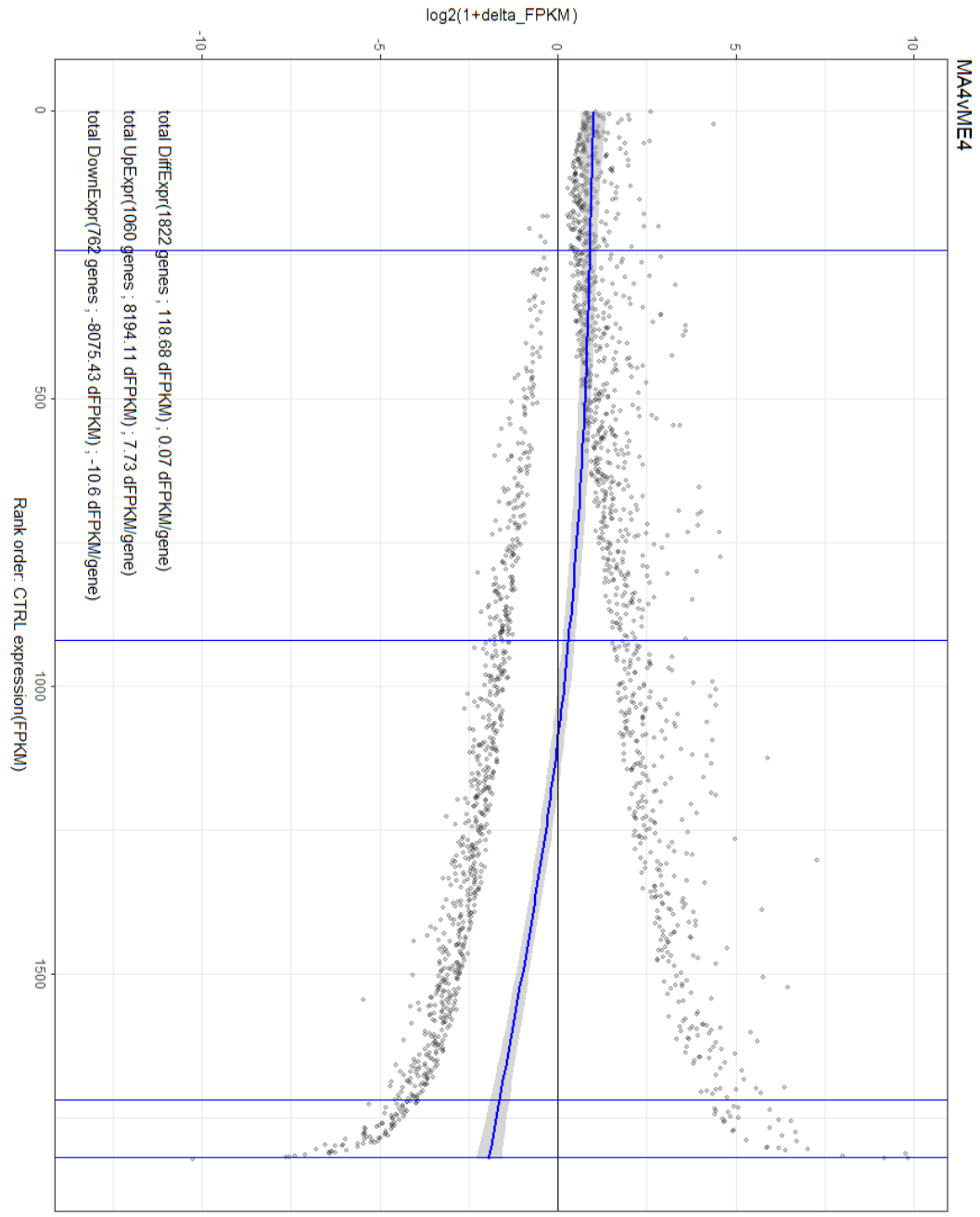

Figure 4c (MMM1 - Day 5.5 - Panobinostat)

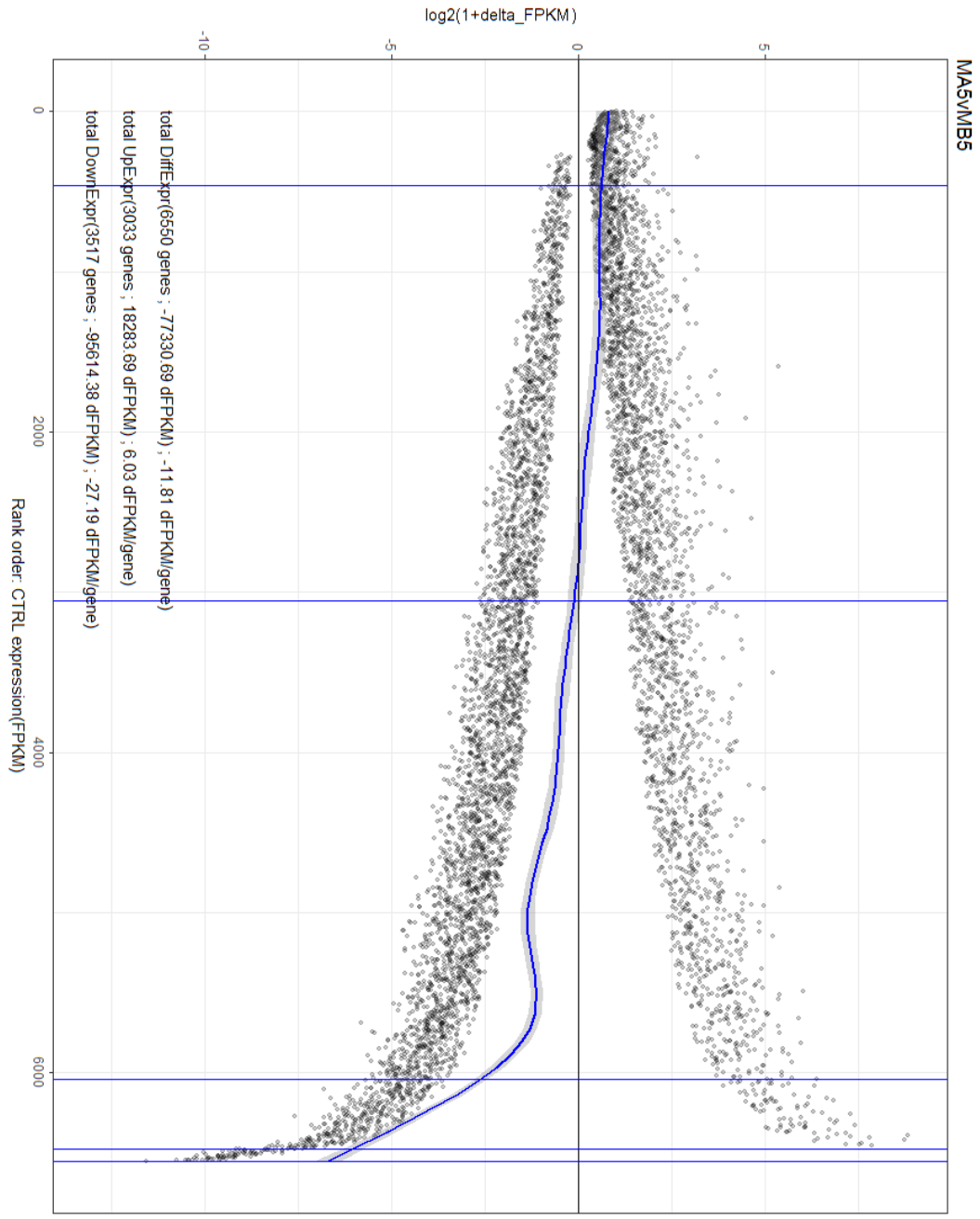

Figure 4d (MMM1 - Day 5.5 - EPZ-6438)

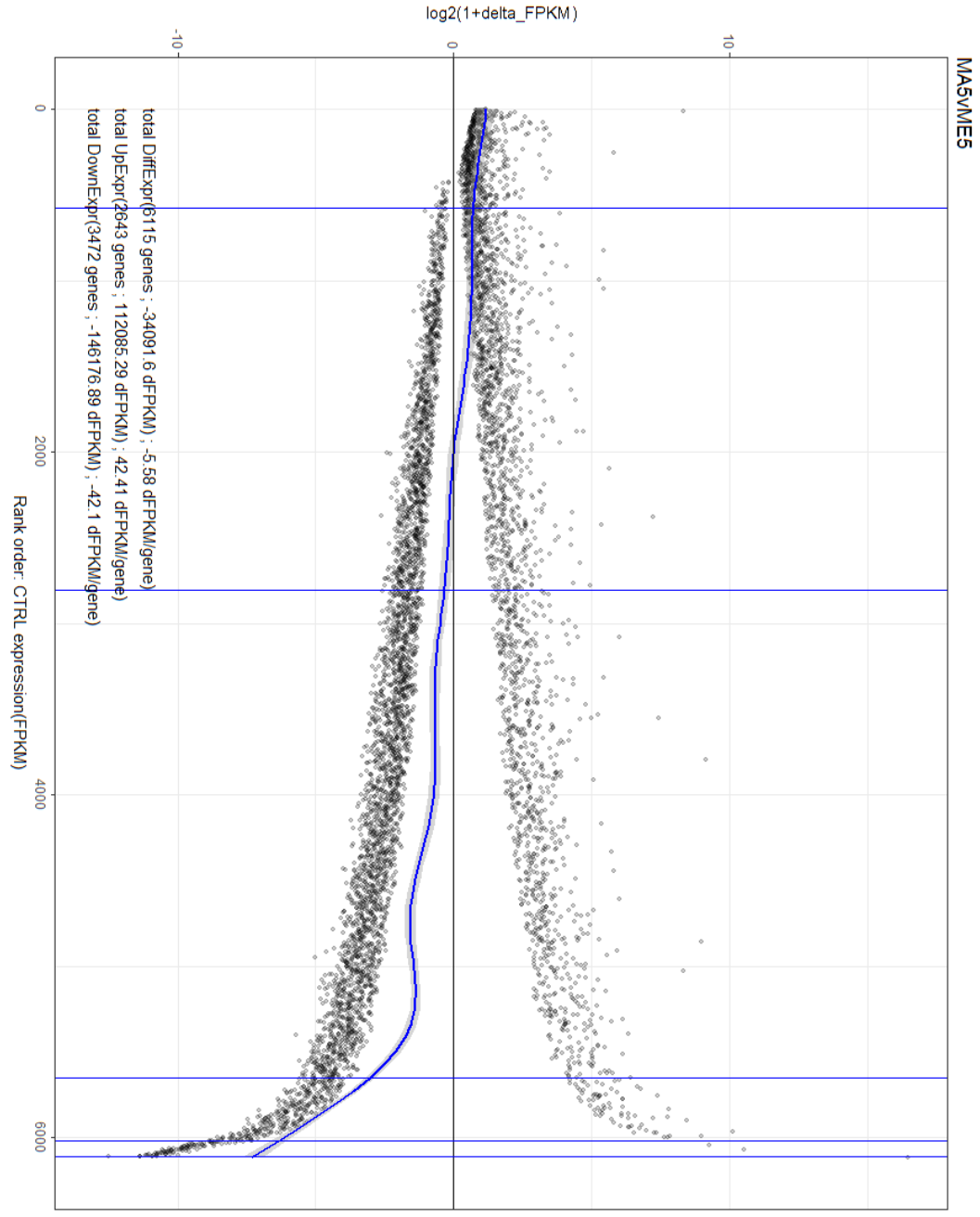

Figure 4e (MMM1 - Day 5.5 – EPZ-6438 + Panobinostat)

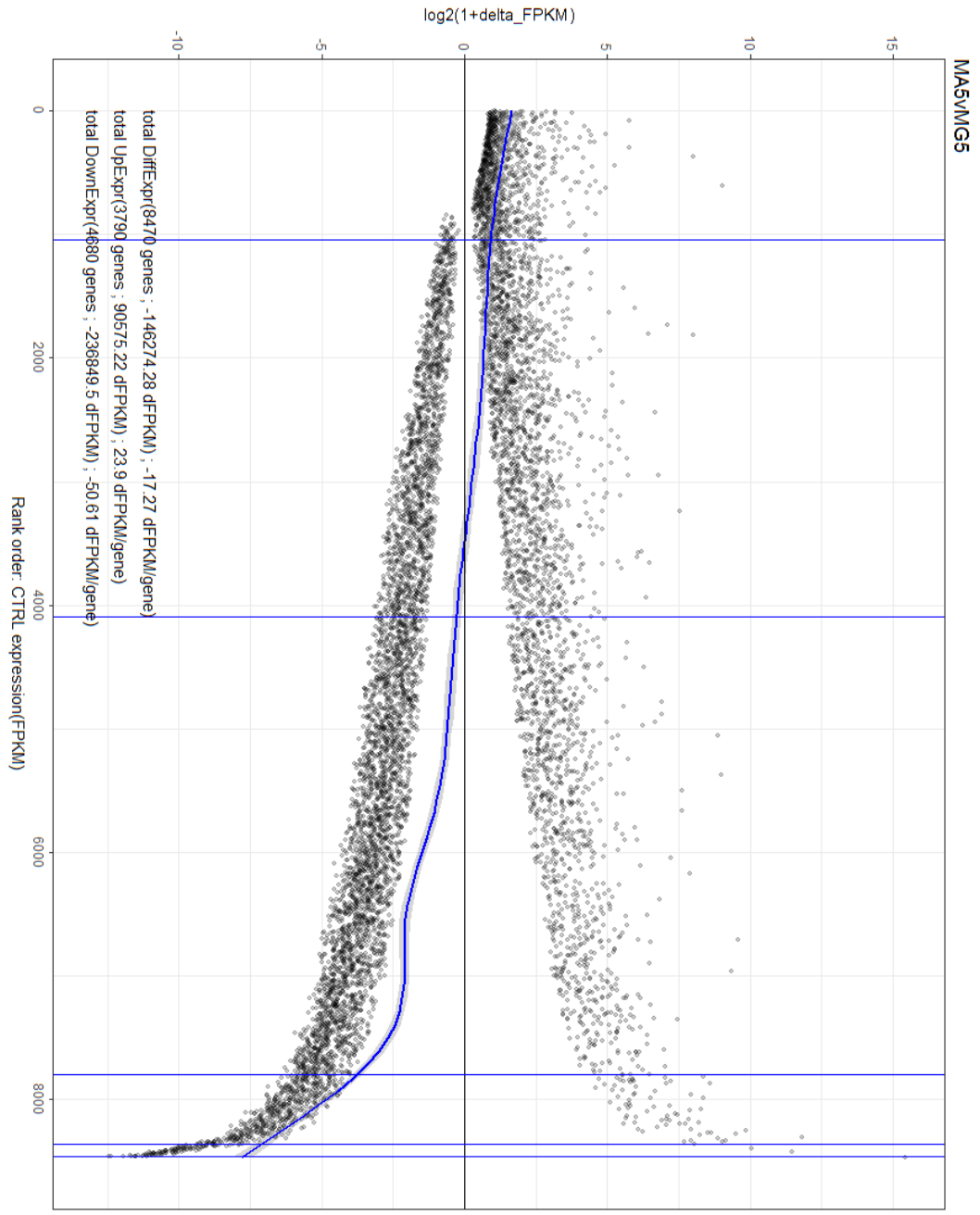

Figure 4f (FLAM76 - Day 1 - EPZ-6438)

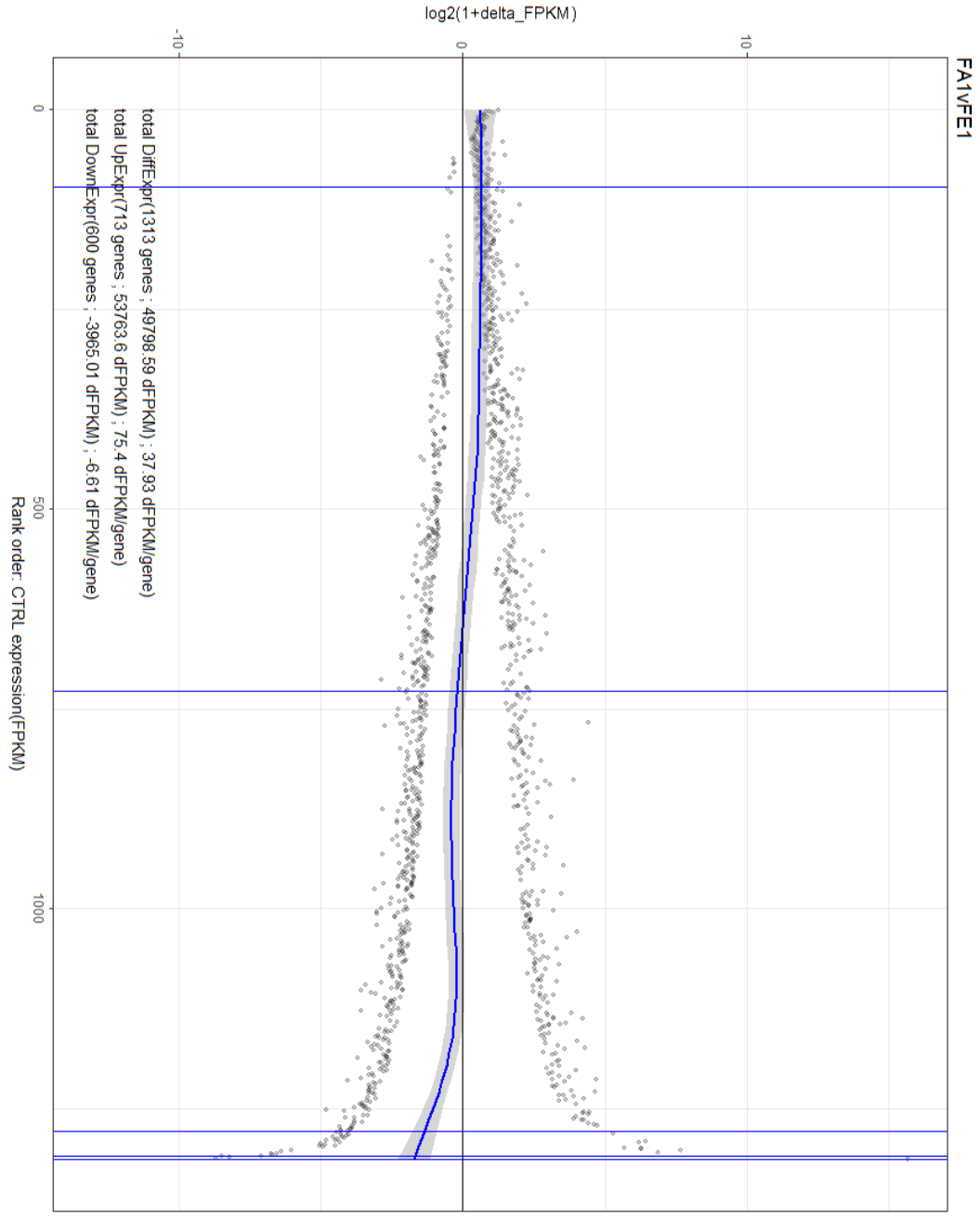

Figure 4g (FLAM76 - Day 4 - EPZ-6438)

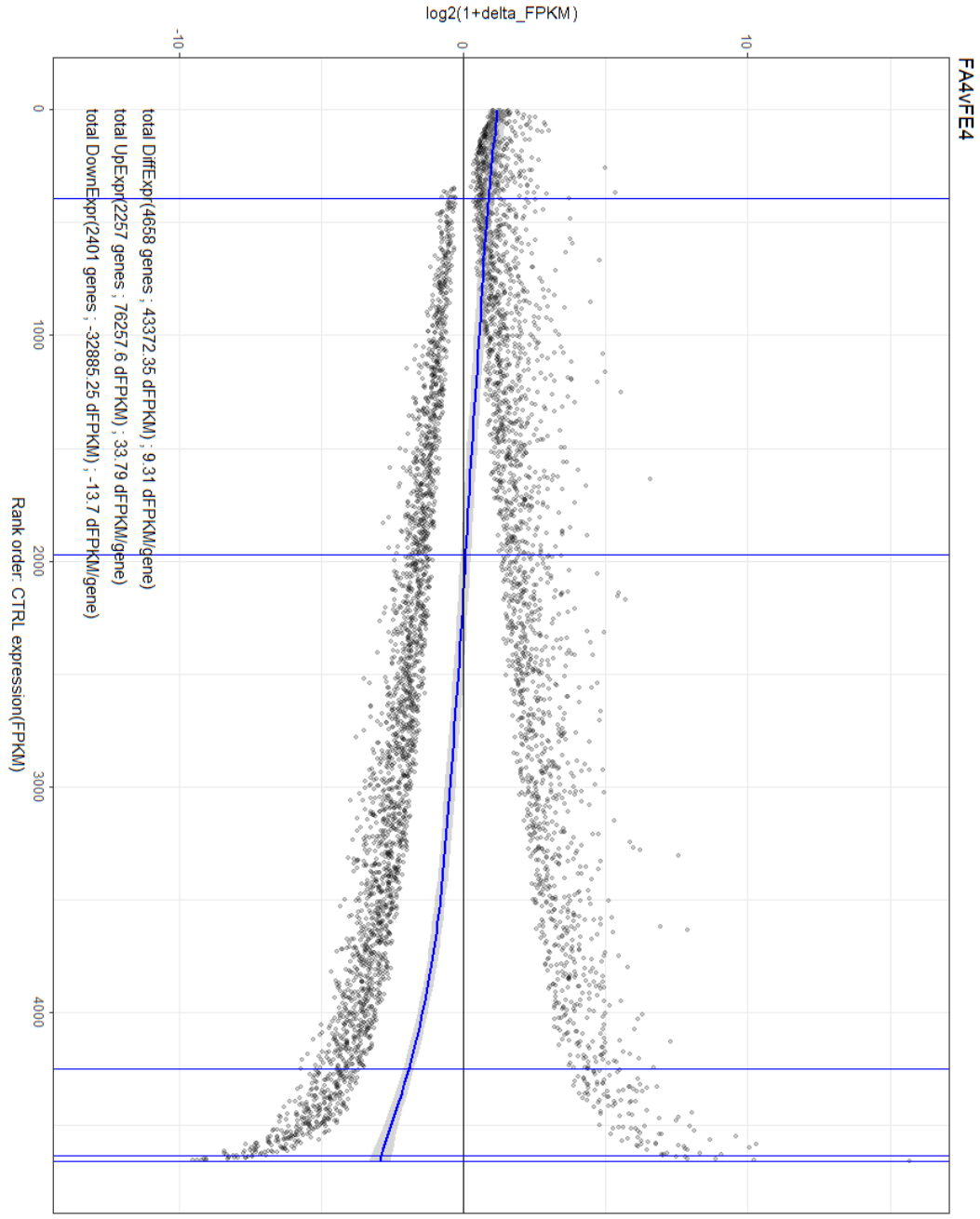

Figure 4h (FLAM76 - Day 5.5 - panobinostat)

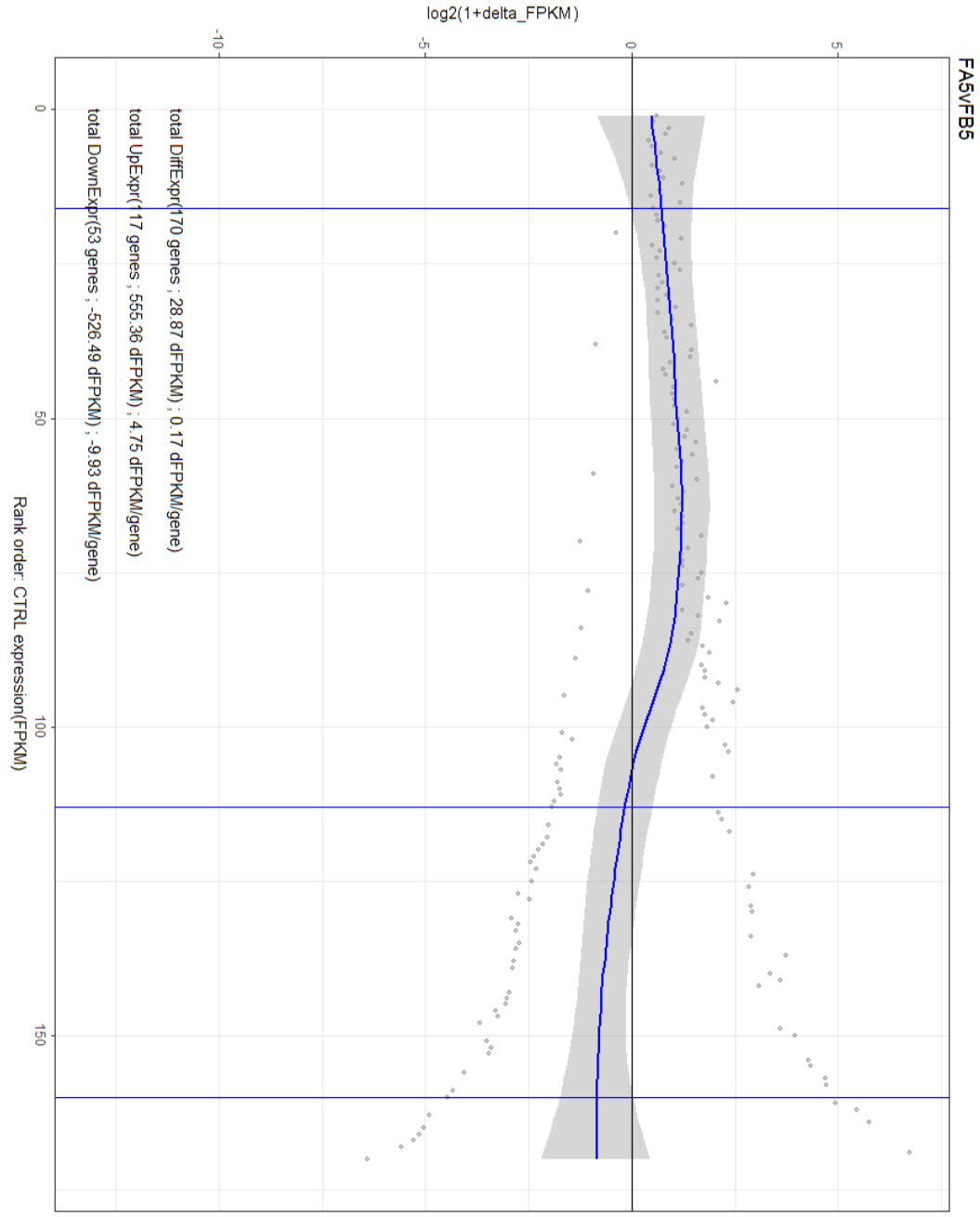

Figure 4i (FLAM76 - Day 5.5 - EPZ-6438)

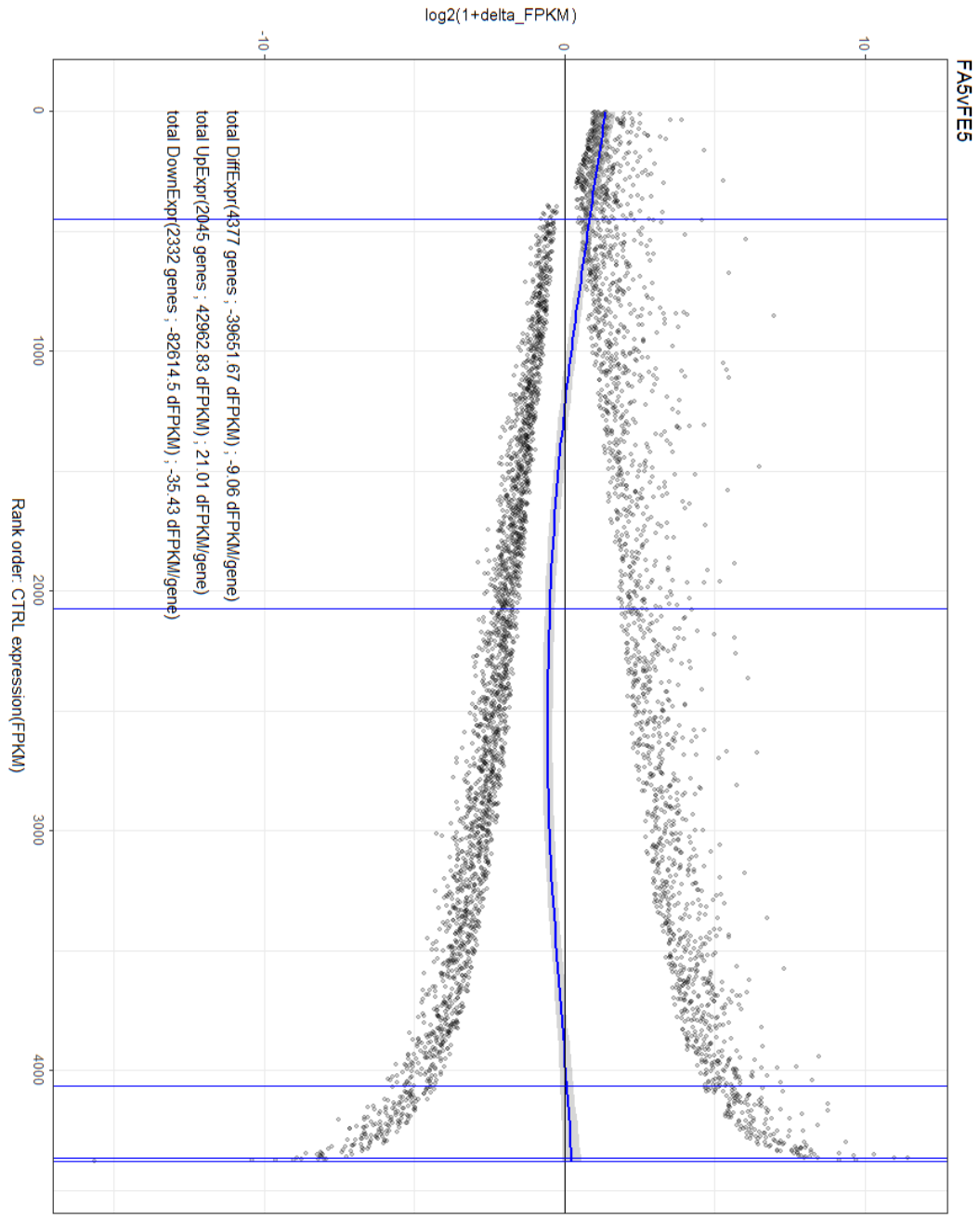

Figure 4j (FLAM76 - Day 5.5 - EPZ-6438 + panobinostat)

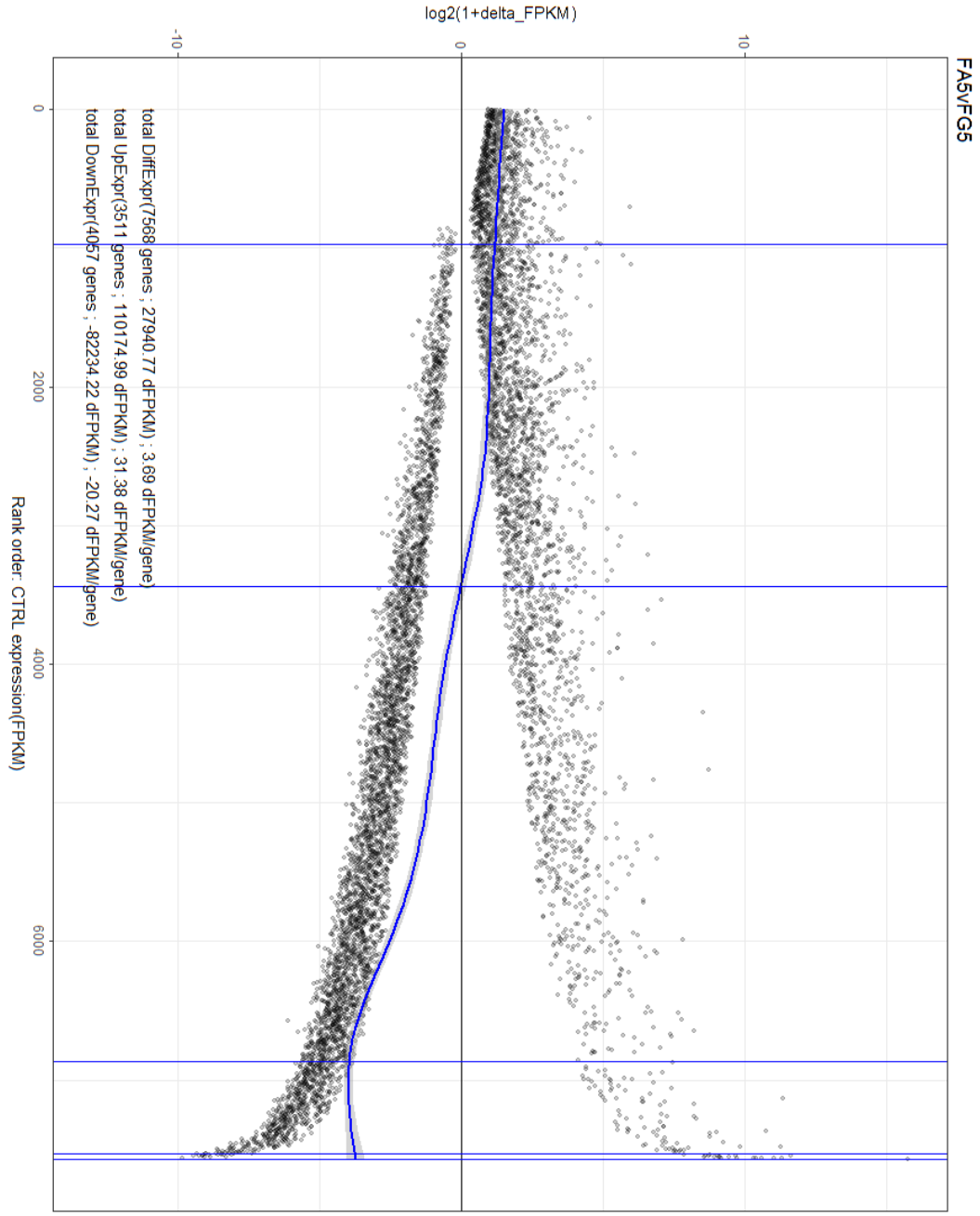

CHAPTER 5

DISCUSSION AND FUTURE AIMS

The next decade will be an incredibly exciting time to be involved in cancer research. New quantitative 'omics' technologies developed in the post-genomic era have vastly expanded our understanding of the biological mechanisms malignant cells use to initiate/sustain erroneous proliferation and evade standard-of-care therapies. The future of oncology will likely see a marriage of these profiling technologies with disease management; a union that will set the stage for precision medicine that utilizes the great body of accumulated knowledge to direct therapy towards the most fruitful outcome [214]. While personalized medicine seeks to categorize patients, other technologies, founded on our increasing understanding of immune biology, have immense promise to broadly target certain malignant cell types via the host immune system [197]. Other broad targeting therapies have begun to emerge from our relatively newfound appreciation for cancer epigenetics. While cancer biology has traditionally been a field that has studies the impact of specific oncogenic/tumor suppressor pathways, interest has surged towards understanding how cancer cells exploit epigenetic regulation of broad cellular processes to govern proliferation and microenvironment interactions [256]. Studies born out of this surge in interest have fomented the development a number of small compound inhibitors that have the potential to exploit cancer epigenomes with broad applicability. While these examples serve to elevate hope in the future of cancer biology, many cantankerous obstacles still block the road to a cure.

The introduction to this dissertation described MM as an immensely complex and highly heterogeneous disease. A diverse set of germinal-center-based genomic lesions initiate pre-malignancy. After terminal differentiation to the plasma cell stage, accumulate additional CNVs, translocations, somatic mutations and a reprogrammed epigenome until the malignant plasma cell burden in the bone marrow microenvironment ultimately prompts the diagnosis of MM [48]. These numerous roads, all leading to the singular diagnosis, exemplify the widespread heterogeneity present between MM patients. It should be no surprise that oncologists struggle to

manage this pernicious and often refractory malignancy with a limited palette of therapeutic options [191].

Addition of certain therapies to standard anti-MM therapeutic regimens (i.e. proteasome inhibitors and immunomodulatory drugs) have positively impacted disease management, however MM remains incurable due to inevitable drug-resistant relapse. In light of this, there is a profound need to expand the number of therapeutic options that are available to clinicians. These include therapies that both target specific sub-sets of the patient population and more broadly target MM despite genomic heterogeneity. Furthermore, such diverse options in treatment must absolutely be accompanied by profiling strategies that direct therapy to the most efficacious option prior to administration of ineffective and resistance-cultivating therapies.

The second chapter of this dissertation outlines a study that identified a 42-gene gene expression profile (GEP) that distinguishes extreme sensitivity/resistance to proteasome inhibitors (PIs). Proteasome inhibitors have been widely applied in MM therapy for over a decade. During this time, the problem of refraction/resistance to PIs has increasingly precipitated studies that have attempted to identify specific biomarkers for sensitivity/resistance. Dutifully following the literature on this subject in recent years have revealed a myriad of factors that seem to contribute to proteasome inhibitor resistance. While some biologically significant information can be gleaned from many of these studies, many of them suffer from the same pitfall: a lack of broad examination across a large number of cell lines [222]. Many studies attempting to distinguish sensitivity and resistance in MM (to PIs and other anti-MM therapies) perform experiments in only a handful of HMCLs, failing to address the broad context of disease heterogeneity.

In this study [217], we executed an unprecedented effort to systematically profile chemosensitivity to four proteasome inhibitors across a large (50+) panel of HMCLs. We observed that our HMCL panel displayed a broad distribution of cytotoxic response to therapy, not unlike the distribution of response present in the MM patient population. We importantly confirmed that all four PIs generally share significant overlap in response distribution. There were, however, some exceptions to this trend, suggesting that in some instances, certain HMCLs have adopted resistance mechanisms that are selective among proteasome inhibitors despite a

seemingly similar mechanism of action. This implies that, in some cases of refraction/relapse, other proteasome inhibitors may remain as therapeutic options. Attempting to elucidate the specific mechanisms that underpin selective resistance among proteasome inhibitors may shed light on interesting pharmacodynamic differences between these inhibitors.

Transcriptomic differences between HMCLs in the top and bottom deciles of the chemo sensitivity distribution revealed a large set of common distinguishing genes. Stringent thresholding to select only the most consistent genes yielded a 42-gene signature. Unsurprisingly several genes identified in this signature are directly or indirectly related to the ubiquitin proteasome system and endoplasmic reticulum stress.

Using this 42-gene signature our then post-doctoral researcher Amit Mitra, Ph.D. used publically available data to cluster patient data and train supervised ensemble machine learning algorithms (random forest and random survival forest). These efforts demonstrated that although our GEP was generated on only a handful of cell lines, these genes can successfully stratify patient populations under PI-including therapeutic regimens between good and poor responders. Importantly this was only true in clinical trial arms that contained PIs, suggesting that this signature is indeed drug specific.

Until recently, the notion of empirically testing GEPs to determine if these expression changes, as a group, are sufficient to drive resistance or therapy was not feasible. The advent of CRISPR-Cas9 genome engineering has raised a number of new possibilities. Specifically, it may be possible to multiplex guide RNAs that direct catalytically null Cas9 nucleases conjugated to enhancers or repressors of transcription (CRISPRa/CRISPRi) to precisely modulate the expression of several genes in tandem [281]. Several technical aspects are obstacles to such an approach. Despite this, it may soon be feasible to test drug-sensitivity GEPs directly in HMCLs to better understand the degree to which these transcriptomic changes are functionally causative.

Our laboratory has begun testing the ability of GEPs to distinguish sensitivity and resistance of sub-clones present in MM samples and cell lines. Single cell sequencing technologies are still in their infancy, yet they have immense promise to identify drug resistant sub-clones within a tumor that may flag a patient as harboring innate resistance to therapy. Our

recent publication [234] provides a bioinformatics pipeline for processing single cell sequencing (targeted) data and identifying drug resistant clones based on a predictive-GEP. This proof-of-principle study suggests that such an approach may have clinical utility. Both this and the experimental methods outlined in the preceding paragraph have just been funded for further evaluation/development and will be a continued area of research in the Van Ness laboratory.

The 3rd and 4th chapters of this dissertation articulate a study that tests methods to target the myeloma epigenome. Therapeutic strategies that target the epigenome have gained great momentum in recent years as epigenetic abnormalities are increasingly recognized as a core aspect of cancer development. MM is no exception to this.

The epigenetic repressor of transcription EZH2 initially became a gene of interest for the Van Ness laboratory in 2005 when a former graduate student, Paula Croonquist, described EZH2 as an oncogene in MM and demonstrated that EZH2 knockdown is sufficient to arrest MM growth [170]. At the time, a lack of small compounds that specifically inhibit EZH2 temporarily stifled our labs interest in EZH2 as we have always been interested in evaluating pre-clinical models that have potential translational impact in therapeutic contexts. Since Paula's 2005 *Oncogene* paper, a compendium of evidence has accumulated implicating EZH2 as a driver of many forms of cancer, namely lymphomas with gain-of-function mutations. Development of compounds that inhibit EZH2, along with new evidence corroborating EZH2 as being aberrantly active in MM, reignited our interest in evaluating EZH2 as a target for therapy in MM.

My study on this subject demonstrated that two EZH2 inhibitors (EZH2i's: EPZ-6438 and GSK-126) do have single agent efficacy in less than half of the HMCLs tested. This initial finding has since been corroborated by other recent publications examining the efficacy of these EZH2i's in MM. We were initially surprised to find that even in cases of resistance, H3K27 was robustly demethylated. This suggested that EZH2 inhibition in HMCLs did induce presumably massive remodeling of the MM epigenetic landscape in all cases, yet this change was only sometimes cytotoxic. This led us to postulate that EZH2i remodeling of the epigenome may potentiate response to current anti-MM therapies. Indeed we found that EZH2i pre-treatment strongly potentiate sensitivity towards the pan-HDAC inhibitor panobinostat in nearly all cases. Excitingly,

this this drug combination was effective even in HMCLs that had previously demonstrated the most extreme resistance to PIs.

While this drug combination is particularly relevant to MM due to the recent FDA approval of panobinostat for relapsed/refractory MM [135,136], it remains possible that other compounds may also be potentiated by EZH2i pre-treatment. EZH2's aberrant activity in MM (contrasting its lack of expression in healthy plasma cells) presents a specific target for EZH2i's. It would be informative to screen HMCLs pre-treated with EZH2i's for induced sensitivity to various anti-cancer compounds. Such a high throughput approach could illuminate new strategies to specifically target malignant plasma cells while also further elucidating the biological scope of EZH2 activity in MM cells.

Transcriptomic analysis revealed that combining of EZH2 inhibition with panobinostat in HMCLs modulates the expression of thousands of genes. This was no surprise as the targets of both drugs are individually known to regulate thousands of genes through canonical modifications of histones and non-canonical modification of non-histone regulators of transcription [127,159]. Interestingly, in combination, these two compounds revealed a large portion of differentially expressed genes that were unique to the combination (~2/3). This was particularly striking in the EZH2i-sensitive HMCL FLAM76, which had little to no transcriptomic response from panobinostat at the doses used in that experiment. This reveals an interesting area of potential research. As discussed in the introduction, epigenetic complexes crosstalk with each-other to form a highly complex network of transcriptomic regulation [111,131]. My data suggests that HDACs and EZH2 cooperate to silence thousands of gene that cannot be upregulated by a loss of either alone. My transcriptomic data represents too few HMCLs to make any conclusions regarding whether or not there is a consistent GEP that represents genes co-regulated in this manner across HMCLs. It would be interesting to perform this transcriptomic analysis in many additional HMCLs to determine if such a signature exists.

Network analysis via IPA revealed a great number of pathways, upstream regulators and GO terms enriched in my transcriptomic data. Many of these findings reflected changes that have been described in other recent studies that have measured EZH2i-induced transcriptomic

changes in lymphoid malignancies and other cancers (referenced in Chapter 3). Many important oncogenic pathways were highlighted as well as many other pathways with less obvious significance. Unfortunately, the differences and similarities between the two lines were far too numerous to derive any specific candidates as factors that distinguish sensitivity. Furthermore, the lack of panobinostat single agent response in one of the two HMCLs subjected to transcriptomic analysis reduced conclusions that could be drawn regarding mechanisms for toxicity in the combination condition.

The general conclusion from this analysis was that EZH2i upregulates many tumor suppressive signaling cascades (e.g. p53 and XAF1) while concomitantly downregulating tumor-promoting pathways (e.g. MYC and BCL2). These changes are enhanced by the addition of HDAC inhibition.

Interestingly, despite the large number of genes identified to be uniquely modulated in the combination condition, relatively few contextually significant pathways, regulators and GO terms were uniquely unveiled at the inclusion of panobinostat. This suggests that unlike EZH2i-induced GEPs, genes upregulated uniquely in the combination treatment may not represent a specific epigenetic program that governs specific pathways but may rather represent non-specific upregulation across the genome. This prompted us to consider the possibility that there may be an element of non-specific transcriptomic stress produced be the massive induction of transcriptomic output. We postulate that it might be possible that, as suggested above, HDAC inhibition exacerbates transcriptomic changes in pathways targeted by EZH2 inhibition. These changes seem to promote a more apoptotic-permissive state that may sensitize these cells to undue transcriptomic stress (over-loading of the transcriptomic machinery). As outlined in Chapter 4 gene expression changes observed in the combination condition have an odd distribution where genes highly expressed in the untreated condition (baseline) are highly biased towards downregulation. This could suggest that undue transcriptomic activation may be overloading the transcriptomic machinery and downregulating highly expressed housekeeping genes and overexpressed MM-related oncogenes (e.g. MYC). Additional studies are required to support the notion of non-specific transcriptomic stress as a mechanism for cytotoxicity in

EZH2i/HDACi combination treatment. If this were to be supported empirically, it would present a novel cytotoxic mechanism to target (via EZH2 inhibition) malignant plasma cells.

This study presents a number of future directions, some of which are alluded to above. The next logical progression in the pre-clinical evaluation of EZH2i/HDACi combination would be to apply this therapeutic strategy in a *murine* xenograft model of MM. We have discussed this prospect with EZH2i-producing companies and have garnered some interest in funding such a study. This study revealed several ongoing questions regarding the biological significance of EZH2 activity in MM and how EZH2 and HDACs coordinate to regulate large portions of the genome. Studies addressing these questions should begin by measuring EZH2/HDAC occupancy on chromatin in response to single agent and combination therapy. Some information exists regarding complex interactions between these two classes of epigenetic regulators [271,276,277], however there is ample room for basic science studies to elucidate the specific molecular and contextual basis for these interactions.

The research presented in this document represents two approaches for overcoming drug resistant MM. The first focuses on using HMCL chemosensitivity screening and subsequent transcriptomic profiling to identify patients that represent extremes in sensitivity to proteasome inhibitors. The second focuses on applying a combination of epigenetic inhibitors to broadly target malignant plasma cells even in cases of extreme resistance to proteasome inhibitors. This next decade holds great promise for new therapeutic strategies that improve MM management. As we continue to combine tumor profiling with efforts to increase our understanding of MM biology, we will inch ever closer to defeating this devastating malignancy.

BIBLIOGRAPHY

1. Dimopoulos MA, Facon T, Editors ET. Multiple Myeloma and Other Plasma Cell Neoplasms. Available from https://link.springer.com/content/pdf/10.1007%2F978-3-319-25586-6.pdf
2. Kuehl WM, Bergsagel PL. Multiple myeloma: evolving genetic events and host interactions. Nat Rev Cancer. Nature Publishing Group; 2002; 2: 175–87. doi: 10.1038/nrc746.
3. Siegel RL, Miller KD, Jemal A. Cancer statistics, 2017. CA Cancer J Clin. 2017; 67: 7–30. doi: 10.3322/caac.21387.
4. Morse D, Dailey RC, Bunn J. Prehistoric multiple myeloma. Bull N Y Acad Med. 1974; 50: 447–58. Available from http://www.ncbi.nlm.nih.gov/pubmed/4594853
5. Solly S. Remarks on the pathology of mollities ossium; with cases. Med Chir Trans. Royal Society of Medicine Press; 1844; 27: 435–498.8. Available from http://www.ncbi.nlm.nih.gov/pubmed/20895811
6. BENCE JONES H. Papers ON CHEMICAL PATHOLOGY; Lancet. Elsevier; 1847; 50: 88–92. doi: 10.1016/S0140-6736(02)86528-X.
7. EDELMAN GM, GALLY JA. The nature of Bence-Jones proteins. Chemical similarities to polypetide chains of myeloma globulins and normal gamma-globulins. J Exp Med. Rockefeller University Press; 1962; 116: 207–27. doi: 10.1084/JEM.116.2.207.
8. Longsworth LG, Shedlovsky T, Macinnes DA. ELECTROPHORETIC PATTERNS OF NORMAL AND PATHOLOGICAL HUMAN BLOOD SERUM AND PLASMA. J Exp Med. Rockefeller University Press; 1939; 70: 399–413. doi: 10.1084/JEM.70.4.399.
9. de Larrea CF, Isola I, Pereira A, Cibeira MT, Magnano L, Tovar N, Rodríguez-Lobato L-G, Calvo X, Aróstegui JI, Díaz T, Lozano E, Rozman M, Yagüe J, et al. Evolving m-protein pattern in patients with smoldering multiple myeloma: impact on early progression. Leukemia. Nature Publishing Group; 2018; : 1. doi: 10.1038/s41375-018-0013-4.
10. Rustizky J. Multiples Myelom. Dtsch Zeitschrift für Chir. Springer Berlin Heidelberg; 1873; 3: 162–72. doi: 10.1007/BF02911073.

11. Wright JH. A CASE OF MULTIPLE MYELOMA. J Boston Soc Med Sci. American Society for Investigative Pathology; 1900; 4: 195–204.5. Available from http://www.ncbi.nlm.nih.gov/pubmed/19971313

12. Kyle RA, Rajkumar S V. Criteria for diagnosis, staging, risk stratification and response assessment of multiple myeloma. Leukemia. Nature Publishing Group; 2009; 23: 3–9. doi: 10.1038/leu.2008.291.

13. Cohen G, Hörl WH. Free Immunoglobulin Light Chains as a Risk Factor in Renal and Extrarenal Complications. Semin Dial. Blackwell Publishing Ltd; 2009; 22: 369–72. doi: 10.1111/j.1525-139X.2009.00582.x.

14. Standal T, Abildgaard N, Fagerli U-M, Stordal B, Hjertner O, Borset M, Sundan A. HGF inhibits BMP-induced osteoblastogenesis: possible implications for the bone disease of multiple myeloma. Blood. American Society of Hematology; 2007; 109: 3024–30. doi: 10.1182/blood-2006-07-034884.

15. Giuliani N, Colla S, Morandi F, Lazzaretti M, Sala R, Bonomini S, Grano M, Colucci S, Svaldi M, Rizzoli V. Myeloma cells block RUNX2/CBFA1 activity in human bone marrow osteoblast progenitors and inhibit osteoblast formation and differentiation. Blood. American Society of Hematology; 2005; 106: 2472–83. doi: 10.1182/blood-2004-12-4986.

16. Oyajobi BO. Multiple myeloma/hypercalcemia. Arthritis Res Ther. BioMed Central; 2007; 9: S4. doi: 10.1186/ar2168.

17. Husby S, Grønbæk K. Mature lymphoid malignancies: origin, stem cells, and chronicity. Blood Adv. 2017; 1: 2444–55. doi: 10.1182/bloodadvances.2017008854.

18. Allman D, Li J, Hardy RR. Commitment to the B lymphoid lineage occurs before DH-JH recombination. J Exp Med. 1999; 189: 735–40. Available from http://www.ncbi.nlm.nih.gov/pubmed/9989989

19. Li YS, Wasserman R, Hayakawa K, Hardy RR. Identification of the earliest B lineage stage in mouse bone marrow. Immunity. 1996; 5: 527–35. Available from http://www.ncbi.nlm.nih.gov/pubmed/8986713

20. Ogawa M, ten Boekel E, Melchers F. Identification of CD19(-)B220(+)c-Kit(+)Flt3/Flk-

2(+)cells as early B lymphoid precursors before pre-B-I cells in juvenile mouse bone marrow. Int Immunol. 2000; 12: 313–24. Available from http://www.ncbi.nlm.nih.gov/pubmed/10700466

21. Kondo M, Weissman IL, Akashi K. Identification of clonogenic common lymphoid progenitors in mouse bone marrow. Cell. 1997; 91: 661–72. Available from http://www.ncbi.nlm.nih.gov/pubmed/9393859

22. Johnson K, Shapiro-Shelef M, Tunyaplin C, Calame K. Regulatory events in early and late B-cell differentiation. Mol Immunol. Pergamon; 2005; 42: 749–61. doi: 10.1016/J.MOLIMM.2004.06.039.

23. Mostoslavsky R, Alt FW, Bassing CH. Chromatin dynamics and locus accessibility in the immune system. Nat Immunol. 2003; 4: 603–6. doi: 10.1038/ni0703-603.

24. Nossal GJV. Negative selection of lymphocytes. Cell. Cell Press; 1994; 76: 229–39. doi: 10.1016/0092-8674(94)90331-X.

25. Driver DJ, McHeyzer-Williams LJ, Cool M, Stetson DB, McHeyzer-Williams MG. Development and maintenance of a B220- memory B cell compartment. J Immunol. 2001; 167: 1393–405. Available from http://www.ncbi.nlm.nih.gov/pubmed/11466358

26. Calame KL. Plasma cells: finding new light at the end of B cell development. Nat Immunol. Nature Publishing Group; 2001; 2: 1103–8. doi: 10.1038/ni1201-1103.

27. Shapiro-Shelef M, Calame K. Regulation of plasma-cell development. Nat Rev Immunol. Nature Publishing Group; 2005; 5: 230–42. doi: 10.1038/nri1572.

28. Shapiro-Shelef M, Calame K. Plasma cell differentiation and multiple myeloma. Curr Opin Immunol. Elsevier Current Trends; 2004; 16: 226–34. doi: 10.1016/J.COI.2004.02.001.

29. Shapiro-Shelef M, Lin K-I, Savitsky D, Liao J, Calame K. Blimp-1 is required for maintenance of long-lived plasma cells in the bone marrow. J Exp Med. Rockefeller University Press; 2005; 202: 1471–6. doi: 10.1084/jem.20051611.

30. Slifka MK, Ahmed R. Long-lived plasma cells: a mechanism for maintaining persistent antibody production. Curr Opin Immunol. 1998; 10: 252–8. Available from http://www.ncbi.nlm.nih.gov/pubmed/9638360

31. Fenton JAL, Pratt G, Rawstron AC, Morgan GJ. Isotype class switching and the pathogenenesis of multiple myeloma. Hematol Oncol. 2002; 20: 75–85. doi: 10.1002/hon.688.

32. Bakkus MH, Van Riet I, Van Camp B, Thielemans K. Evidence that the clonogenic cell in multiple myeloma originates from a pre-switched but somatically mutated B cell. Br J Haematol. 1994; 87: 68–74. Available from http://www.ncbi.nlm.nih.gov/pubmed/7947257

33. Bakkus MH, Heirman C, Van Riet I, Van Camp B, Thielemans K. Evidence that multiple myeloma Ig heavy chain VDJ genes contain somatic mutations but show no intraclonal variation. Blood. 1992; 80: 2326–35. Available from http://www.ncbi.nlm.nih.gov/pubmed/1421403

34. Goossens T, Klein U, Küppers R. Frequent occurrence of deletions and duplications during somatic hypermutation: implications for oncogene translocations and heavy chain disease. Proc Natl Acad Sci U S A. 1998; 95: 2463–8. Available from http://www.ncbi.nlm.nih.gov/pubmed/9482908

35. Kyle RA, Therneau TM, Rajkumar SV, Offord JR, Larson DR, Plevak MF, Melton LJ. A Long-Term Study of Prognosis in Monoclonal Gammopathy of Undetermined Significance. N Engl J Med. Massachusetts Medical Society ; 2002; 346: 564–9. doi: 10.1056/NEJMoa01133202.

36. Bladé J, Rosiñol L, Cibeira MT, de Larrea CF. Pathogenesis and progression of monoclonal gammopathy of undetermined significance. Leukemia. Nature Publishing Group; 2008; 22: 1651–7. doi: 10.1038/leu.2008.203.

37. Kyle RA, Rajkumar SV. Monoclonal gammopathy of undetermined significance and smouldering multiple myeloma: emphasis on risk factors for progression. Br J Haematol. Blackwell Publishing Ltd; 2007; 139: 730–43. doi: 10.1111/j.1365-2141.2007.06873.x.

38. Kyle RA, Remstein ED, Therneau TM, Dispenzieri A, Kurtin PJ, Hodnefield JM, Larson DR, Plevak MF, Jelinek DF, Fonseca R, Melton LJ, Rajkumar SV. Clinical Course and Prognosis of Smoldering (Asymptomatic) Multiple Myeloma. N Engl J Med. Massachusetts Medical Society ; 2007; 356: 2582–90. doi: 10.1056/NEJMoa070389.

39. Albarracin F, Fonseca R. Plasma cell leukemia. Blood Rev. Elsevier; 2011; 25: 107–12. doi: 10.1016/j.blre.2011.01.005.

40. Lohr JG, Stojanov P, Carter SL, Cruz-Gordillo P, Lawrence MS, Auclair D, Sougnez C, Knoechel B, Gould J, Saksena G, Cibulskis K, McKenna A, Chapman MA, et al. Widespread genetic heterogeneity in multiple myeloma: implications for targeted therapy. Cancer Cell. 2014; 25: 91–101. doi: 10.1016/j.ccr.2013.12.015.

41. Bahlis NJ. Darwinian evolution and tiding clones in multiple myeloma. Blood. 2012; 120: 927–8. doi: 10.1182/blood-2012-06-430645.

42. Bolli N, Avet-Loiseau H, Wedge DC, Van Loo P, Alexandrov LB, Martincorena I, Dawson KJ, Iorio F, Nik-Zainal S, Bignell GR, Hinton JW, Li Y, Tubio JMC, et al. Heterogeneity of genomic evolution and mutational profiles in multiple myeloma. Nat Commun. Nature Publishing Group; 2014; 5: 2997. doi: 10.1038/ncomms3997.

43. Walker BA, Wardell CP, Melchor L, Brioli A, Johnson DC, Kaiser MF, Mirabella F, Lopez-Corral L, Humphray S, Murray L, Ross M, Bentley D, Gutiérrez NC, et al. Intraclonal heterogeneity is a critical early event in the development of myeloma and precedes the development of clinical symptoms. Leukemia. 2014; 28: 384–90. doi: 10.1038/leu.2013.199.

44. Walker BA, Boyle EM, Wardell CP, Murison A, Begum DB, Dahir NM, Proszek PZ, Johnson DC, Kaiser MF, Melchor L, Aronson LI, Scales M, Pawlyn C, et al. Mutational Spectrum, Copy Number Changes, and Outcome: Results of a Sequencing Study of Patients With Newly Diagnosed Myeloma. J Clin Oncol. 2015; 33: 3911–20. doi: 10.1200/JCO.2014.59.1503.

45. Walker BA, Wardell CP, Melchor L, Brioli A, Johnson DC, Kaiser MF, Mirabella F, Lopez-Corral L, Humphray S, Murray L, Ross M, Bentley D, Gutiérrez NC, et al. Intraclonal heterogeneity is a critical early event in the development of myeloma and precedes the development of clinical symptoms. Leukemia. 2014; 28: 384–90. doi: 10.1038/leu.2013.199.

46. Bolli N, Li Y, Sathiaseelan V, Raine K, Jones D, Ganly P, Cocito F, Bignell G, Chapman

MA, Sperling AS, Anderson KC, Avet-Loiseau H, Minvielle S, et al. A DNA target-enrichment approach to detect mutations, copy number changes and immunoglobulin translocations in multiple myeloma. Blood Cancer J. 2016; 6: e467. doi: 10.1038/bcj.2016.72.

47. Chapman MA, Lawrence MS, Keats JJ, Cibulskis K, Sougnez C, Schinzel AC, Harview CL, Brunet J-P, Ahmann GJ, Adli M, Anderson KC, Ardlie KG, Auclair D, et al. Initial genome sequencing and analysis of multiple myeloma. Nature. Nature Publishing Group; 2011; 471: 467–72. doi: 10.1038/nature09837.

48. Manier S, Salem KZ, Park J, Landau DA, Getz G, Ghobrial IM. Genomic complexity of multiple myeloma and its clinical implications. Nat Rev Clin Oncol. Nature Publishing Group; 2017; 14: 100–13. doi: 10.1038/nrclinonc.2016.122.

49. Stella F, Pedrazzini E, Agazzoni M, Ballester O, Slavutsky I. Cytogenetic Alterations in Multiple Myeloma: Prognostic Significance and the Choice of Frontline Therapy. Cancer Invest. Informa HealthcareNew York; 2015; 33: 496–504. doi: 10.3109/07357907.2015.1080833.

50. Taub R, Kirsch I, Morton C, Lenoir G, Swan D, Tronick S, Aaronson S, Leder P. Translocation of the c-myc gene into the immunoglobulin heavy chain locus in human Burkitt lymphoma and murine plasmacytoma cells. Proc Natl Acad Sci. 1982; 79.

51. Walker BA, Wardell CP, Johnson DC, Kaiser MF, Begum DB, Dahir NB, Ross FM, Davies FE, Gonzalez D, Morgan GJ. Characterization of IGH locus breakpoints in multiple myeloma indicates a subset of translocations appear to occur in pregerminal center B cells. Blood. American Society of Hematology; 2013; 121: 3413–9. doi: 10.1182/blood-2012-12-471888.

52. Walker BA, Boyle EM, Wardell CP, Murison A, Begum DB, Dahir NM, Proszek PZ, Johnson DC, Kaiser MF, Melchor L, Aronson LI, Scales M, Pawlyn C, et al. Mutational Spectrum, Copy Number Changes, and Outcome: Results of a Sequencing Study of Patients With Newly Diagnosed Myeloma. J Clin Oncol. 2015; 33: 3911–20. doi: 10.1200/JCO.2014.59.1503.

53. Debes-Marun CS, Dewald GW, Bryant S, Picken E, Santana-Dávila R, González-Paz N, Winkler JM, Kyle RA, Gertz MA, Witzig TE, Dispenzieri A, Lacy MQ, Rajkumar S V, et al. Chromosome abnormalities clustering and its implications for pathogenesis and prognosis in myeloma. Leukemia. Nature Publishing Group; 2003; 17: 427–36. doi: 10.1038/sj.leu.2402797.

54. Chng WJ, Winkler JM, Greipp PR, Jalal SM, Bergsagel PL, Chesi M, Trendle MC, Ahmann GJ, Henderson K, Blood E, Oken MM, Hulbert A, Wier SA Van, et al. Ploidy status rarely changes in myeloma patients at disease progression. Leuk Res. Pergamon; 2006; 30: 266–71. doi: 10.1016/J.LEUKRES.2005.07.004.

55. Avet-Loiseau H, Gerson F, Magrangeas F, Minvielle S, Harousseau JL, Bataille R, Intergroupe Francophone du Myélome. Rearrangements of the c-myc oncogene are present in 15% of primary human multiple myeloma tumors. Blood. 2001; 98: 3082–6. Available from http://www.ncbi.nlm.nih.gov/pubmed/11698294

56. Walker BA, Leone PE, Chiecchio L, Dickens NJ, Jenner MW, Boyd KD, Johnson DC, Gonzalez D, Dagrada GP, Protheroe RKM, Konn ZJ, Stockley DM, Gregory WM, et al. A compendium of myeloma-associated chromosomal copy number abnormalities and their prognostic value. Blood. 2010; 116: e56–65. doi: 10.1182/blood-2010-04-279596.

57. Dimopoulos K, Gimsing P, Grønbæk K. The role of epigenetics in the biology of multiple myeloma. Blood Cancer J. 2014; 4: e207. doi: 10.1038/bcj.2014.29.

58. Alzrigat M, Párraga AA, Jernberg-Wiklund H. Epigenetics in multiple myeloma: From mechanisms to therapy. Semin Cancer Biol. 2017; . doi: 10.1016/j.semcancer.2017.09.007.

59. Christofides A, Karantanos T, Bardhan K, Boussiotis VA. Epigenetic regulation of cancer biology and anti-tumor immunity by EZH2. Oncotarget. 2016; 7: 85624–40. doi: 10.18632/oncotarget.12928.

60. Issa ME, Takhsha FS, Chirumamilla CS, Perez-Novo C, Vanden Berghe W, Cuendet M. Epigenetic strategies to reverse drug resistance in heterogeneous multiple myeloma. Clin Epigenetics. BioMed Central; 2017; 9: 17. doi: 10.1186/s13148-017-0319-5.

61. Jones PA. Functions of DNA methylation: islands, start sites, gene bodies and beyond. Nat Rev Genet. Nature Publishing Group; 2012; 13: 484–92. doi: 10.1038/nrg3230.

62. Liang G, Weisenberger DJ. DNA methylation aberrancies as a guide for surveillance and treatment of human cancers. Epigenetics. 2017; 12: 416–32. doi: 10.1080/15592294.2017.1311434.

63. Kaiser MF, Johnson DC, Wu P, Walker BA, Brioli A, Mirabella F, Wardell CP, Melchor L, Davies FE, Morgan GJ. Global methylation analysis identifies prognostically important epigenetically inactivated tumor suppressor genes in multiple myeloma. Blood. 2013; 122: 219–26. doi: 10.1182/blood-2013-03-487884.

64. Heuck CJ, Mehta J, Bhagat T, Gundabolu K, Yu Y, Khan S, Chrysofakis G, Schinke C, Tariman J, Vickrey E, Pulliam N, Nischal S, Zhou L, et al. Myeloma Is Characterized by Stage-Specific Alterations in DNA Methylation That Occur Early during Myelomagenesis. J Immunol. 2013; 190: 2966–75. doi: 10.4049/jimmunol.1202493.

65. Walker BA, Wardell CP, Chiecchio L, Smith EM, Boyd KD, Neri A, Davies FE, Ross FM, Morgan GJ. Aberrant global methylation patterns affect the molecular pathogenesis and prognosis of multiple myeloma. Blood. 2011; 117: 553–62. doi: 10.1182/blood-2010-04-279539.

66. Bollati V, Fabris S, Pegoraro V, Ronchetti D, Mosca L, Deliliers GL, Motta V, Bertazzi PA, Baccarelli A, Neri A. Differential repetitive DNA methylation in multiple myeloma molecular subgroups. Carcinogenesis. 2009; 30: 1330–5. doi: 10.1093/carcin/bgp149.

67. Agirre X, Castellano G, Pascual M, Heath S, Kulis M, Segura V, Bergmann A, Esteve A, Merkel A, Raineri E, Agueda L, Blanc J, Richardson D, et al. Whole-epigenome analysis in multiple myeloma reveals DNA hypermethylation of B cell-specific enhancers. Genome Res. Cold Spring Harbor Laboratory Press; 2015; 25: 478–87. doi: 10.1101/gr.180240.114.

68. Houde C, Li Y, Song L, Barton K, Zhang Q, Godwin J, Nand S, Toor A, Alkan S, Smadja NV, Avet-Loiseau H, Lima CS, Miele L, et al. Overexpression of the NOTCH ligand JAG2 in malignant plasma cells from multiple myeloma patients and cell lines. Blood. American

Society of Hematology; 2004; 104: 3697–704. doi: 10.1182/blood-2003-12-4114.

69. Bi C, Chung T-H, Huang G, Zhou J, Yan JJ, Fonseca R, Chng WJ, Bi C, Chung T-H, Huang G, Zhou J, Yan JJ, Fonseca R, et al. Genome-wide pharmacologic unmasking identifies tumor suppressive microRNAs in multiple myeloma. Oncotarget. Impact Journals; 2015; 6: 26508–18. doi: 10.18632/oncotarget.4769.

70. Zhang W, Wang YE, Zhang Y, Leleu X, Reagan M, Zhang Y, Mishima Y, Glavey S, Manier S, Sacco A, Jiang B, Roccaro AM, Ghobrial IM. Global Epigenetic Regulation of MicroRNAs in Multiple Myeloma. Zhang Y, editor. PLoS One. Public Library of Science; 2014; 9: e110973. doi: 10.1371/journal.pone.0110973.

71. Wong KY, Huang X, Chim CS. DNA methylation of microRNA genes in multiple myeloma. Carcinogenesis. Oxford University Press; 2012; 33: 1629–38. doi: 10.1093/carcin/bgs212.

72. Brinkman AB, Gu H, Bartels SJJ, Zhang Y, Matarese F, Simmer F, Marks H, Bock C, Gnirke A, Meissner A, Stunnenberg HG. Sequential ChIP-bisulfite sequencing enables direct genome-scale investigation of chromatin and DNA methylation cross-talk. Genome Res. Cold Spring Harbor Laboratory Press; 2012; 22: 1128–38. doi: 10.1101/gr.133728.111.

73. Reddington JP, Perricone SM, Nestor CE, Reichmann J, Youngson NA, Suzuki M, Reinhardt D, Dunican DS, Prendergast JG, Mjoseng H, Ramsahoye BH, Whitelaw E, Greally JM, et al. Redistribution of H3K27me3 upon DNA hypomethylation results in de-repression of Polycomb target genes. Genome Biol. BioMed Central; 2013; 14: R25. doi: 10.1186/gb-2013-14-3-r25.

74. Pawlyn C, Kaiser MF, Heuck C, Melchor L, Wardell CP, Murison A, Chavan SS, Johnson DC, Begum DB, Dahir NM, Proszek PZ, Cairns DA, Boyle EM, et al. The Spectrum and Clinical Impact of Epigenetic Modifier Mutations in Myeloma. Clin Cancer Res. American Association for Cancer Research; 2016; 22: 5783–94. doi: 10.1158/1078-0432.CCR-15-1790.

75. Corthals SL, Sun SM, Kuiper R, de Knegt Y, Broyl A, van der Holt B, Beverloo HB, Peeters JK, el Jarari L, Lokhorst HM, Zweegman S, Jongen-Lavrencic M, Sonneveld P.

MicroRNA signatures characterize multiple myeloma patients. Leukemia. Nature Publishing Group; 2011; 25: 1784–9. doi: 10.1038/leu.2011.147.

76. Bi C, Chng WJ. MicroRNA: important player in the pathobiology of multiple myeloma. Biomed Res Int. Hindawi; 2014; 2014: 521586. doi: 10.1155/2014/521586.

77. Rastgoo N, Abdi J, Hou J, Chang H. Role of epigenetics-microRNA axis in drug resistance of multiple myeloma. J Hematol Oncol. 2017; 10: 121. doi: 10.1186/s13045-017-0492-1.

78. Liu X, Ling Z-Q. Role of isocitrate dehydrogenase 1/2 (IDH 1/2) gene mutations in human tumors. Histol Histopathol. 2015; 30: 1155–60. doi: 10.14670/HH-11-643.

79. Du J, Johnson LM, Jacobsen SE, Patel DJ. DNA methylation pathways and their crosstalk with histone methylation. Nat Rev Mol Cell Biol. 2015; 16: 519–32. doi: 10.1038/nrm4043.

80. Kiziltepe T, Hideshima T, Catley L, Raje N, Yasui H, Shiraishi N, Okawa Y, Ikeda H, Vallet S, Pozzi S, Ishitsuka K, Ocio EM, Chauhan D, et al. 5-Azacytidine, a DNA methyltransferase inhibitor, induces ATR-mediated DNA double-strand break responses, apoptosis, and synergistic cytotoxicity with doxorubicin and bortezomib against multiple myeloma cells. Mol Cancer Ther. American Association for Cancer Research; 2007; 6: 1718–27. doi: 10.1158/1535-7163.MCT-07-0010.

81. Maes K, De Smedt E, Kassambara A, Hose D, Seckinger A, Van Valckenborgh E, Menu E, Klein B, Vanderkerken K, Moreaux J, De Bruyne E. In vivo treatment with epigenetic modulating agents induces transcriptional alterations associated with prognosis and immunomodulation in multiple myeloma. Oncotarget. 2015; 6: 3319–34. doi: 10.18632/oncotarget.3207.

82. Fratta E, Montico B, Rizzo A, Colizzi F, Sigalotti L, Dolcetti R, Fratta E, Montico B, Rizzo A, Colizzi F, Sigalotti L, Dolcetti R. Epimutational profile of hematologic malignancies as attractive target for new epigenetic therapies. Oncotarget. Impact Journals; 2016; 7: 57327–50. doi: 10.18632/oncotarget.10033.

83. Alexander RP, Fang G, Rozowsky J, Snyder M, Gerstein MB. Annotating non-coding regions of the genome. Nat Rev Genet. Nature Publishing Group; 2010; 11: 559–71. doi: 10.1038/nrg2814.

84. Kapranov P, Cheng J, Dike S, Nix DA, Duttagupta R, Willingham AT, Stadler PF, Hertel J, Hackermüller J, Hofacker IL, Bell I, Cheung E, Drenkow J, et al. RNA maps reveal new RNA classes and a possible function for pervasive transcription. Science. American Association for the Advancement of Science; 2007; 316: 1484–8. doi: 10.1126/science.1138341.

85. Carninci P, Kasukawa T, Katayama S, Gough J, Frith MC, Maeda N, Oyama R, Ravasi T, Lenhard B, Wells C, Kodzius R, Shimokawa K, Bajic VB, et al. The transcriptional landscape of the mammalian genome. Science. American Association for the Advancement of Science; 2005; 309: 1559–63. doi: 10.1126/science.1112014.

86. Bartel DP. MicroRNAs: Genomics, Biogenesis, Mechanism, and Function. Cell. Cell Press; 2004; 116: 281–97. doi: 10.1016/S0092-8674(04)00045-5.

87. Tüfekci KU, Meuwissen RLJ, Genç Ş. The Role of MicroRNAs in Biological Processes. Humana Press, Totowa, NJ; 2014. p. 15–31. doi: 10.1007/978-1-62703-748-8_2.

88. Kent OA, Mendell JT. A small piece in the cancer puzzle: microRNAs as tumor suppressors and oncogenes. Oncogene. Nature Publishing Group; 2006; 25: 6188–96. doi: 10.1038/sj.onc.1209913.

89. Chan S-H, Wang L-H. Regulation of cancer metastasis by microRNAs. J Biomed Sci. BioMed Central; 2015; 22: 9. doi: 10.1186/s12929-015-0113-7.

90. Lionetti M, Musto P, Di Martino MT, Fabris S, Agnelli L, Todoerti K, Tuana G, Mosca L, Gallo Cantafio ME, Grieco V, Bianchino G, D'Auria F, Statuto T, et al. Biological and clinical relevance of miRNA expression signatures in primary plasma cell leukemia. Clin Cancer Res. American Association for Cancer Research; 2013; 19: 3130–42. doi: 10.1158/1078-0432.CCR-12-2043.

91. Chi J, Ballabio E, Chen X-H, Kušec R, Taylor S, Hay D, Tramonti D, Saunders NJ, Littlewood T, Pezzella F, Boultwood J, Wainscoat JS, Hatton CS, et al. MicroRNA expression in multiple myeloma is associated with genetic subtype, isotype and survival. Biol Direct. BioMed Central; 2011; 6: 23. doi: 10.1186/1745-6150-6-23.

92. Seckinger A, Meißner T, Moreaux J, Benes V, Hillengass J, Castoldi M, Zimmermann J,

Ho AD, Jauch A, Goldschmidt H, Klein B, Hose D. miRNAs in multiple myeloma--a survival relevant complex regulator of gene expression. Oncotarget. Impact Journals, LLC; 2015; 6: 39165–83. doi: 10.18632/oncotarget.5381.

93. Sarasquete ME, Gutiérrez NC, Misiewicz-Krzeminska I, Paiva B, Chillón MC, Alcoceba M, García-Sanz R, Hernández JM, González M, San-Miguel JF, Hernández JM, Sureda A, Palomera L, et al. Upregulation of Dicer is more frequent in monoclonal gammopathies of undetermined significance than in multiple myeloma patients and is associated with longer survival in symptomatic myeloma patients. Haematologica. Haematologica; 2011; 96: 468–71. doi: 10.3324/haematol.2010.033845.

94. Martino M Di, Gullà A, Cantafio M, Oncotarget ML-, 2013 undefined. In vitro and in vivo anti-tumor activity of miR-221/222 inhibitors in multiple myeloma. ncbi.nlm.nih.gov. Available from https://www.ncbi.nlm.nih.gov/pmc/articles/PMC3712570/

95. Gutiérrez NC, Sarasquete ME, Misiewicz-Krzeminska I, Delgado M, De Las Rivas J, Ticona F V, Fermiñán E, Martín-Jiménez P, Chillón C, Risueño A, Hernández JM, García-Sanz R, González M, et al. Deregulation of microRNA expression in the different genetic subtypes of multiple myeloma and correlation with gene expression profiling. Leukemia. Nature Publishing Group; 2010; 24: 629–37. doi: 10.1038/leu.2009.274.

96. Mercer TR, Dinger ME, Mattick JS. Long non-coding RNAs: insights into functions. Nat Rev Genet. Nature Publishing Group; 2009; 10: 155–9. doi: 10.1038/nrg2521.

97. Majidinia M, Yousefi B. Long non-coding RNAs in cancer drug resistance development. DNA Repair (Amst). Elsevier; 2016; 45: 25–33. doi: 10.1016/J.DNAREP.2016.06.003.

98. Bhan A, Soleimani M, Mandal SS. Long Noncoding RNA and Cancer: A New Paradigm. Cancer Res. American Association for Cancer Research; 2017; 77: 3965–81. doi: 10.1158/0008-5472.CAN-16-2634.

99. Schmitt AM, Chang HY. Long Noncoding RNAs: At the Intersection of Cancer and Chromatin Biology. Cold Spring Harb Perspect Med. NIH Public Access; 2017; 7. doi: 10.1101/cshperspect.a026492.

100. Bartonicek N, Maag JL V., Dinger ME. Long noncoding RNAs in cancer: mechanisms of

action and technological advancements. Mol Cancer. BioMed Central; 2016; 15: 43. doi: 10.1186/s12943-016-0530-6.

101. Ronchetti D, Agnelli L, Taiana E, Galletti S, Manzoni M, Todoerti K, Musto P, Strozzi F, Neri A. Distinct lncRNA transcriptional fingerprints characterize progressive stages of multiple myeloma. Oncotarget. Impact Journals, LLC; 2016; 7: 14814–30. doi: 10.18632/oncotarget.7442.

102. Binder S, Hösler N, Riedel D, Zipfel I, Buschmann T, Kämpf C, Reiche K, Burger R, Gramatzki M, Hackermüller J, Stadler PF, Horn F. STAT3-induced long noncoding RNAs in multiple myeloma cells display different properties in cancer. Sci Rep. Nature Publishing Group; 2017; 7: 7976. doi: 10.1038/s41598-017-08348-5.

103. Shen Y, Feng Y, Chen H, Huang L, Wang F, Bai J, Yang Y, Wang J, Zhao W, Jia Y, Peng Y, Lei X, He A. Focusing on long non-coding RNA dysregulation in newly diagnosed multiple myeloma. Life Sci. 2018; 196: 133–42. doi: 10.1016/j.lfs.2018.01.025.

104. Liu H, Wang H, Wu B, Yao K, Liao A, Miao M, Li Y, Yang W. Down-regulation of long non-coding RNA MALAT1 by RNA interference inhibits proliferation and induces apoptosis in multiple myeloma. Clin Exp Pharmacol Physiol. 2017; 44: 1032–41. doi: 10.1111/1440-1681.12804.

105. Luger K, Mäder AW, Richmond RK, Sargent DF, Richmond TJ. Crystal structure of the nucleosome core particle at 2.8 Å resolution. Nature. 1997; 389: 251–60. doi: 10.1038/38444.

106. Medvedeva YA, Lennartsson A, Ehsani R, Kulakovskiy I V, Vorontsov IE, Panahandeh P, Khimulya G, Kasukawa T, FANTOM Consortium TF, Drabløs F. EpiFactors: a comprehensive database of human epigenetic factors and complexes. Database (Oxford). Oxford University Press; 2015; 2015: bav067. doi: 10.1093/database/bav067.

107. Biterge B, Schneider R. Histone variants: key players of chromatin. Cell Tissue Res. 2014; 356: 457–66. doi: 10.1007/s00441-014-1862-4.

108. Khare SP, Habib F, Sharma R, Gadewal N, Gupta S, Galande S. HIstome--a relational knowledgebase of human histone proteins and histone modifying enzymes. Nucleic Acids

Res. Oxford University Press; 2012; 40: D337-42. doi: 10.1093/nar/gkr1125.

109. Kouzarides T. Chromatin Modifications and Their Function. Cell. Cell Press; 2007; 128: 693–705. doi: 10.1016/J.CELL.2007.02.005.

110. Rothbart SB, Strahl BD. Interpreting the language of histone and DNA modifications. Biochim Biophys Acta - Gene Regul Mech. 2014; 1839: 627–43. doi: 10.1016/j.bbagrm.2014.03.001.

111. Zhang T, Cooper S, Brockdorff N. The interplay of histone modifications - writers that read. EMBO Rep. 2015; 16: 1467–81. doi: 10.15252/embr.201540945.

112. Ernst J, Kheradpour P, Mikkelsen TS, Shoresh N, Ward LD, Epstein CB, Zhang X, Wang L, Issner R, Coyne M, Ku M, Durham T, Kellis M, et al. Mapping and analysis of chromatin state dynamics in nine human cell types. Nature. Nature Publishing Group; 2011; 473: 43–9. doi: 10.1038/nature09906.

113. Filion GJ, van Bemmel JG, Braunschweig U, Talhout W, Kind J, Ward LD, Brugman W, de Castro IJ, Kerkhoven RM, Bussemaker HJ, van Steensel B. Systematic protein location mapping reveals five principal chromatin types in Drosophila cells. Cell. NIH Public Access; 2010; 143: 212–24. doi: 10.1016/j.cell.2010.09.009.

114. Voigt P, Tee W-W, Reinberg D. A double take on bivalent promoters. Genes Dev. 2013; 27: 1318–38. doi: 10.1101/gad.219626.113.

115. Harikumar A, Meshorer E. Chromatin remodeling and bivalent histone modifications in embryonic stem cells. EMBO Rep. 2015; 16: 1609–19. doi: 10.15252/embr.201541011.

116. Li B, Carey M, Workman JL. The Role of Chromatin during Transcription. Cell. Cell Press; 2007; 128: 707–19. doi: 10.1016/J.CELL.2007.01.015.

117. Zhang Y, Lv J, Liu H, Zhu J, Su J, Wu Q, Qi Y, Wang F, Li X. HHMD: the human histone modification database. Nucleic Acids Res. Oxford University Press; 2010; 38: D149-54. doi: 10.1093/nar/gkp968.

118. Füllgrabe J, Kavanagh E, Joseph B. Histone onco-modifications. Oncogene. Nature Publishing Group; 2011; 30: 3391–403. doi: 10.1038/onc.2011.121.

119. Torres IO, Fujimori DG. Functional coupling between writers, erasers and readers of

histone and DNA methylation. Curr Opin Struct Biol. 2015; 35: 68–75. doi: 10.1016/j.sbi.2015.09.007.

120. Hyun K, Jeon J, Park K, Kim J. Writing, erasing and reading histone lysine methylations. Exp Mol Med. 2017; 49: e324–e324. doi: 10.1038/emm.2017.11.

121. Dupéré-Richer D, Licht JD. Epigenetic regulatory mutations and epigenetic therapy for multiple myeloma. Curr Opin Hematol. 2017; 24: 336–44. doi: 10.1097/MOH.0000000000000358.

122. Morin RD, Mungall K, Pleasance E, Mungall AJ, Goya R, Huff RD, Scott DW, Ding J, Roth A, Chiu R, Corbett RD, Chan FC, Mendez-Lago M, et al. Mutational and structural analysis of diffuse large B-cell lymphoma using whole-genome sequencing. Blood. American Society of Hematology; 2013; 122: 1256–65. doi: 10.1182/blood-2013-02-483727.

123. Li H, Kaminski MS, Li Y, Yildiz M, Ouillette P, Jones S, Fox H, Jacobi K, Saiya-Cork K, Bixby D, Lebovic D, Roulston D, Shedden K, et al. Mutations in linker histone genes HIST1H1 B, C, D, and E; OCT2 (POU2F2); IRF8; and ARID1A underlying the pathogenesis of follicular lymphoma. Blood. American Society of Hematology; 2014; 123: 1487–98. doi: 10.1182/blood-2013-05-500264.

124. Shain AH, Pollack JR. The Spectrum of SWI/SNF Mutations, Ubiquitous in Human Cancers. Kashanchi F, editor. PLoS One. Public Library of Science; 2013; 8: e55119. doi: 10.1371/journal.pone.0055119.

125. Struhl K. Histone acetylation and transcriptional regulatory mechanisms. Genes Dev. Cold Spring Harbor Laboratory Press; 1998; 12: 599–606. Available from http://www.ncbi.nlm.nih.gov/pubmed/9499396

126. Parbin S, Kar S, Shilpi A, Sengupta D, Deb M, Rath SK, Patra SK. Histone deacetylases: a saga of perturbed acetylation homeostasis in cancer. J Histochem Cytochem. Histochemical Society; 2014; 62: 11–33. doi: 10.1369/0022155413506582.

127. Haberland M, Montgomery RL, Olson EN. The many roles of histone deacetylases in development and physiology: implications for disease and therapy. Nat Rev Genet. NIH

Public Access; 2009; 10: 32–42. doi: 10.1038/nrg2485.

128. Pasqualucci L, Dominguez-Sola D, Chiarenza A, Fabbri G, Grunn A, Trifonov V, Kasper LH, Lerach S, Tang H, Ma J, Rossi D, Chadburn A, Murty V V., et al. Inactivating mutations of acetyltransferase genes in B-cell lymphoma. Nature. Nature Publishing Group; 2011; 471: 189–95. doi: 10.1038/nature09730.

129. Mithraprabhu S, Kalff A, Chow A, Khong T, Spencer A. Dysregulated Class I histone deacetylases are indicators of poor prognosis in multiple myeloma. Epigenetics. Taylor & Francis; 2014; 9: 1511–20. doi: 10.4161/15592294.2014.983367.

130. Choudhary C, Kumar C, Gnad F, Nielsen ML, Rehman M, Walther TC, Olsen J V, Mann M. Lysine acetylation targets protein complexes and co-regulates major cellular functions. Science. American Association for the Advancement of Science; 2009; 325: 834–40. doi: 10.1126/science.1175371.

131. Yang X-J, Seto E. Lysine Acetylation: Codified Crosstalk with Other Posttranslational Modifications. Mol Cell. Cell Press; 2008; 31: 449–61. doi: 10.1016/J.MOLCEL.2008.07.002.

132. Pei X-Y, Dai Y, Grant S. Synergistic Induction of Oxidative Injury and Apoptosis in Human Multiple Myeloma Cells by the Proteasome Inhibitor Bortezomib and Histone Deacetylase Inhibitors. Clin Cancer Res. 2004; 10: 3839–52. doi: 10.1158/1078-0432.CCR-03-0561.

133. Catley L, Weisberg E, Kiziltepe T, Tai Y-T, Hideshima T, Neri P, Tassone P, Atadja P, Chauhan D, Munshi NC, Anderson KC. Aggresome induction by proteasome inhibitor bortezomib and -tubulin hyperacetylation by tubulin deacetylase (TDAC) inhibitor LBH589 are synergistic in myeloma cells. Blood. 2006; 108: 3441–9. doi: 10.1182/blood-2006-04-016055.

134. San-Miguel JF, Hungria VTM, Yoon S-S, Beksac M, Dimopoulos MA, Elghandour A, Jedrzejczak WW, Guenther A, Nakorn TN, Siritanaratkul N, Schlossman RL, Hou J, Moreau P, et al. Final Analysis of Overall Survival from the Phase 3 Panorama 1 Trial of Panobinostat Plus Bortezomib and Dexamethasone Versus Placebo Plus Bortezomib and Dexamethasone in Patients with Relapsed or Relapsed and Refractory Multiple Myeloma.

Blood. 2015; 126. Available from http://www.bloodjournal.org/content/126/23/3026?sso-checked=true

135. Raedler LA. Farydak (Panobinostat): First HDAC Inhibitor Approved for Patients with Relapsed Multiple Myeloma. Am Heal drug benefits. Engage Healthcare Communications, LLC; 2016; 9: 84–7. Available from http://www.ncbi.nlm.nih.gov/pubmed/27668050

136. Wahaib K, Beggs AE, Campbell H, Kodali L, Ford PD. Panobinostat: A histone deacetylase inhibitor for the treatment of relapsed or refractory multiple myeloma. Am J Heal Pharm. 2016; 73: 441–50. doi: 10.2146/ajhp150487.

137. Allfrey VG, Mirsky AE. Structural Modifications of Histones and their Possible Role in the Regulation of RNA Synthesis. Science (80-). 1964; 144: 559–559. doi: 10.1126/science.144.3618.559.

138. Rea S, Eisenhaber F, O'Carroll D, Strahl BD, Sun Z-W, Schmid M, Opravil S, Mechtler K, Ponting CP, Allis CD, Jenuwein T. Regulation of chromatin structure by site-specific histone H3 methyltransferases. Nature. 2000; 406: 593–9. doi: 10.1038/35020506.

139. Shi Y, Lan F, Matson C, Mulligan P, Whetstine JR, Cole PA, Casero RA, Shi Y. Histone Demethylation Mediated by the Nuclear Amine Oxidase Homolog LSD1. Cell. 2004; 119: 941–53. doi: 10.1016/j.cell.2004.12.012.

140. Tsukada Y, Fang J, Erdjument-Bromage H, Warren ME, Borchers CH, Tempst P, Zhang Y. Histone demethylation by a family of JmjC domain-containing proteins. Nature. 2006; 439: 811–6. doi: 10.1038/nature04433.

141. Musselman CA, Khorasanizadeh S, Kutateladze TG. Towards understanding methyllysine readout. Biochim Biophys Acta - Gene Regul Mech. 2014; 1839: 686–93. doi: 10.1016/j.bbagrm.2014.04.001.

142. Keats JJ, Maxwell CA, Taylor BJ, Hendzel MJ, Chesi M, Bergsagel PL, Larratt LM, Mant MJ, Reiman T, Belch AR, Pilarski LM. Overexpression of transcripts originating from the MMSET locus characterizes all t(4;14)(p16;q32)-positive multiple myeloma patients. Blood. American Society of Hematology; 2005; 105: 4060–9. doi: 10.1182/blood-2004-09-3704.

143. Oyer JA, Huang X, Zheng Y, Shim J, Ezponda T, Carpenter Z, Allegretta M, Okot-Kotber CI, Patel JP, Melnick A, Levine RL, Ferrando A, MacKerell AD, et al. Point mutation E1099K in MMSET/NSD2 enhances its methyltranferase activity and leads to altered global chromatin methylation in lymphoid malignancies. Leukemia. Nature Publishing Group; 2014; 28: 198–201. doi: 10.1038/leu.2013.204.

144. Shah MY, Martinez-Garcia E, Phillip JM, Chambliss AB, Popovic R, Ezponda T, Small EC, Will C, Phillip MP, Neri P, Bahlis NJ, Wirtz D, Licht JD. MMSET/WHSC1 enhances DNA damage repair leading to an increase in resistance to chemotherapeutic agents. Oncogene. Nature Publishing Group; 2016; 35: 5905–15. doi: 10.1038/onc.2016.116.

145. Kuo AJ, Cheung P, Chen K, Zee BM, Kioi M, Lauring J, Xi Y, Park BH, Shi X, Garcia BA, Li W, Gozani O. NSD2 Links Dimethylation of Histone H3 at Lysine 36 to Oncogenic Programming. Mol Cell. Cell Press; 2011; 44: 609–20. doi: 10.1016/J.MOLCEL.2011.08.042.

146. Martinez-Garcia E, Popovic R, Min D-J, Sweet SMM, Thomas PM, Zamdborg L, Heffner A, Will C, Lamy L, Staudt LM, Levens DL, Kelleher NL, Licht JD. The MMSET histone methyl transferase switches global histone methylation and alters gene expression in t(4;14) multiple myeloma cells. Blood. American Society of Hematology; 2011; 117: 211–20. doi: 10.1182/blood-2010-07-298349.

147. Popovic R, Martinez-Garcia E, Giannopoulou EG, Zhang Q, Zhang Q, Ezponda T, Shah MY, Zheng Y, Will CM, Small EC, Hua Y, Bulic M, Jiang Y, et al. Histone methyltransferase MMSET/NSD2 alters EZH2 binding and reprograms the myeloma epigenome through global and focal changes in H3K36 and H3K27 methylation. Milne T, editor. PLoS Genet. 2014; 10: e1004566. doi: 10.1371/journal.pgen.1004566.

148. Min D-J, Ezponda T, Kim MK, Will CM, Martinez-Garcia E, Popovic R, Basrur V, Elenitoba-Johnson KS, Licht JD. MMSET stimulates myeloma cell growth through microRNA-mediated modulation of c-MYC. Leukemia. Nature Publishing Group; 2013; 27: 686–94. doi: 10.1038/leu.2012.269.

149. Vakoc CR, Mandat SA, Olenchock BA, Blobel GA. Histone H3 Lysine 9 Methylation and

HP1γ Are Associated with Transcription Elongation through Mammalian Chromatin. Mol Cell. Cell Press; 2005; 19: 381–91. doi: 10.1016/J.MOLCEL.2005.06.011.

150. De Bruyne E, Bos TJ, Schuit F, Van Valckenborgh E, Menu E, Thorrez L, Atadja P, Jernberg-Wiklund H, Vanderkerken K. IGF-1 suppresses Bim expression in multiple myeloma via epigenetic and posttranslational mechanisms. Blood. American Society of Hematology; 2010; 115: 2430–40. doi: 10.1182/blood-2009-07-232801.

151. Ohguchi H, Hideshima T, Bhasin MK, Gorgun GT, Santo L, Cea M, Samur MK, Mimura N, Suzuki R, Tai Y-T, Carrasco RD, Raje N, Richardson PG, et al. The KDM3A–KLF2–IRF4 axis maintains myeloma cell survival. Nat Commun. Nature Publishing Group; 2016; 7: 10258. doi: 10.1038/ncomms10258.

152. Ezponda T, Dupéré-Richer D, Will CM, Small EC, Varghese N, Patel T, Nabet B, Popovic R, Oyer J, Bulic M, Zheng Y, Huang X, Shah MY, et al. UTX/KDM6A Loss Enhances the Malignant Phenotype of Multiple Myeloma and Sensitizes Cells to EZH2 inhibition. Cell Rep. 2017; 21: 628–40. doi: 10.1016/j.celrep.2017.09.078.

153. van Haaften G, Dalgliesh GL, Davies H, Chen L, Bignell G, Greenman C, Edkins S, Hardy C, O'Meara S, Teague J, Butler A, Hinton J, Latimer C, et al. Somatic mutations of the histone H3K27 demethylase gene UTX in human cancer. Nat Genet. Nature Publishing Group; 2009; 41: 521–3. doi: 10.1038/ng.349.

154. Margueron R, Reinberg D. The Polycomb complex PRC2 and its mark in life. Nature. Nature Publishing Group; 2011; 469: 343–9. doi: 10.1038/nature09784.

155. Lewis EB. A gene complex controlling segmentation in Drosophila. Nature. 1978; 276: 565–70. Available from http://www.ncbi.nlm.nih.gov/pubmed/103000

156. Jürgens G. A group of genes controlling the spatial expression of the bithorax complex in Drosophila. Nature. Nature Publishing Group; 1985; 316: 153–5. doi: 10.1038/316153a0.

157. Dorafshan E, Kahn TG, Schwartz YB. Hierarchical recruitment of Polycomb complexes revisited. Nucleus. Taylor & Francis; 2017; 8: 496–505. doi: 10.1080/19491034.2017.1363136.

158. Holoch D, Margueron R. Mechanisms Regulating PRC2 Recruitment and Enzymatic

Activity. Trends Biochem Sci. Elsevier Current Trends; 2017; 42: 531–42. doi: 10.1016/J.TIBS.2017.04.003.

159. Sashida G, Iwama A. Multifaceted role of the polycomb-group gene EZH2 in hematological malignancies. Int J Hematol. 2017; 105: 23–30. doi: 10.1007/s12185-016-2124-x.

160. Lee JM, Lee JS, Kim H, Kim K, Park H, Kim J-Y, Lee SH, Kim IS, Kim J, Lee M, Chung CH, Seo S-B, Yoon J-B, et al. EZH2 Generates a Methyl Degron that Is Recognized by the DCAF1/DDB1/CUL4 E3 Ubiquitin Ligase Complex. Mol Cell. 2012; 48: 572–86. doi: 10.1016/j.molcel.2012.09.004.

161. Dasgupta M, Dermawan JKT, Willard B, Stark GR. STAT3-driven transcription depends upon the dimethylation of K49 by EZH2. Proc Natl Acad Sci U S A. National Academy of Sciences; 2015; 112: 3985–90. doi: 10.1073/pnas.1503152112.

162. Yan J, Ng S-B, Tay JL-S, Lin B, Koh TL, Tan J, Selvarajan V, Liu S-C, Bi C, Wang S, Choo S-N, Shimizu N, Huang G, et al. EZH2 overexpression in natural killer/T-cell lymphoma confers growth advantage independently of histone methyltransferase activity. Blood. 2013; 121: 4512–20. doi: 10.1182/blood-2012-08-450494.

163. Shi B, Liang J, Yang X, Wang Y, Zhao Y, Wu H, Sun L, Zhang Y, Chen Y, Li R, Zhang Y, Hong M, Shang Y. Integration of Estrogen and Wnt Signaling Circuits by the Polycomb Group Protein EZH2 in Breast Cancer Cells. Mol Cell Biol. 2007; 27: 5105–19. doi: 10.1128/MCB.00162-07.

164. Jung H-Y, Jun S, Lee M, Kim H-C, Wang X, Ji H, McCrea PD, Park J-I. PAF and EZH2 Induce Wnt/β-Catenin Signaling Hyperactivation. Mol Cell. 2013; 52: 193–205. doi: 10.1016/j.molcel.2013.08.028.

165. Zovoilis A, Cifuentes-Rojas C, Chu H-P, Hernandez AJ, Lee JT. Destabilization of B2 RNA by EZH2 Activates the Stress Response. Cell. 2016; 167: 1788–1802.e13. doi: 10.1016/j.cell.2016.11.041.

166. Karantanos T, Boussiotis VA. JAK3-mediated phosphorylation of EZH2: a novel mechanism of non-canonical EZH2 activation and oncogenic function. Transl Cancer Res.

2016; 5: S1208–11. doi: 10.21037/tcr.2016.11.11.

167. Béguelin W, Popovic R, Teater M, Jiang Y, Bunting KL, Rosen M, Shen H, Yang SN, Wang L, Ezponda T, Martinez-Garcia E, Zhang H, Zheng Y, et al. EZH2 Is Required for Germinal Center Formation and Somatic EZH2 Mutations Promote Lymphoid Transformation. Cancer Cell. Cell Press; 2013; 23: 677–92. doi: 10.1016/J.CCR.2013.04.011.

168. Zhan F, Hardin J, Kordsmeier B, Bumm K, Zheng M, Tian E, Sanderson R, Yang Y, Wilson C, Zangari M, Anaissie E, Morris C, Muwalla F, et al. Global gene expression profiling of multiple myeloma, monoclonal gammopathy of undetermined significance, and normal bone marrow plasma cells. Blood. 2002; 99: 1745–57. Available from http://www.ncbi.nlm.nih.gov/pubmed/11861292

169. Zhan F, Tian E, Bumm K, Smith R, Barlogie B, Shaughnessy J. Gene expression profiling of human plasma cell differentiation and classification of multiple myeloma based on similarities to distinct stages of late-stage B-cell development. Blood. 2003; 101: 1128–40. doi: 10.1182/blood-2002-06-1737.

170. Croonquist PA, Van Ness B. The polycomb group protein enhancer of zeste homolog 2 (EZH2) is an oncogene that influences myeloma cell growth and the mutant ras phenotype. Oncogene. 2005; 24: 6269–80. doi: 10.1038/sj.onc.1208771.

171. Kim KH, Roberts CWM. Targeting EZH2 in cancer. Nat Med. 2016; 22: 128–34. doi: 10.1038/nm.4036.

172. Yamaguchi H, Hung M-C. Regulation and Role of EZH2 in Cancer. Cancer Res Treat. Korean Cancer Association; 2014; 46: 209–22. doi: 10.4143/crt.2014.46.3.209.

173. Herviou L, Cavalli G, Cartron G, Klein B, Moreaux J. EZH2 in normal hematopoiesis and hematological malignancies. Oncotarget. 2016; 7: 2284–96. doi: 10.18632/oncotarget.6198.

174. McCabe MT, Graves AP, Ganji G, Diaz E, Halsey WS, Jiang Y, Smitheman KN, Ott HM, Pappalardi MB, Allen KE, Chen SB, Della Pietra A, Dul E, et al. Mutation of A677 in histone methyltransferase EZH2 in human B-cell lymphoma promotes hypertrimethylation

of histone H3 on lysine 27 (H3K27). Proc Natl Acad Sci. 2012; 109: 2989–94. doi: 10.1073/pnas.1116418109.

175. Morin RD, Johnson NA, Severson TM, Mungall AJ, An J, Goya R, Paul JE, Boyle M, Woolcock BW, Kuchenbauer F, Yap D, Humphries RK, Griffith OL, et al. Somatic mutations altering EZH2 (Tyr641) in follicular and diffuse large B-cell lymphomas of germinal-center origin. Nat Genet. Nature Publishing Group; 2010; 42: 181–5. doi: 10.1038/ng.518.

176. Majer CR, Jin L, Scott MP, Knutson SK, Kuntz KW, Keilhack H, Smith JJ, Moyer MP, Richon VM, Copeland RA, Wigle TJ. A687V EZH2 is a gain-of-function mutation found in lymphoma patients. FEBS Lett. No longer published by Elsevier; 2012; 586: 3448–51. doi: 10.1016/J.FEBSLET.2012.07.066.

177. Sneeringer CJ, Scott MP, Kuntz KW, Knutson SK, Pollock RM, Richon VM, Copeland RA. Coordinated activities of wild-type plus mutant EZH2 drive tumor-associated hypertrimethylation of lysine 27 on histone H3 (H3K27) in human B-cell lymphomas. Proc Natl Acad Sci U S A. National Academy of Sciences; 2010; 107: 20980–5. doi: 10.1073/pnas.1012525107.

178. Honma D, Kanno O, Watanabe J, Kinoshita J, Hirasawa M, Nosaka E, Shiroishi M, Takizawa T, Yasumatsu I, Horiuchi T, Nakao A, Suzuki K, Yamasaki T, et al. Novel orally bioavailable EZH1/2 dual inhibitors with greater antitumor efficacy than an EZH2 selective inhibitor. Cancer Sci. Wiley-Blackwell; 2017; 108: 2069–78. doi: 10.1111/cas.13326.

179. Alzrigat M, Párraga AA, Agarwal P, Zureigat H, Österborg A, Nahi H, Ma A, Jin J, Nilsson K, Öberg F, Kalushkova A, Jernberg-Wiklund H. EZH2 inhibition in multiple myeloma downregulates myeloma associated oncogenes and upregulates microRNAs with potential tumor suppressor functions. Oncotarget. 2016; 8: 10213–24. doi: 10.18632/oncotarget.14378.

180. Pawlyn C, Bright MD, Buros AF, Stein CK, Walters Z, Aronson LI, Mirabella F, Jones JR, Kaiser MF, Walker BA, Jackson GH, Clarke PA, Bergsagel PL, et al. Overexpression of EZH2 in multiple myeloma is associated with poor prognosis and dysregulation of cell

cycle control. Blood Cancer J. 2017; 7: e549. doi: 10.1038/bcj.2017.27.

181. Gaudichon J, Milano F, Cahu J, DaCosta L, Martens AC, Renoir J-M, Sola B. Deazaneplanocin A Is a Promising Drug to Kill Multiple Myeloma Cells in Their Niche. Eckert RL, editor. PLoS One. 2014; 9: e107009. doi: 10.1371/journal.pone.0107009.

182. Agarwal P, Alzrigat M, Párraga AA, Enroth S, Singh U, Ungerstedt J, Österborg A, Brown PJ, Ma A, Jin J, Nilsson K, Öberg F, Kalushkova A, et al. Genome-wide profiling of histone H3 lysine 27 and lysine 4 trimethylation in multiple myeloma reveals the importance of Polycomb gene targeting and highlights EZH2 as a potential therapeutic target. Oncotarget. 2016; 7: 6809–23. doi: 10.18632/oncotarget.6843.

183. Hernando H, Gelato KA, Lesche R, Beckmann G, Koehr S, Otto S, Steigemann P, Stresemann C. EZH2 Inhibition Blocks Multiple Myeloma Cell Growth through Upregulation of Epithelial Tumor Suppressor Genes. Mol Cancer Ther. 2016; 15: 287–98. doi: 10.1158/1535-7163.MCT-15-0486.

184. Zeng D, Liu M, Pan J. Blocking EZH2 methylation transferase activity by GSK126 decreases stem cell-like myeloma cells. Oncotarget. 2016; 8: 3396–411. doi: 10.18632/oncotarget.13773.

185. Kikuchi J, Koyama D, Wada T, Izumi T, Hofgaard PO, Bogen B, Furukawa Y. Phosphorylation-mediated EZH2 inactivation promotes drug resistance in multiple myeloma. J Clin Invest. 2015; 125: 4375–90. doi: 10.1172/JCI80325.

186. Kalushkova A, Fryknäs M, Lemaire M, Fristedt C, Agarwal P, Eriksson M, Deleu S, Atadja P, Österborg A, Nilsson K, Vanderkerken K, Öberg F, Jernberg-Wiklund H. Polycomb Target Genes Are Silenced in Multiple Myeloma. Imhof A, editor. PLoS One. 2010; 5: e11483. doi: 10.1371/journal.pone.0011483.

187. Knutson SK, Kawano S, Minoshima Y, Warholic NM, Huang K-C, Xiao Y, Kadowaki T, Uesugi M, Kuznetsov G, Kumar N, Wigle TJ, Klaus CR, Allain CJ, et al. Selective Inhibition of EZH2 by EPZ-6438 Leads to Potent Antitumor Activity in EZH2-Mutant Non-Hodgkin Lymphoma. Mol Cancer Ther. 2014; 13: 842–54. doi: 10.1158/1535-7163.MCT-13-0773.

188. McCabe MT, Ott HM, Ganji G, Korenchuk S, Thompson C, Van Aller GS, Liu Y, Graves AP, III ADP, Diaz E, LaFrance L V., Mellinger M, Duquenne C, et al. EZH2 inhibition as a therapeutic strategy for lymphoma with EZH2-activating mutations. Nature. 2012; 492: 108–12. doi: 10.1038/nature11606.

189. Konze KD, Ma A, Li F, Barsyte-Lovejoy D, Parton T, MacNevin CJ, Liu F, Gao C, Huang X-P, Kuznetsova E, Rougie M, Jiang A, Pattenden SG, et al. An Orally Bioavailable Chemical Probe of the Lysine Methyltransferases EZH2 and EZH1. ACS Chem Biol. 2013; 8: 1324–34. doi: 10.1021/cb400133j.

190. Tan J, Yan Y, Wang X, Jiang Y, Xu HE. EZH2: biology, disease, and structure-based drug discovery. Acta Pharmacol Sin. 2014; 35: 161–74. doi: 10.1038/aps.2013.161.

191. Kumar SK, Rajkumar V, Kyle RA, van Duin M, Sonneveld P, Mateos M-V, Gay F, Anderson KC. Multiple myeloma. Nat Rev Dis Prim. Nature Publishing Group; 2017; 3: 17046. doi: 10.1038/nrdp.2017.46.

192. Alexanian R, Haut A, Khan AU, Lane M, McKelvey EM, Migliore PJ, Stuckey WJ, Wilson HE. Treatment for multiple myeloma. Combination chemotherapy with different melphalan dose regimens. JAMA. 1969; 208: 1680–5. Available from http://www.ncbi.nlm.nih.gov/pubmed/5818682

193. Palumbo A, Bringhen S, Ludwig H, Dimopoulos MA, Blade J, Mateos M V., Rosinol L, Boccadoro M, Cavo M, Lokhorst H, Zweegman S, Terpos E, Davies F, et al. Personalized therapy in multiple myeloma according to patient age and vulnerability: a report of the European Myeloma Network (EMN). Blood. 2011; 118: 4519–29. doi: 10.1182/blood-2011-06-358812.

194. Attal M, Harousseau J-L, Stoppa A-M, Sotto J-J, Fuzibet J-G, Rossi J-F, Casassus P, Maisonneuve H, Facon T, Ifrah N, Payen C, Bataille R. A Prospective, Randomized Trial of Autologous Bone Marrow Transplantation and Chemotherapy in Multiple Myeloma. N Engl J Med. 1996; 335: 91–7. doi: 10.1056/NEJM199607113350204.

195. Palumbo A, Cavallo F, Gay F, Di Raimondo F, Ben Yehuda D, Petrucci MT, Pezzatti S, Caravita T, Cerrato C, Ribakovsky E, Genuardi M, Cafro A, Marcatti M, et al. Autologous

Transplantation and Maintenance Therapy in Multiple Myeloma. N Engl J Med. 2014; 371: 895–905. doi: 10.1056/NEJMoa1402888.

196. Rosenblatt J, Avigan D. Targeting the PD-1/PD-L1 axis in multiple myeloma: a dream or a reality? Blood. 2017; 129: 275–9. doi: 10.1182/blood-2016-08-731885.

197. Ghosh A, Mailankody S, Giralt SA, Landgren CO, Smith EL, Brentjens RJ. CAR T cell therapy for multiple myeloma: where are we now and where are we headed? Leuk Lymphoma. 2017; : 1–12. doi: 10.1080/10428194.2017.1393668.

198. CAR T-cell Therapy Impresses in Multiple Myeloma. Cancer Discov. 2018; 8: OF2-OF2. doi: 10.1158/2159-8290.CD-NB2017-181.

199. Grigoreva TA, Tribulovich VG, Garabadzhiu A V, Melino G, Barlev NA. The 26S proteasome is a multifaceted target for anti-cancer therapies. Oncotarget. Impact Journals, LLC; 2015; 6: 24733–49. doi: 10.18632/oncotarget.4619.

200. Tsakiri EN, Trougakos IP. The Amazing Ubiquitin-Proteasome System: Structural Components and Implication in Aging. Int Rev Cell Mol Biol. Academic Press; 2015; 314: 171–237. doi: 10.1016/BS.IRCMB.2014.09.002.

201. Kisselev AF, Goldberg AL. Proteasome inhibitors: from research tools to drug candidates. Chem Biol. Cell Press; 2001; 8: 739–58. doi: 10.1016/S1074-5521(01)00056-4.

202. Hideshima T, Mitsiades C, Akiyama M, Hayashi T, Chauhan D, Richardson P, Schlossman R, Podar K, Munshi NC, Mitsiades N, Anderson KC, Stirling DI, Anderson KC. Molecular mechanisms mediating antimyeloma activity of proteasome inhibitor PS-341. Blood. American Society of Hematology; 2003; 101: 1530–4. doi: 10.1182/blood-2002-08-2543.

203. Gao M, Kong Y, Yang G, Gao L, Shi J. Multiple myeloma cancer stem cells. Oncotarget. 2016; 7: 35466–77. doi: 10.18632/oncotarget.8154.

204. Yang W-C, Lin S-F. Mechanisms of Drug Resistance in Relapse and Refractory Multiple Myeloma. Biomed Res Int. Hindawi Limited; 2015; 2015: 341430. doi: 10.1155/2015/341430.

205. Oerlemans R, Franke NE, Assaraf YG, Cloos J, van Zantwijk I, Berkers CR, Scheffer GL,

Debipersad K, Vojtekova K, Lemos C, van der Heijden JW, Ylstra B, Peters GJ, et al. Molecular basis of bortezomib resistance: proteasome subunit 5 (PSMB5) gene mutation and overexpression of PSMB5 protein. Blood. 2008; 112: 2489–99. doi: 10.1182/blood-2007-08-104950.

206. Vtorushin S V, Khristenko KY, Zavyalova M V, Perelmuter VM, Litviakov N V, Denisov E V, Dulesova AY, Cherdyntseva N V. THE PHENOMENON OF MULTI-DRUG RESISTANCE IN THE TREATMENT OF MALIGNANT TUMORS. Exp Oncol. 2014; 36: 144–56. Available from http://exp-oncology.com.ua/wp/wp-content/uploads/2014/09/2128.pdf?upload=

207. Di Marzo L, Desantis V, Solimando AG, Ruggieri S, Annese T, Nico B, Fumarulo R, Vacca A, Frassanito MA. Microenvironment drug resistance in multiple myeloma: emerging new players. Oncotarget. 2016; 7: 60698–711. doi: 10.18632/oncotarget.10849.

208. Furukawa Y, Kikuchi J. Epigenetic mechanisms of cell adhesion-mediated drug resistance in multiple myeloma. Int J Hematol. Springer Japan; 2016; 104: 281–92. doi: 10.1007/s12185-016-2048-5.

209. Shaughnessy JD, Zhan F, Burington BE, Huang Y, Colla S, Hanamura I, Stewart JP, Kordsmeier B, Randolph C, Williams DR, Xiao Y, Xu H, Epstein J, et al. A validated gene expression model of high-risk multiple myeloma is defined by deregulated expression of genes mapping to chromosome 1. Blood. American Society of Hematology; 2007; 109: 2276–84. doi: 10.1182/blood-2006-07-038430.

210. Decaux O, Lodé L, Magrangeas F, Charbonnel C, Gouraud W, Jézéquel P, Attal M, Harousseau J-L, Moreau P, Bataille R, Campion L, Avet-Loiseau H, Minvielle S, et al. Prediction of Survival in Multiple Myeloma Based on Gene Expression Profiles Reveals Cell Cycle and Chromosomal Instability Signatures in High-Risk Patients and Hyperdiploid Signatures in Low-Risk Patients: A Study of the Intergroupe Francophone du Myélome. J Clin Oncol. 2008; 26: 4798–805. doi: 10.1200/JCO.2007.13.8545.

211. Kuiper R, Broyl A, de Knegt Y, van Vliet MH, van Beers EH, van der Holt B, el Jarari L, Mulligan G, Gregory W, Morgan G, Goldschmidt H, Lokhorst HM, van Duin M, et al. A

gene expression signature for high-risk multiple myeloma. Leukemia. 2012; 26: 2406–13. doi: 10.1038/leu.2012.127.

212. Zhan F, Huang Y, Colla S, Stewart JP, Hanamura I, Gupta S, Epstein J, Yaccoby S, Sawyer J, Burington B, Anaissie E, Hollmig K, Pineda-Roman M, et al. The molecular classification of multiple myeloma. Blood. American Society of Hematology; 2006; 108: 2020–8. doi: 10.1182/blood-2005-11-013458.

213. van Laar R, Flinchum R, Brown N, Ramsey J, Riccitelli S, Heuck C, Barlogie B, Shaughnessy Jr JD. Translating a gene expression signature for multiple myeloma prognosis into a robust high-throughput assay for clinical use. BMC Med Genomics. 2014; 7: 25. doi: 10.1186/1755-8794-7-25.

214. Szalat R, Avet-Loiseau H, Munshi NC. Gene Expression Profiles in Myeloma: Ready for the Real World? Clin Cancer Res. NIH Public Access; 2016; 22: 5434–42. doi: 10.1158/1078-0432.CCR-16-0867.

215. Stessman HAF, Baughn LB, Sarver A, Xia T, Deshpande R, Mansoor A, Walsh SA, Sunderland JJ, Dolloff NG, Linden MA, Zhan F, Janz S, Myers CL, et al. Profiling Bortezomib Resistance Identifies Secondary Therapies in a Mouse Myeloma Model. Mol Cancer Ther. 2013; 12: 1140–50. doi: 10.1158/1535-7163.MCT-12-1151.

216. Ghasemi M, Alpsoy S, Türk S, Malkan ÜY, Atakan Ş, Haznedaroğlu İC, Güneş G, Gündüz M, Yılmaz B, Etgül S, Aydın S, Aslan T, Sayınalp N, et al. Expression Profiles of the Individual Genes Corresponding to the Genes Generated by Cytotoxicity Experiments with Bortezomib in Multiple Myeloma. Turkish J Haematol Off J Turkish Soc Haematol. Galenos Yayinevi; 2016; 33: 286–92. doi: 10.4274/tjh.2015.0145.

217. Mitra AK, Harding T, Mukherjee UK, Jang JS, Li Y, HongZheng R, Jen J, Sonneveld P, Kumar S, Kuehl WM, Rajkumar V, Van Ness B. A gene expression signature distinguishes innate response and resistance to proteasome inhibitors in multiple myeloma. Blood Cancer J. Nature Publishing Group; 2017; 7: e581. doi: 10.1038/bcj.2017.56.

218. Marin JJ, Briz O, Monte MJ, Blazquez AG, Macias RI. Genetic variants in genes involved in mechanisms of chemoresistance to anticancer drugs. Curr Cancer Drug Targets. ;

2012; 12: 402–38.

219. Richardson PG, Sonneveld P, Schuster MW, Irwin D, Stadtmauer EA, Facon T. Safety and efficacy of bortezomib in high-risk and elderly patients with relapsed multiple myeloma. Br J Haematol. ; 2007; 137: 429–35.

220. Fonseca R, Bergsagel PL, Drach J, Shaughnessy J, Gutierrez N, Stewart AK. International Myeloma Working Group molecular classification of multiple myeloma: spotlight review. Leukemia. ; 2009; 23: 2210–21.

221. Vangsted A, Klausen TW, Vogel U. Genetic variations in multiple myeloma II: association with effect of treatment. Eur J Haematol. ; 2012; 88: 93–117.

222. Kumar S, Rajkumar S V. Many facets of bortezomib resistance/susceptibility. Blood. ; 2008; 112: 2177–8.

223. Rajkumar S V, Dimopoulos MA, Palumbo A, Blade J, Merlini G, Mateos M V. International Myeloma Working Group updated criteria for the diagnosis of multiple myeloma. Lancet Oncol. ; 2014; 15: e538–48.

224. Rajkumar SV. Myeloma today: Disease definitions and treatment advances. Am J Hematol. 2016; 91: 90–100. doi: 10.1002/ajh.24236.

225. Mitsiades CS, Davies FE, Laubach JP, Joshua D, San Miguel J, Anderson KC. Future directions of next-generation novel therapies, combination approaches, and the development of personalized medicine in myeloma. J Clin Oncol. ; 2011; 29: 1916–23.

226. Richardson PG, Hungria VT, Yoon SS, Beksac M, Dimopoulos MA, Elghandour A. Panobinostat plus bortezomib and dexamethasone in relapsed/relapsed and refractory myeloma: outcomes by prior treatment. Blood. ; 2016; 127: 713–21.

227. Moreau P, Richardson PG, Cavo M, Orlowski RZ, San Miguel JF, Palumbo A. Proteasome inhibitors in multiple myeloma: 10 years later. Blood. ; 2012; 120: 947–59.

228. Lightcap ES, McCormack TA, Pien CS, Chau V, Adams J, Elliott PJ. Proteasome inhibition measurements: clinical application. Clin Chem. ; 2000; 46: 673–83.

229. Adams J, Palombella VJ, Sausville EA, Johnson J, Destree A, Lazarus DD. Proteasome inhibitors: a novel class of potent and effective antitumor agents. Cancer Res. ; 1999; 59:

2615–22.

230. Kortuem KM, Stewart AK. Carfilzomib. Blood. ; 2013; 121: 893–7.

231. Rajkumar SV. Multiple myeloma: 2016 update on diagnosis, risk-stratification, and management. Am J Hematol. NIH Public Access; 2016; 91: 719–34. doi: 10.1002/ajh.24402.

232. Moreaux J, Klein B, Bataille R, Descamps G, Maiga S, Hose D. A high-risk signature for patients with multiple myeloma established from the molecular classification of human myeloma cell lines. Haematologica. ; 2011; 96: 574–82.

233. Hastie T, Tibshirani R, Friedman JH. No Title. The Elements Of Statistical Learning: Data Mining, Inference, And Prediction. ; 2009.

234. Mitra AK, Mukherjee UK, Harding T, Jang JS, Stessman H, Li Y. Single-cell analysis of targeted transcriptome predicts drug sensitivity of single cells within human myeloma tumors. Leukemia. ; 2016; 30: 1094–102.

235. Kumar SK, LaPlant B, Roy V, Reeder CB, Lacy MQ, Gertz MA. Phase 2 trial of ixazomib in patients with relapsed multiple myeloma not refractory to bortezomib. Blood Cancer J. ; 2015; 5: e338.

236. Mulligan G, Mitsiades C, Bryant B, Zhan F, Chng WJ, Roels S. Gene expression profiling and correlation with outcome in clinical trials of the proteasome inhibitor bortezomib. Blood. ; 2007; 109: 3177–88.

237. Ishwaran H, Kogalur UB, Blackstone EH, Lauer MS. Random survival forests. Ann Appl Stat. ; 2008; 2: 841–60.

238. Somers RH. A new asymmetric measure of association for ordinal variables. Am Sociol Rev. ; 1962; 27: 799–811.

239. Hartigan JA, Wong MA. A K-means clustering algorithm. J R Stat Soc C Appl Stat. ; 1979; 28: 100–8.

240. Altman DG. No Title. Analysis Of Survival Times. ; 1991.

241. Marubini E, Valsecchi MG. No Title. Analysing Survival Data From Clinical Trials And Observational Studies. ; 2004.

242. Hosmer JDW, Lemeshow S, Sturdivant RX. No Title. Applied Logistic Regression. ;

243. Thomas S, Bonchev D. A survey of current software for network analysis in molecular biology. Hum Genomics. ; 2010; 4: 353–60.

244. Rajkumar S V, Harousseau JL, Durie B, Anderson KC, Dimopoulos M, Kyle R. Consensus recommendations for the uniform reporting of clinical trials: report of the International Myeloma Workshop Consensus Panel 1. Blood. ; 2011; 117: 4691–5.

245. Krämer A, Green J, Pollard J, Tugendreich S. Causal analysis approaches in Ingenuity Pathway Analysis. Bioinformatics. Oxford University Press; 2014; 30: 523–30. doi: 10.1093/bioinformatics/btt703.

246. Zhan F, Barlogie B, Mulligan G, Shaughnessy JJD, Bryant B. High-risk myeloma: a gene expression based risk-stratification model for newly diagnosed multiple myeloma treated with high-dose therapy is predictive of outcome in relapsed disease treated with single-agent bortezomib or high-dose dexamethasone. Blood. ; 2008; 111: 968–9.

247. Fonseca SG, Ishigaki S, Oslowski CM, Lu S, Lipson KL, Ghosh R. Wolfram syndrome 1 gene negatively regulates ER stress signaling in rodent and human cells. J Clin Invest. ; 2010; 120: 744–55.

248. Gambella M, Rocci A, Passera R, Gay F, Omede P, Crippa C. High XBP1 expression is a marker of better outcome in multiple myeloma patients treated with bortezomib. Haematologica. ; 2014; 99: e14–6.

249. Leung-Hagesteijn C, Erdmann N, Cheung G, Keats JJ, Stewart AK, Reece DE. Xbp1s-negative tumor B cells and pre-plasmablasts mediate therapeutic proteasome inhibitor resistance in multiple myeloma. Cancer Cell. ; 2013; 24: 289–304.

250. Cea M, Cagnetta A, Patrone F, Nencioni A, Gobbi M, Anderson KC. Intracellular NAD(+) depletion induces autophagic death in multiple myeloma cells. Autophagy. ; 2013; 9: 410–2.

251. Lu JP, Wang Y, Sliter DA, Pearce MM, Wojcikiewicz RJ. RNF170 protein, an endoplasmic reticulum membrane ubiquitin ligase, mediates inositol 1,4,5-trisphosphate receptor ubiquitination and degradation. J Biol Chem. ; 2011; 286: 24426–33.

252. Bataille R, Delmas PD, Chappard D, Sany J. Abnormal serum bone Gla protein levels in multiple myeloma. Crucial role of bone formation and prognostic implications. Cancer. ; 1990; 66: 167–72.

253. Stessman HA, Lulla A, Xia T, Mitra A, Harding T, Mansoor A. High-throughput drug screening identifies compounds and molecular strategies for targeting proteasome inhibitor-resistant multiple myeloma. Leukemia. ; 2014; 28: 2263–7.

254. Mullard A. Learning from exceptional drug responders. Nat Rev Drug Discov. ; 2014; 13: 401–2.

255. Maes K, Menu E, Van Valckenborgh E, Van Riet I, Vanderkerken K, De Bruyne E. Epigenetic Modulating Agents as a New Therapeutic Approach in Multiple Myeloma. Cancers (Basel). Multidisciplinary Digital Publishing Institute; 2013; 5: 430–61. doi: 10.3390/cancers5020430.

256. Goyama S, Kitamura T. Epigenetics in normal and malignant hematopoiesis: An overview and update 2017. Cancer Sci. 2017; 108: 553–62. doi: 10.1111/cas.13168.

257. Afifi S, Michael A, Azimi M, Rodriguez M, Lendvai N, Landgren O. Role of Histone Deacetylase Inhibitors in Relapsed Refractory Multiple Myeloma: A Focus on Vorinostat and Panobinostat. Pharmacother J Hum Pharmacol Drug Ther. 2015; 35: 1173–88. doi: 10.1002/phar.1671.

258. Sashida G, Iwama A. Multifaceted role of the polycomb-group gene EZH2 in hematological malignancies. Int J Hematol. 2017; 105: 23–30. doi: 10.1007/s12185-016-2124-x.

259. Herviou L, Cavalli G, Cartron G, Klein B, Moreaux J. EZH2 in normal hematopoiesis and hematological malignancies. Oncotarget. 2016; 7: 2284–96. doi: 10.18632/oncotarget.6198.

260. Wen Y, Cai J, Hou Y, Huang Z, Wang Z. Role of EZH2 in cancer stem cells: from biological insight to a therapeutic target. Oncotarget. 2015; 8: 37974–90. doi: 10.18632/oncotarget.16467.

261. Alzrigat M, Párraga AA, Majumder MM, Ma A, Jin J, Österborg A, Nahi H, Nilsson K,

Heckman CA, Öberg F, Kalushkova A, Jernberg-Wiklund H. The polycomb group protein BMI-1 inhibitor PTC-209 is a potent anti-myeloma agent alone or in combination with epigenetic inhibitors targeting EZH2 and the BET bromodomains. Oncotarget. 2017; 5. Available from https://www.researchgate.net/profile/Mohammad_Alzrigat/publication/320575442_The_polycomb_group_protein_BMI-1_inhibitor_PTC-209_is_a_potent_anti-myeloma_agent_alone_or_in_combination_with_epigenetic_inhibitors_targeting_EZH2_and_the_BET_bromodomains/links

262. Qi W, Chan H, Teng L, Li L, Chuai S, Zhang R, Zeng J, Li M, Fan H, Lin Y, Gu J, Ardayfio O, Zhang J-H, et al. Selective inhibition of Ezh2 by a small molecule inhibitor blocks tumor cells proliferation. Proc Natl Acad Sci. 2012; 109: 21360–5. doi: 10.1073/pnas.1210371110.

263. Stessman HAF, Baughn LB, Sarver A, Xia T, Deshpande R, Mansoor A, Walsh SA, Sunderland JJ, Dolloff NG, Linden MA, Zhan F, Janz S, Myers CL, et al. Profiling Bortezomib Resistance Identifies Secondary Therapies in a Mouse Myeloma Model. Mol Cancer Ther. 2013; 12: 1140–50. doi: 10.1158/1535-7163.MCT-12-1151.

264. Afgan E, Baker D, van den Beek M, Blankenberg D, Bouvier D, Čech M, Chilton J, Clements D, Coraor N, Eberhard C, Grüning B, Guerler A, Hillman-Jackson J, et al. The Galaxy platform for accessible, reproducible and collaborative biomedical analyses: 2016 update. Nucleic Acids Res. Oxford University Press; 2016; 44: W3–10. doi: 10.1093/nar/gkw343.

265. Bradley WD, Arora S, Busby J, Balasubramanian S, Gehling VS, Nasveschuk CG, Vaswani RG, Yuan C-C, Hatton C, Zhao F, Williamson KE, Iyer P, Méndez J, et al. EZH2 Inhibitor Efficacy in Non-Hodgkin's Lymphoma Does Not Require Suppression of H3K27 Monomethylation. Chem Biol. 2014; 21: 1463–75. doi: 10.1016/j.chembiol.2014.09.017.

266. Quantitative analysis of dose-effect relationships: the combined effects of multiple drugs or enzyme inhibitors. Adv Enzyme Regul. Pergamon; 1984; 22: 27–55. doi: 10.1016/0065-2571(84)90007-4.

267. Poole CJ, van Riggelen J. MYC-Master Regulator of the Cancer Epigenome and Transcriptome. Genes (Basel). Multidisciplinary Digital Publishing Institute (MDPI); 2017; 8. doi: 10.3390/genes8050142.

268. Iannetti A, Ledoux AC, Tudhope SJ, Sellier H, Zhao B, Mowla S, Moore A, Hummerich H, Gewurz BE, Cockell SJ, Jat PS, Willmore E, Perkins ND. Regulation of p53 and Rb links the alternative NF-κB pathway to EZH2 expression and cell senescence. PLoS Genet. Public Library of Science; 2014; 10: e1004642. doi: 10.1371/journal.pgen.1004642.

269. Jin Y, Huo B, Fu X, Hao T, Zhang Y, Guo Y, Hu X. LSD1 collaborates with EZH2 to regulate expression of interferon-stimulated genes. Biomed Pharmacother. Elsevier Masson; 2017; 88: 728–37. doi: 10.1016/J.BIOPHA.2017.01.055.

270. Zhao X, Lwin T, Zhang X, Huang A, Wang J, Marquez VE, Chen-Kiang S, Dalton WS, Sotomayor E, Tao J. Disruption of the MYC-miRNA-EZH2 loop to suppress aggressive B-cell lymphoma survival and clonogenicity. Leukemia. NIH Public Access; 2013; 27: 2341–50. doi: 10.1038/leu.2013.94.

271. Zhang X, Zhao X, Fiskus W, Lin J, Lwin T, Rao R, Zhang Y, Chan JC, Fu K, Marquez VE, Chen-Kiang S, Moscinski LC, Seto E, et al. Coordinated silencing of MYC-mediated miR-29 by HDAC3 and EZH2 as a therapeutic target of histone modification in aggressive B-Cell lymphomas. Cancer Cell. NIH Public Access; 2012; 22: 506–23. doi: 10.1016/j.ccr.2012.09.003.

272. Kim KH, Kim W, Howard TP, Vazquez F, Tsherniak A, Wu JN, Wang W, Haswell JR, Walensky LD, Hahn WC, Orkin SH, Roberts CWM. SWI/SNF-mutant cancers depend on catalytic and non-catalytic activity of EZH2. Nat Med. NIH Public Access; 2015; 21: 1491–6. doi: 10.1038/nm.3968.

273. Mondello P, Brea EJ, De Stanchina E, Toska E, Chang AY, Fennell M, Seshan V, Garippa R, Scheinberg DA, Baselga J, Wendel H-G, Younes A. Panobinostat acts synergistically with ibrutinib in diffuse large B cell lymphoma cells with MyD88 L265 mutations. JCI Insight. 2017; 2: e90196. doi: 10.1172/jci.insight.90196.

274. Zhang L, Tai Y-T, Ho MZG, Qiu L, Anderson KC. Interferon-alpha-based immunotherapies

in the treatment of B cell-derived hematologic neoplasms in today's treat-to-target era. Exp Hematol Oncol. BioMed Central; 2017; 6: 20. doi: 10.1186/s40164-017-0081-6.

275. Grinshtein N, Rioseco CC, Marcellus R, Uehling D, Aman A, Lun X, Muto O, Podmore L, Lever J, Shen Y, Blough MD, Cairncross GJ, Robbins SM, et al. Small molecule epigenetic screen identifies novel EZH2 and HDAC inhibitors that target glioblastoma brain tumor-initiating cells. Oncotarget. Impact Journals, LLC; 2016; 7: 59360–76. doi: 10.18632/oncotarget.10661.

276. Huang JP, Ling K. EZH2 and histone deacetylase inhibitors induce apoptosis in triple negative breast cancer cells by differentially increasing H3 Lys27 acetylation in the BIM gene promoter and enhancers. Oncol Lett. Spandidos Publications; 2017; 14: 5735–42. doi: 10.3892/ol.2017.6912.

277. Takashina T, Kinoshita I, Kikuchi J, Shimizu Y, Sakakibara-Konishi J, Oizumi S, Nishimura M, Dosaka-Akita H. Combined inhibition of EZH2 and histone deacetylases as a potential epigenetic therapy for non-small-cell lung cancer cells. Cancer Sci. 2016; 107: 955–62. doi: 10.1111/cas.12957.

278. Fiskus W, Wang Y, Sreekumar A, Buckley KM, Shi H, Jillella A, Ustun C, Rao R, Fernandez P, Chen J, Balusu R, Koul S, Atadja P, et al. Combined epigenetic therapy with the histone methyltransferase EZH2 inhibitor 3-deazaneplanocin A and the histone deacetylase inhibitor panobinostat against human AML cells. Blood. American Society of Hematology; 2009; 114: 2733–43. doi: 10.1182/blood-2009-03-213496.

279. Xu B, On DM, Ma A, Parton T, Konze KD, Pattenden SG, Allison DF, Cai L, Rockowitz S, Liu S, Liu Y, Li F, Vedadi M, et al. Selective inhibition of EZH2 and EZH1 enzymatic activity by a small molecule suppresses MLL-rearranged leukemia. Blood. American Society of Hematology; 2015; 125: 346–57. doi: 10.1182/blood-2014-06-581082.

280. Rizq O, Mimura N, Oshima M, Saraya A, Koide S, Kato Y, Aoyama K, Nakajima-Takagi Y, Wang C, Chiba T, Ma A, Jin J, Iseki T, et al. Dual Inhibition of EZH2 and EZH1 Sensitizes PRC2-Dependent Tumors to Proteasome Inhibition. Clin Cancer Res. American Association for Cancer Research; 2017; 23: 4817–30. doi: 10.1158/1078-0432.CCR-16-

2735.

281. Kampmann M. CRISPRi and CRISPRa Screens in Mammalian Cells for Precision Biology and Medicine. ACS Chem Biol. American Chemical Society; 2018; 13: 406–16. doi: 10.1021/acschembio.7b00657.